ENGINEERING APPENDIX A

APPENDIX 1

HYDRAULIC ENGINEERING APPENDIX -BRAZOS RIVER FLOODGATES

MOTT MACDONALD

Hydraulic Engineering Appendix

Brazos River Floodgates

February 14th, 2019

Texas Department of Transportation (TXDOT)

Mott MacDonald
10415 Morado Circle
Building One
Suite 300
Austin TX 78759
United States of America

T +1 (512) 342 9516
F +1 (512) 342 9708
mottmac.com

Texas Department of Transportation (TXDOT)

Hydraulic Engineering Appendix

Brazos River Floodgates

For Inclusion in Feasibility Report

February 14th, 2019

Issue and revision record

Revision	Date	Originator	Checker	Approver	Description
0	9/1/17	P. McLaughlin C. Harter	J. Carter	J. Carter	Engineering Appendix, first draft
1	1/3/18	P. McLaughlin C. Harter	J. Carter	J. Carter	Engineering Appendix, second draft
2	2/2/18	P. McLaughlin C. Harter	J. Carter	J. Carter	Engineering Appendix, third draft
3	2/8/18	P. McLaughlin C. Harter	J. Carter	J. Carter	Engineering Appendix, fourth draft
4	2/16/18	P. McLaughlin C. Harter	J. Carter	J. Carter	Engineering Appendix, fifth draft
5	5/4/18	P. McLaughlin C. Harter	J. Carter	J. Carter	Engineering Appendix, sixth draft
6	6/19/18	P. McLaughlin C. Harter	J. Carter	J. Carter	Engineering Appendix, seventh draft
7	11/13/18	P. McLaughlin C. Harter	J. Carter	J. Carter	Engineering Appendix, eighth draft
8	1/7/19	P. McLaughlin C. Harter	J. Carter	J. Carter	Engineering Appendix, ninth draft
9	2/14/19	P. McLaughlin C. Harter	J. Carter	J. Carter	Engineering Appendix, tenth draft

Document reference: 357463 | A | 0

Information class: Standard

This document is issued for the party which commissioned it and for specific purposes connected with the above-captioned project only. It should not be relied upon by any other party or used for any other purpose.

We accept no responsibility for the consequences of this document being relied upon by any other party, or being used for any other purpose, or containing any error or omission which is due to an error or omission in data supplied to us by other parties.

This document contains confidential information and proprietary intellectual property. It should not be shown to other parties without consent from us and from the party which commissioned it.

Contents

1 Introduction 1

2 Data Collection & Project Site Conditions 2

2.1.1 River Hydraulics and Basin Hydrology 3
2.1.2 Bathymetric and Topographic Data 10
2.1.3 Tidal Elevations 11
2.1.4 Relative Sea Level Rise 11
2.1.5 Winds 18
2.1.6 Waves 21

3 Hydrodynamic Analysis 24

3.1 Hydrodynamic Processes Modeling 24
3.1.1 Model Description 24
3.1.2 Mesh & Bathymetric Surface Development 24
3.1.3 Hydrodynamic Model Setup 26
3.1.4 Sensitivity Testing and Calibration 27
3.1.5 Validation of Calibrated Model 29
3.2 Hydrodynamic Alternatives Analysis 33
3.2.1 Impacts on Relative Sea Level Rise on River Velocity 47
3.3 Storm Surge Analysis 48
3.3.1 Mesh Development & Model Setup 49
3.3.2 Model Calibration & Validation 50
3.3.3 Storm Surge Alternatives Analysis 53

4 Salinity Analysis 57

4.1 Introduction 57
4.2 Data Collection 57
4.3 Model Setup 57
4.4 Results 58
4.5 RSLR Salinity Results 64

5 Sedimentation Analysis 66

5.1 Site Conditions 66
5.1.1 Sediment Sampling 66
5.1.2 Suspended Sediment Concentrations 67
5.1.3 Dredging History 68
5.1.4 Historical Sedimentation Analysis 70
5.1.5 Hurricane Harvey 72

5.2 Sedimentation Modeling 75
5.2.1 Model setup 75
5.2.2 Calibration & Validation 75
5.2.3 Model Sensitivity to Sand Load 79
5.3 Alternatives Analysis 81
5.3.1 Scaling of Sedimentation Rates 89
5.3.2 Impact of Sea Level Rise on Sedimentation Rate 90
5.4 Open San Bernard Mouth Modeling 94
5.4.1 Sedimentation Modeling 94
5.4.2 Water Surface Elevation Analysis 96
5.4.3 Inlet Stability Analysis 99

6 Navigation Analysis 104
6.1 Introduction 104
6.2 Project Site Conditions 104
6.2.1 Existing Closure & Delay Criteria 104
6.2.2 Available Data for Navigation Analysis 104
6.3 Navigation Assessment 104
6.4 Navigation Analysis Methodology 105
6.5 Existing Condition Results 105
6.5.1 Measured Data Delays 105
6.5.2 Modeled Delays 106
6.6 Navigation Hindcasting 113
6.7 Alternatives Analysis 114
6.8 GIWW & Freeport Velocity Analysis 118

7 References 122

Tables

Table 1. Navigation restrictions at the BRFG 3
Table 2. USGS gaging station map legend. 4
Table 3. Long-term daily USGS stations discharge statistics for Brazos River at Rosharon (1903-2015) and San Bernard River at Boling (1954-2015). 4
Table 4. Long-term daily USGS stations discharge extremal analysis by annual maximum for Brazos River at Rosharon (1903-2015) and San Bernard River at Boling (1954-2015). Annual Exceedance Probability (AEP) shown in parenthesis 4
Table 5. GIWW Brazos Crossing Data Stations Summary 7
Table 6. Brazos River and San Bernard River qualitative summary of hydrologic process. 9
Table 7. Tidal Datums at NOAA Station 8772447. 11
Table 8. Summary of storms that have made landfall near the project site. 21
Table 9. Return period of extreme winds. 21
Table 10. General statistics computed for WIS Station 73062 from 1980-2013. 23

Table 11. Percent occurrence of wave height and wave period at WIS station 73062. 23
Table 12. Extreme Values of Wave Heights at WIS 73062. 23
Table 13. Available overlapping data between July 2004 and January 2005 among all USGS stations to be used in calibration and validation. 27
Table 14: High Water Mark Comparison (Modeled vs. Measured) 52
Table 15: High Water Mark Comparison (Modeled vs. Measured) 53
Table 16: Maximum velocity at proposed or existing structures 55
Table 17. Mean salinity (and change for alt-existing) [ppt], October – December 59
Table 18. Mean salinity (and change for alt-existing), June – August. 59
Table 19. Influence of relative sea level rise (RSLR) on seasonal average salinity in each zone of influence for all proposed alternatives. Salinity concentrations in ppt. 65
Table 20. Grab sample sediment class distributions and median grain size. 67
Table 21. Average sedimentation rates from Station 566+000 to Station 615+000 using survey data from 2012 through 2016. Note that cells stating No Data indicate areas where there were no consecutive surveys for the specified time period. 72
Table 22. Calculated sedimentation volumes based on pre- and post-storm surveys. 73
Table 23. Sedimentation model sediment parameters. 75
Table 24. Validation of volumetric sedimentation rates in the West GIWW, Brazos Basin, and East GIWW. 78
Table 25. Model sensitivity simulation to sand load sediment parameters. 80
Table 26. Sedimentation volumes in zones of influence for sensitivity simulations with and without 20% sand load. 80
Table 27. Changes in deposition rates based on sand load. 81
Table 28. Summary of sedimentation volumes in cubic yards for a one year period for each alternative and all zones of influence. 86
Table 29. Summary of sedimentation volume change from existing conditions in cubic yards (and percent) for each alternative and all zones of influence. 86
Table 30. Scale ratio for East GIWW, Brazos Basin and West GIWW for Existing Conditions to account for the difference between sedimentation volume and dredge volume. 90
Table 31. Summary of modeled and scaled annual sedimentation rates in cubic yards 90
Table 32. Summary of sedimentation volumes and percent change from the base condition for all alternatives and RSLR conditions. Percent changes, in parentheses are relative to the base condition for each zone of influence. 91
Table 33. Annualized Sedimentation Rate in West GIWW [Cubic Yards/Year] 95
Table 34. Annualized Sedimentation Rate in San Bernard Gulf Channel [Cubic Yards/Year] 96
Table 35. Annualized Sedimentation Rate in San Bernard Inlet [Cubic Yards/Year] 96
Table 36: Rivers End change in WSE [ft.] from existing (closed) conditions for selected CDF intervals. 98
Table 37: Sanders Road change in WSE [ft.] from existing (closed) conditions for selected CDF intervals. 99
Table 38: Annual Sediment Transport Rates at the Mouth of the San Bernard (from Kraus & Lin, 2002) 101
Table 39: Summary of Ω/M ratios for existing and proposed conditions 102
Table 40. Closure criteria. 104

Table 41. Recorded limited passage delays and closure conditions between March 2015 and April 2016 when the threshold head difference and velocity for limited passage was exceeded. 106
Table 42. Comparison of what causes modeled limited passage conditions. 108
Table 43. Comparison of what causes modeled closures. 108
Table 44. Comparison between modeled and hindcast delay statistics. 114
Table 45. Summary of closure condition causes and total closure % for alternatives. 116
Table 46. Summary of limited passage conditions and % of time under limited passage restrictions for alternatives. 116
Table 47. Summary of limited passage conditions, closure conditions, and total event conditions as a percentage of the model simulation period. 116

Figures

Figure 1. Brazos River Floodgates location map. 2
Figure 2. (left) USGS Gaging Stations used in the hydrodynamic processes analysis near Brazos River Floodgates, and (right) detailed view of USGS gaging stations used in the hydrodynamic processes analysis near Brazos River Floodgates, see Table 2 for legend. 3
Figure 3. Long-term monthly mean streamflow discharge at USGS stations Brazos River near Richmond (upstream in blue), Brazos River near Rosharon (downstream in red) and San Bernard River near Boling. Data is shown in water year from October 1st to September 30th. 5
Figure 4. Streamflow discharge at USGS station Bernard River near Boling and detrended discharge data at USGS station San Bernard River upstream of the GIWW July 2004 to February 2005 (USGS, undated). 6
Figure 5: Station 8117300 gage locations 6
Figure 6. Brazos River long-term monthly mean freshwater inflow hydrology data over the period from 1977 to 2009. Data is shown in water year from October 1st to September 30th (Texas Water Development Board, 2011). 8
Figure 7. San Bernard River long-term monthly mean freshwater inflow hydrology data over the period from 1977 to 2009. Data is shown in water year from October 1st to September 30th (Texas Water Development Board, 2011). 9
Figure 8. Historical storm tracks near the project site. 10
Figure 9. USACE projected RLSR, at NOAA gage 8772440, Freeport TX over 100-Year Period of Analysis (2025 Base Year/2075 End of 50-Year Project Economic Life, 2125 End of Project Planning Horizon). 12
Figure 10. Project inundation map for mean sea level in the year 2125 under the high sea level rise scenario. 12
Figure 11. Annual peak discharges on the Brazos River near Rosharon, TX. 13
Figure 12. Annual peak discharges on the San Bernard River near Boling, TX. 13
Figure 13. Annual peak instantaneous flow trends at the Brazos River near Rosharon, TX pulled from USACE Climate Hydrology Assessment Tool. 14
Figure 14. Projected changes in seasonal precipitation, 2085 vs. 1985 mm (from USACE, 2015). Texas region circled with red oval. 15

Figure 15. Watershed vulnerability for the Brazos River watershed (HUC 1207) from the USACE watershed vulnerability tool. 16
Figure 16. Trends in mean modeled annual maximum streamflow. The mean (blue line) is the average of 93 Climate-Change Hydrology Models of HUC 1207 17
Figure 17. WIS hindcast data stations near Brazos River Floodgates. 18
Figure 18. Wind Rose at WIS 73062 for overall (top), summer (left) and winter (right) months. 20
Figure 19. Wave Rose as WIS 73062 for overall (top), summer (left) and winter (right) months. 22
Figure 20. Brazos River Floodgates ADH circulation model mesh. 25
Figure 21. Bathymetry correction between the BRFG and the Gulf of Mexico. 26
Figure 22. Time series of water surface elevation showing the model sensitivity to friction coefficient (top), river flow rate (mid-top), gate operations (mid-bottom) and the combined effect of gate operations and an open San Bernard River inlet (bottom). 29
Figure 23: River discharges during the model validation period. 30
Figure 24: Time series comparison of water surface elevation at the Freeport Gage (top) and the river side of the West Gate (middle) and of velocity at the Brazos River Gage (bottom) 31
Figure 25: (top) measured vs. modeled water surface elevation at every gage in the domain and for every time step in the model period. (Middle) measured vs. modeled water surface elevation at the east and west river gages for every time step in the model period. (Bottom) measured vs. modeled water surface elevation at the east and west lock gages for every time step in the model period. Color bar indicates point density calculated as the number of points within a 0.25 ft. radius of the point specified. 32
Figure 26. Project zones of influence. 33
Figure 27. Model mesh resolution and bathymetry for all proposed TSP alternatives 34
Figure 28. Existing conditions model alignment and bathymetry. 35
Figure 29. Existing Conditions peak ebb velocity (top) and flood velocity (bottom) at the Brazos River - GIWW intersection. 35
Figure 30. Alternative 3a model alignment and bathymetry. 36
Figure 31. Alternative 3a peak ebb velocity (top) and flood velocity (bottom) at the Brazos River - GIWW intersection. 37
Figure 32. Alternative 3a.1 model alignment and bathymetry. 37
Figure 33. Alternative 3a.1 peak ebb velocity (top) and flood velocity (bottom) at the Brazos River - GIWW intersection. 38
Figure 34. Alternative 9a model alignment and bathymetry. 39
Figure 35. Alternative 9a peak ebb velocity (top) and flood velocity (bottom) at the Brazos River - GIWW intersection. 39
Figure 36. Alternative 9b model alignment and bathymetry. 40
Figure 37. Alternative 9b peak ebb velocity (top) and flood velocity (bottom) at the Brazos River - GIWW intersection. 41
Figure 38. Alternative 9c model alignment and bathymetry. 42
Figure 39. Alternative 9c peak ebb velocity (top) and flood velocity (bottom) at the Brazos River - GIWW intersection. 42
Figure 40. Probability of water level non-exceedance in West GIWW for Alternative 3a. 43

Figure 41. Probability of water level non-exceedance in West GIWW for Alternative 3a.1. 44
Figure 42. Probability of water level non-exceedance in West GIWW for Alternative 9a. 44
Figure 43. Probability of water level non-exceedance in West GIWW for Alternatives 9b and 9c (negligible difference). 45
Figure 44. Probability of Non-Exceedance (PNE) for WSE [ft. MSL] at Rivers End. 46
Figure 45. Probability of Non-Exceedance (PNE) for WSE [ft. MSL] at Sanders Rd. 46
Figure 46. PNE of velocities extracted just north of the Brazos River Crossing for Existing Conditions/2a (top left) and all proposed alternatives for existing conditions, +1.0 ft. RSLR and +2.0 ft. RSLR. 48
Figure 47. Full mesh domain. 49
Figure 48: Resolution of Mesh at Project Site (approximately 65 m or 213 ft) 50
Figure 49. Maximum modeled water surface elevation from Hurricane Claudette (ft MSL) 51
Figure 50: Maximum Water Surface Elevation (ft MSL) for design storm. 54
Figure 51: Maximum velocity [ft/sec] at the Brazos River from Storm surge runs. 55
Figure 52: Increase in Water Surface Elevation [ft] from Existing conditions. 56
Figure 53. Initial salinity concentration in the model domain. 58
Figure 54. Validation of Salinity at USGS gage 08117300 (top) and flow rates in the Brazos and San Bernard Rivers (bottom). 58
Figure 55. Change in mean salinity for summer and late-fall between Existing Conditions and Alternative 3a. 60
Figure 56. Change in mean salinity for summer and late-fall between Existing Conditions and Alternative 3a.1. 61
Figure 57. Change in mean salinity for summer and late-fall between Existing Conditions and Alternative 9a. 62
Figure 58. Change in mean salinity for summer and late-fall between Existing Conditions and Alternative 9b. 63
Figure 59. Change in mean salinity for summer and late-fall between Existing Conditions and Alternative 9c. 64
Figure 60. Locations of sediment grab samples. 66
Figure 61. Grab sample sediment class distributions. 67
Figure 62. Sediment load curve at Brazos River, Rosharon gage based on measured data. 95% confidence intervals shown as dotted lines. 68
Figure 63. Sediment load curve at San Bernard Boling gage based on measured data. 95% confidence intervals shown as dotted lines. 68
Figure 64. Station numbers along the GIWW channel alignment; survey and dredging data was investigated for the reach of channel extending from Station 566+000 to Station 615+000. 69
Figure 65. Summary of surveys and dredging activities from 2012 through 2016 along the reach of the GIWW channel from Station 566+000 to Station 615+000. Blue indicates surveys documenting existing conditions (EX); red indicates surveys documenting post-dredging conditions (AD); and green indicates surveys documenting pre-dredging conditions (BD). 70
Figure 66. Sedimentation rates within the GIWW from Station 566+000 to Station 615+000 based on surveys from 2012 to 2016. 71
Figure 67. Sedimentation pattern in the W-GIWW due to Hurricane Harvey. 73

Figure 68. Sedimentation pattern in the Brazos Basin due to Hurricane Harvey. 74
Figure 69. Sedimentation pattern in the E-GIWW due to Hurricane Harvey. 74
Figure 70. Comparison of measured (top) and modeled (bottom) sedimentation rates in the West GIWW. 76
Figure 71. Comparison of measured (top) and modeled (bottom) sedimentation rates in the Brazos Basin. 77
Figure 72. Comparison of measured (top) and modeled (bottom) sedimentation rates in the East GIWW. 77
Figure 73. Channel centerline for comparison of modeled vs. measured sedimentation depth between the Freeport Harbor and the San Bernard River. 79
Figure 74. Comparison of measured vs. modeled sedimentation depth along the GIWW channel centerline between the Freeport Harbor and the San Bernard River. 79
Figure 75. Sediment load vs river discharge for existing conditions and Alt 3a. 81
Figure 76. Sedimentation rate vs river discharge for existing conditions and Alt 3a. 82
Figure 77. Sediment load vs river discharge for existing conditions and Alt 3a.1. 82
Figure 78. Sedimentation rate vs river discharge for existing conditions and Alt 3a.1. 82
Figure 79. Sediment load vs river discharge for existing conditions and Alt 9a. 83
Figure 80. Sedimentation rate vs river discharge for existing conditions and Alt 9a. 83
Figure 81. Sediment load vs river discharge for existing conditions and Alt 9b. 84
Figure 82. Sedimentation rate vs river discharge for existing conditions and Alt 9b. 84
Figure 83. Sediment load vs river discharge for existing conditions and Alt 9c. 84
Figure 84. Sedimentation rate vs river discharge for existing conditions and Alt 9c. 85
Figure 85. Sedimentation pattern zones master figure. 87
Figure 86. Sedimentation pattern at the Brazos River - GIWW intersection for all alternatives. 88
Figure 87. Sedimentation pattern in the West GIWW for all alternatives. 88
Figure 88. Sedimentation pattern in the East GIWW for all alternatives. 89
Figure 89. Sedimentation pattern in the Freeport Harbor and channel. 89
Figure 90. Sedimentation volume in the West GIWW for all alternatives and sea-level conditions. 92
Figure 91. Sedimentation volume in the Brazos Basin for all alternatives and sea-level conditions. 92
Figure 92. Sedimentation volume in the East GIWW for all alternatives and sea-level conditions. 93
Figure 93. Sedimentation volume in the Freeport Harbor for all alternatives and sea-level conditions. 93
Figure 94. Bathymetry for open San Bernard condition 94
Figure 95. Locations of the West GIWW, San Bernard Gulf Channel, and San Bernard Inlet zones of impact. 95
Figure 96. Probability of Non-Exceedance at Sanders Road for open/closed conditions. 97
Figure 97. Probability of Non-Exceedance at Rivers End for open/closed conditions. 98
Figure 98. Extraction Arc Used for Inlet Stability Analysis 100
Figure 99. Box and whisker plot showing the range of inlet stability 102

Figure 100. Existing condition model bathymetry and extraction points for navigation analysis. 107
Figure 101. Filtering results for west river extraction point (top), west lock extraction point (middle), and the water surface elevation difference (west river – west lock) between the two gages (bottom). 108
Figure 102. Comparison of recorded and modeled close and limited passage events. 109
Figure 103. Modeled head differential (River – GIWW) at west gate (top), east gate (middle), and modeled river velocity. Grey shaded areas represent recorded limited passage conditions, while black shaded areas represent recorded periods of closure. 110
Figure 104. Relationship between modeled gate closure conditions and flow rate in the Brazos River (top), flow rate in the San Bernard River (middle), and the combined flows in both rivers (bottom). 111
Figure 105. Relationship between modeled limited passage conditions and flow rate in the Brazos River (top), flow rate in the San Bernard River (middle), and the combined flows in both rivers (bottom). 112
Figure 106. Existing condition hindcast training results. 114
Figure 107. Alternatives modeled and extraction points for navigation analysis. 115
Figure 108. Probability of Non-Exceedance for head differential at west gate (top) and east gate (bottom). 117
Figure 109. Probability of Non-Exceedance of velocity at gate locations (Existing/2a, 3a, 3a.1 east, 9b, 9c), and open GIWW (3a.1 west, 9a). 118
Figure 110. Spatial distribution of the 25th, 50th, and 95th percentiles of river velocity along the west GIWW for existing conditions (grey) and the TSP (red). 119
Figure 111. Spatial Distribution of the 25th, 50th, and 95th percentiles of river velocity along the Freeport Channel for existing conditions (grey) and the TSP (red). 120
Figure 112. CDF curve for selected extraction points along Freeport Channel comparing velocity for existing conditions (black) and alt. 3a.1 (red). 121

1 Introduction

This report describes the hydraulic modeling and analysis conducted at the Brazos River Floodgates to support the US Army Corps of Engineers Feasibility Study. Hydraulic modeling was conducted for existing conditions to simulate the system hydraulics, salinity, and sedimentation. The models were calibrated to available measured data. These models were then used to simulate hydraulics, salinity, and sedimentation for the proposed Alternatives 2a, 3a, 9a, and 9c. Alternative 2a involves major rehabilitation of the existing floodgates. Alternative 3a involves setting the floodgates farther back along the existing alignment and widening the chamber wall opening to 125 feet. Alternative 9a involves an open channel north of the existing alignment. Alternative 9b involves construction of 125-foot-wide floodgates along the same alignment as 9a and closing off the existing alignment. Finally, Alternative 9c involves construction of 125-foot-wide floodgates with a flow control sluice gate constructed at the existing west gate. Note that Alternative 2a involves major rehabilitation of existing gate structures, but is assumed to not change the guide wall orientation, gate operations, or bathymetry and therefore the hydraulics and resulting salinity and sedimentation are assumed to be identical to existing conditions. Throughout this document, results for Alternative 2a will not be presented separately but will instead be considered the same as exiting conditions results.

The hydraulic modeling was also used to understand changes to the navigation of the system and evaluated the changes to the navigation restrictions and closures due do to system hydraulics.

2 Data Collection & Project Site Conditions

The Brazos River Floodgates are located at the intersection of the Gulf Intracoastal Waterway (GIWW) and the Brazos River in Brazoria County, TX (Figure 1). The drainage area of the Brazos River is approximately 45,560 sq. mi. The Brazos River is the only significant source of sediment for the central Texas coast. In 1929, the Brazos River was diverted 8 miles south of its mouth at Freeport by the Galveston District to reduce flooding and shoaling in the Port of Freeport (USACE, 2002). The intent for the relocation was for the Brazos River Diversion Channel (BRDC) to divert the sediment load of the Brazos River from the Freeport Ship Channel. The GIWW crosses the BRDC 7,000 ft. upstream from its mouth. Tidal and fluvial flows into the GIWW are controlled by the Brazos River Floodgates constructed and controlled by the Corps of Engineers in 1943 (USACE, 1988).

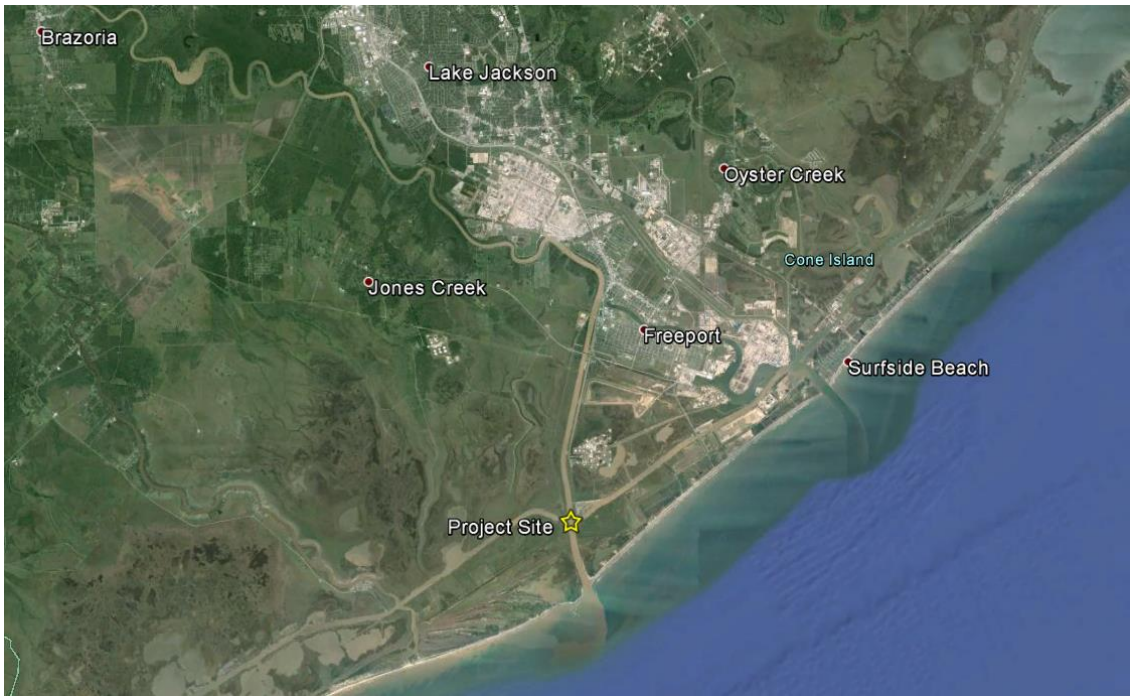

Figure 1. Brazos River Floodgates location map.

The floodgates serve to control flood flows from the Brazos River to the GIWW, improve navigation safety by controlling traffic flow and currents at the intersection of the Brazos River's connection with the GIWW and to control sand and silt deposition from the Brazos River into the GIWW. The total commercial tonnage traversing the Brazos River Floodgates is 45 million tons with an estimated value of $4.5 billion in cargo per year. When the floodgates were built in 1943, barges were typically 26 ft. to 35 ft. wide. The floodgate chamber is 75 ft. wide, and the maximum width of the barge it can accommodate is 55 ft. Today, it is common for towboat operators to push two 35-ft dry cargo barges side by side, for a total width of 70 ft. A typical tank barge measures 54 ft. across, so tank barges must transit singly. The necessity to break the tow to pass individual barges through the Floodgates causes time delays (George, 2016).

Frequent accidents occur when tows strike the facilities while trying to line up to enter the floodgates after crossing the Brazos River. The floodgates are only approximately 600 ft. from the river. When crossing the river, towboat operators do not have enough time to recover their

course after struggling with the river currents. As a result, an average of 36 accidents occurs per year, causing damages worth approximately $800,000 annually to the facility and to the barges (TXDOT, 2015). When these accidents involve tank barges, there is also a risk for hazardous material spills. Navigation traffic delay costs are estimated to exceed $10 million annually (TXDOT, 2015).

Due to the navigation hazards at the BRFG, navigation restrictions have been included in the Code of Federal Regulations (33 CFR 207.187). The restrictions are summarized in Table 1.

Table 1. Navigation restrictions at the BRFG

Restriction	Velocity [ft/s]	Head Difference [ft]
Unlimited passage	< 2.0	< 0.7
Limited passage	2.0 – 5.0	0.7 – 1.8
Gate closure	> 5.0	> 1.8

2.1.1 River Hydraulics and Basin Hydrology

Hydrology and hydraulic data such as rainfall-runoff and river discharge are required for hydraulic engineering analysis as well as numerical modeling of existing conditions and any proposed alternatives of Brazos River Floodgates. Historical rainfall and river discharge data are used to derive river statistics, namely for design and navigation purposes. Simultaneous discharge measurements at different locations within the Brazos River, GIWW, and San Bernard River network are used develop an understanding of the local hydraulics and to calibrate numerical hydrodynamic models.

2.1.1.1 River Hydraulics

Publicly available data from USGS stream gaging stations are available. The available existing hydraulic data for the Brazos River and San Bernard River have been acquired and analyzed. USGS gages are shown on Figure 2 and Table 2 (USGS, 2015) (Jeffery, 2015).

Figure 2. (left) USGS Gaging Stations used in the hydrodynamic processes analysis near Brazos River Floodgates, and (right) detailed view of USGS gaging stations used in the hydrodynamic processes analysis near Brazos River Floodgates, see Table 2 for legend.

Table 2. USGS gaging station map legend.

USGS gage ID	Gage location
08114000	Brazos River at Richmond, TX
08116650	Brazos River at Rosharon, TX
08117300	Brazos River at GIWW Flood Gates near Freeport, TX
08117290	Brazos River at Freeport, TX
08117500	San Bernard River near Boling, TX
08117730	San Bernard River Upstream of GIWW near Freeport, TX
08117740	San Bernard River Downstream of GIWW near Freeport, TX
285217095263001	GIWW East of the San Bernard River, near Freeport, TX

Various statistical parameters were computed for Brazos River and San Bernard River from the available daily mean discharge as a way of summarizing the large dataset. Table 3 provides the long-term daily discharge statistics for Brazos River at Rosharon and San Bernard River at Boling (see Figure 2). It is evident Brazos River discharge is an order of magnitude larger than San Bernard River which is associated with the size of the catchment, 43,339 sq mi and 727 sq mi, respectively. Extreme value statistics on long-term daily discharge data from Brazos River at Rosharon and San Bernard River at Boling were also performed and are shown on Table 3.

Table 3. Long-term daily USGS stations discharge statistics for Brazos River at Rosharon (1903-2015) and San Bernard River at Boling (1954-2015).

Discharge	Brazos River at Rosharon Q [cfs]	San Bernard River at Boling Q [cfs]
Contributing drainage area	45,339 sq mi	727 sq mi
Maximum	123,000	31,300
Minimum	35	0.4
Mean	7,392	519
Standard deviation	11,846	1,389

Table 4. Long-term daily USGS stations discharge extremal analysis by annual maximum for Brazos River at Rosharon (1903-2015) and San Bernard River at Boling (1954-2015). Annual Exceedance Probability (AEP) shown in parenthesis

Return Period [yrs] (AEP Value)	Brazos River at Rosharon Q [cfs]	San Bernard River at Boling Q [cfs]
1 (1.0)	56,997	5,971
2 (0.5)	64,887	9,057
5 (0.2)	72,988	13,536
10 (0.1)	78,207	17,108
20 (0.05)	82,927	20,798
25 (0.04)	84,363	22,006
50 (0.02)	88,615	25,818
75 (0.013)	90,974	28,084
100 (0.010)	92,599	29,707
250 (0.004)	97,537	34,949
500 (0.002)	101,067	38,984

Figure 3 provides the long-term monthly mean discharge at Brazos River Richmond gage (upstream) for the period 1940-2016, Brazos River Rosharon gage (downstream) for the period 1967-2016 and San Bernard River at Boling for the period 1954-2016. Brazos River at Richmond monthly discharge distribution is seemingly unimodal having one evident monthly peak discharge in May. The unimodal quality fades downstream at Rosharon since two local

maximum discharge are observed in the moths of March and June as opposed to a single maximum in May.

The comparison of these data shows that over the entire period of record, the monthly mean peak discharge attenuates in the downstream direction. The maximum monthly mean discharge drops from 14,200 cfs to 12,400 cfs in May. Such attenuation is expected in the lower sections of the Brazos River, “as elevated flows enter storage in the low elevation terrain and are released over longer time periods” (USGS, undated). Conversely the lower flows seen during November, December, January, February, March, April, June, July, April, and September increase in the downstream reach.

Differences are observed when comparing the Brazos (at Rosharon) and San Bernard (at Boling) monthly mean discharges. As shown on Figure 3, the San Bernard River at Boling distribution is multimodal having three local maximum discharges – October, February, and June. Opposite behaviors are observed in October and March when the high flows on San Bernard match the low flows of Brazos and vice versa. In June, however, the highest monthly average discharge occurs for both the San Bernard and Brazos River.

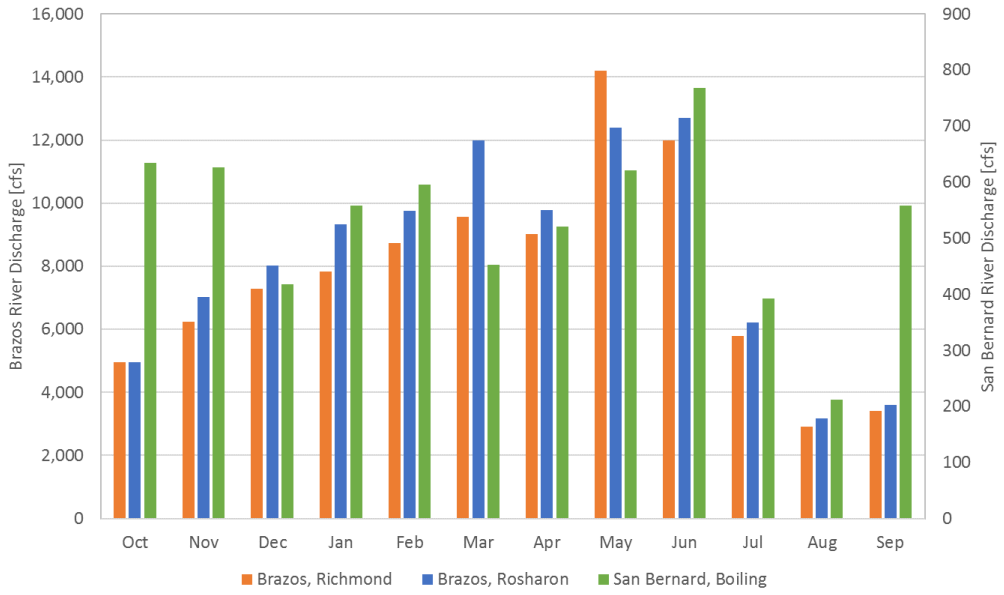

Figure 3. Long-term monthly mean streamflow discharge at USGS stations Brazos River near Richmond (upstream in blue), Brazos River near Rosharon (downstream in red) and San Bernard River near Boling. Data is shown in water year from October 1st to September 30th.

As shown in Figure 4, attenuation is also present in the San Bernard River. Peak flows in the San Bernard River are attenuated from the USGS Boling station to the intersection with the GIWW in the lower sections of River due to elevated flows storage (USGS, undated), which is similar to the trend observed for Brazos River. The high flows at San Bernard in October are associated with local precipitation events that do not reach the headwaters of Brazos River; such high precipitation-discharge events are related to the hurricane/storm season in the Gulf Coast.

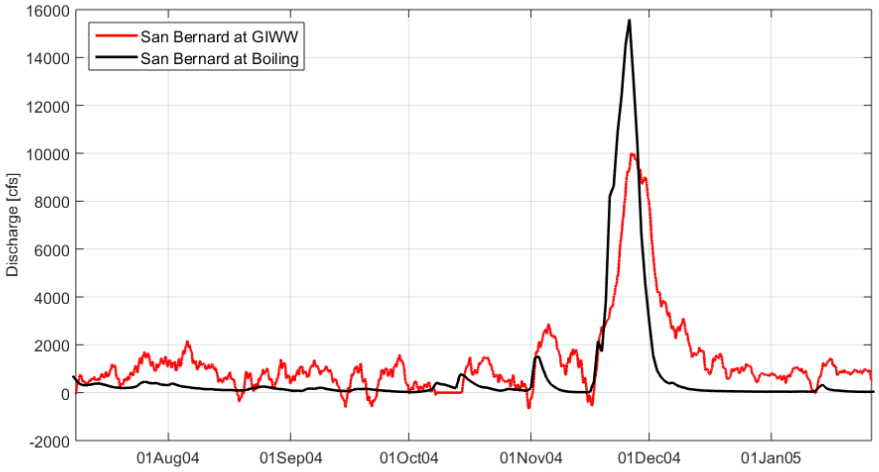

Figure 4. Streamflow discharge at USGS station Bernard River near Boling and detrended discharge data at USGS station San Bernard River upstream of the GIWW July 2004 to February 2005 (USGS, undated).

According to an undated USGS report on the discharge at the intersection of the San Bernard River and the GIWW, the magnitude of discharge in the San Bernard River downstream of the GIWW intersection is much less than flow upstream of the GIWW and the vast majority of water flowing in the San Bernard River immediately upstream of the GIWW intersection (08117730 on Figure 2) flows east into the GIWW (285217095263001 on Figure 2) (USGS, undated).

Several data measurements are available near the GIWW crossing of the Brazos River. USGS station 08117300 is located at the project site and consists of water level gages on either side of both the East and West Gates (4 total). Station 08117300 also includes velocity gages on the river side of both the East and West Gates as well as one velocity gage in the Brazos River approximately 400 feet upstream of the GIWW. The USGS gage locations are shown in Figure 5 and a summary of available data is shown in Table 5.

Figure 5: Station 8117300 gage locations

These gages have recorded historical hourly stage and velocity since 2008. Starting in 2014, these gages recorded stage and velocity at 15-minute intervals. A summary of the available data at the gauges shown is described in Table 5 (USGS, 2017). The gages adjacent to the

gates (East Lock, East River, West Lock, West River) are strongly influenced by the opening and closings which cause large, rapid fluctuations in the stage and velocity.

The sampling intervals of the measured gage data (hourly before 2014, 15 mins after 2014) are such that these opening/closing events, which take between 2 and 5 minutes, cannot be captured and fully resolved. This relatively coarse sampling interval long with the very close location of the gages to the gates result in very noisy data with little apparent discernable meaningful signal. It is difficult to interpret head differentials at the gates using the gage data.

The Brazos River velocity gage provides a good record of the river velocity. However, the gage is located close to the river bank and does not capture the representative velocities in the River. The Lockmaster stated they do not base decisions to restrict navigation based on measurements from this gage because of this fact (George, 2016).

Table 5. GIWW Brazos Crossing Data Stations Summary

Data Station	Data Available	Recording Period	Sampling Interval
USGS 08117300 - East Lock	Stage	1/1/2008 - 9/30/2011, 2/1/2014 - Present	Hourly (Velocity, Stage until 9/30/2011), 15-minute (Stage starting 2/1/14)
USGS 08117300 - East River	Velocity, Stage	1/1/2008 - 9/30/2011, 2/1/2014 - Present	Hourly (Velocity, Stage until 9/30/2011), 15-minute (Stage starting 2/1/14
USGS 08117300 - West Lock	Stage	1/1/2008 - 9/30/2011, 2/1/2014 - Present	Hourly (Velocity, Stage until 9/30/2011), 15-minute (Stage starting 2/1/14
USGS 08117300 - West River	Velocity, Stage	1/1/2008 - 9/30/2011, 2/1/2014 - Present	Hourly (Velocity, Stage until 9/30/2011), 15-minute (Stage starting 2/1/14
USGS 08117300 – Brazos River Upstream	Velocity	1/1/2008 - 9/30/2011, 2/1/2014 - Present	Hourly Velocity until 9/30/2011 15-minute (Stage starting 2/1/14

2.1.1.2 Basin Hydrology

Existing hydrology data in the project vicinity were compiled. The following hydrology data corresponds to the hydrology studies completed by the Texas Water Development Board for Brazos River (Figure 6) and San Bernard River (Figure 7) (Texas Water Development Board, 2011):

- Brazos River Estuary Hydrology Study; covers period from 1977 to 2009
- San Bernard River Estuary Hydrology Study; covers period from 1977 to 2009

Hydrology analysis results provide a volumetric runoff balance in acre-ft. which includes the following contributions:

$$Balance = gaged + modeled - diversion + return - evaporation + precipitation$$

Note that there is no gaged data at the coastal sub-watershed (near the mouth of the river). Therefore, a rainfall-runoff hydrology model is needed. The modeled runoff from the local coastal sub-watershed is added to the upstream gaged data to get a total runoff discharge into the GIWW. Where gaged flows are obtained from USGS gages, modeled are rainfall-runoff values estimated using the Texas Rainfall-Runoff Model (TxRR) model, diversions and returns are flows associated with water rights and holders of discharge permits, and evaporation and precipitation include at contribution from each process on the bay surface area exclusively (Texas Water Development Board, 2011). Note that the TxRR model results were obtained from the Texas Water Development Board. The TxRR model is conceptually similar to the

Agricultural Research Service which is based on the Soil Conservation Service curve number method.

Figure 6 shows over the study period, gaged inflow from the USGS station at Brazos River near Rosharon accounted for approximately 86 percent of combined inflow, while modeled flows (rainfall-runoff) accounted for almost 3 percent of the balance. Hence, the river discharge at the Brazos River Floodgates is significantly dominated by upstream riverine processes rather than precipitation-induced discharges in the coastal plain. Therefore, precipitation processes can be ignored in the analysis. Such behavior is expected due large drainage area. It is possible that heavy local rainfall between the Rosharon gage and the GIWW-Brazos River intersection could influence hydrodynamics at the project site. However long-term trends (as shown in Figure 6) indicate that is an infrequent event, which would likely not alter the long-term hydrodynamics that govern sediment deposition and river flows at the project site.

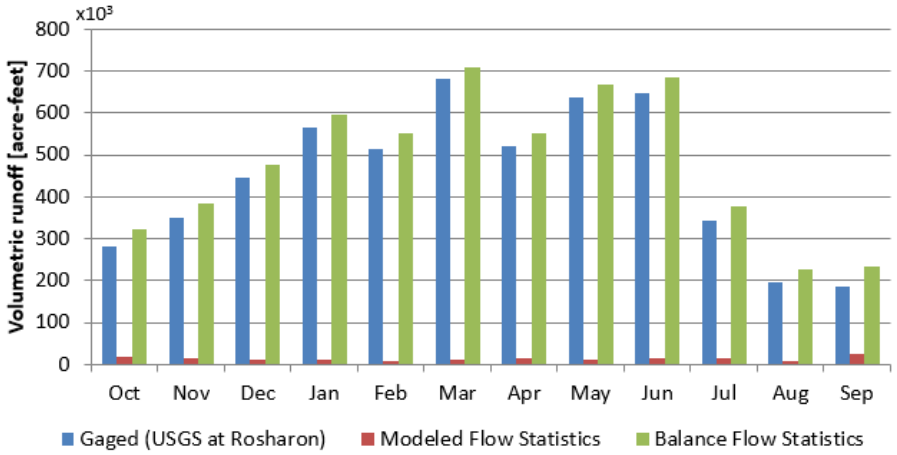

Figure 6. Brazos River long-term monthly mean freshwater inflow hydrology data over the period from 1977 to 2009. Data is shown in water year from October 1st to September 30th (Texas Water Development Board, 2011).

Conversely, Figure 7 shows that over the study period gaged inflows from the USGS gage station at San Bernard River near Boling accounted for approximately 64 percent of the combined inflows, while ungaged flows (modeled rainfall-runoff) accounted for approximately 40 percent of the balance (balance= gaged + modeled - diversion + return - evaporation + precipitation). Therefore, the San Bernard river discharge at the intersection with the GIWW is heavily influenced by precipitation-induced discharge in addition to upstream riverine processes. The rainfall-runoff for San Bernard River (Figure 7) overall trend agrees with the trend overserved at the Boling station, where high flows are observed in September/October and June.

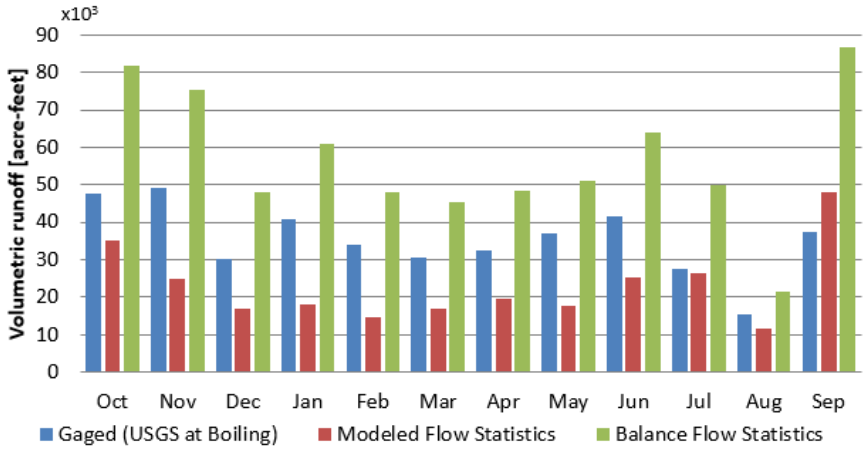

Figure 7. San Bernard River long-term monthly mean freshwater inflow hydrology data over the period from 1977 to 2009. Data is shown in water year from October 1st to September 30th (Texas Water Development Board, 2011).

Table 6 presents a qualitative summary of the data analysis of hydrologic process in Brazos and San Bernard Rivers.

Table 6. Brazos River and San Bernard River qualitative summary of hydrologic process.

River	High Discharge	Driving Mechanism	Peak Attenuation
Brazos (at Rosharon)	March June	Headwater processes	From Richmond to Rosharon Flood plain storage
San Bernard (at Boling)	October February June	Headwater processes Local rainfall-runoff	From Boling to GIWW Flood plain storage

2.1.1.3 Storm Surge

Historical recorded storms are necessary for calibrating and validating the storm surge model. The FEMA Flood Insurance Study (FIS) for Texas Coastal Counties (FEMA, 1999) was referenced to determine the best storms to use for validation.

Since the FEMA FIS analyzed the entire Texas coast, the selected storms for validation spanned across the Gulf Coast. The storms were Carla (1961), Claudette (2003), Rita (2005), and Ike (2008) as potential validation storms due to their intensity and proximity to the project site. The storm tracks for these storms are shown in Figure 8. The FIS study noted that the two most recent storms (Rita and Ike) had the most accurate and comprehensive measurements for wind, atmospheric pressure, waves and surge levels. Due to the storm track's proximity to the project site and data available, Hurricane Claudette was selected as the storm to be used for calibration and Carla was used to validate the model.

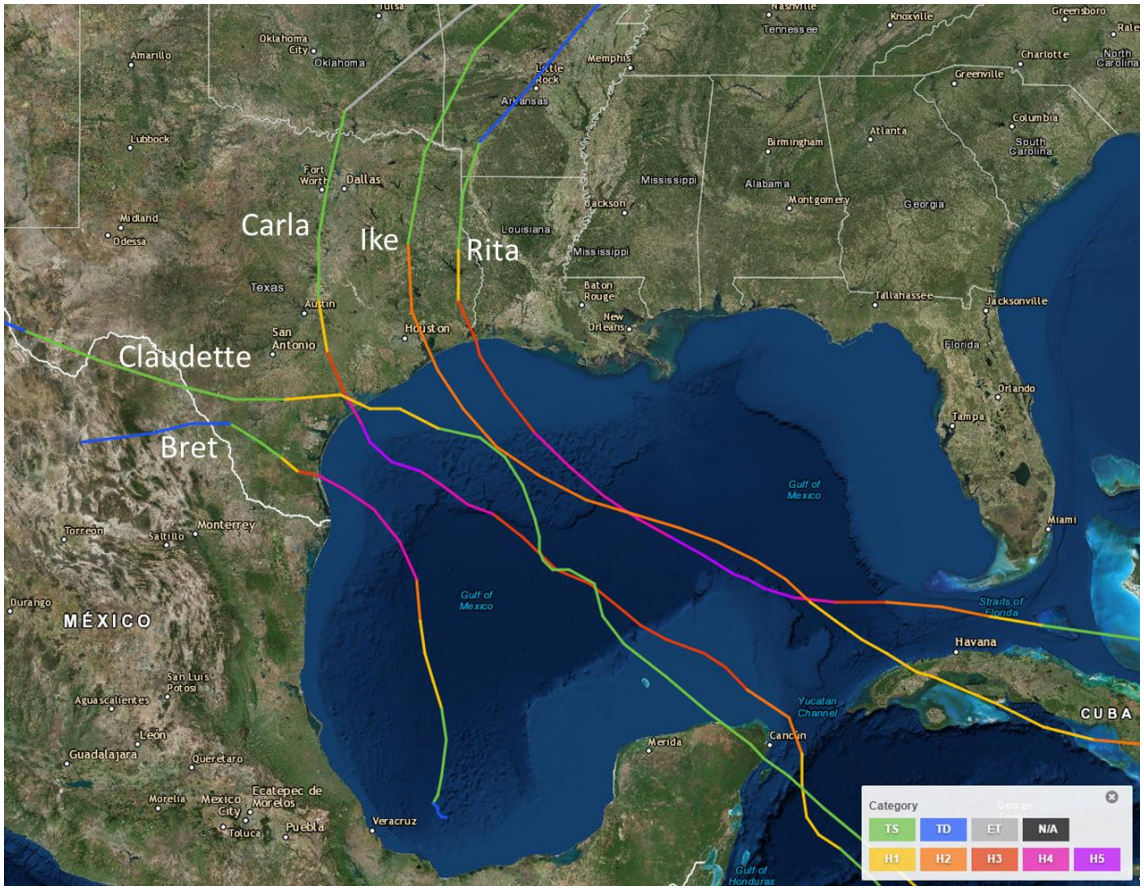

Figure 8. Historical storm tracks near the project site.

To calibrate and validate the model and ensure the model is producing realistic results, the water surface elevation output from the model will need to be compared to measured high water marks. Therefore, for the calibration model run, the surveyed high-water marks for Hurricane Claudette would be necessary to ensure the inundation on the model matches historical storm surge.

The National Hurricane Center compiles reports on each named Tropical Cyclone. These reports include high water marks from both gages impacted by the cyclone and surveyed high water marks taken after the storm impacts an area. The points where the high-water marks were listed in the Hurricane Claudette report (Beven, 2003) are included as observation nodes within the ADCIRC+SWAN model to extract the water surface elevation time series at these locations. If the maximum modeled water surface elevation matches the surveyed high-water mark within the stated error (1 ft, on average), the model can be termed calibrated and will be used for the validation run.

Further discussion of storm surge model development is conducted in Section 3.3.

2.1.2 Bathymetric and Topographic Data

Available bathymetric and topographic data sets were used to build the bathymetric surface to be used for wave and current modeling described in later Sections. Multibeam bathymetric surveys of the Brazos Locks and Basin from 2012 – 2016 were collected. Single beam surveys of the GIWW approximately twice a year from 2012 – 2016 between Freeport and the San Bernard River were collected. Transects of the single beam surveys are spaced at

approximately 200 ft. In addition to survey data, this analysis includes data from the Coastal Relief Model, and EC2012 ADCIRC Tidal Database Mesh. The bathymetry sets used to create the modeling surface are further described in Section 3.1.

2.1.3 Tidal Elevations

Tidal elevations at the project site were extracted from NOAA Station 8772447 in Freeport, TX approximately 6 miles northeast of the project site. The tidal elevations used for this study are shown below in Table 7. Tide levels relative to NAVD88 were found using VDatum (Parker et al. 2003).

Table 7. Tidal Datums at NOAA Station 8772447.

Tide Level	Description	MLLW (Epoch 1983-2001) [ft.]
MHHW	Mean Higher-High Water	1.80
MSL	Mean Sea Level	0.97
MLLW	Mean Lower-Low Water	0.00
NAVD88	North-American Vertical Datum, 1988	-0.04

2.1.4 Relative Sea Level Rise

The Brazos River Floodgates are located in the coastal zone. The existing system as well as any proposed alternatives have the potential to be affected by relative sea level rise. Therefore, it is important to document the robustness of the project alternative selections to climate change, and how the hydraulics and hydrology analysis will change with the changing climate.

The project start date is assumed to be 2025. Since the project life was assumed to be 50 years, the future extent of sea level change was determined using the USACE climate change website http://corpsmapu.usace.army.mil/rccinfo/slc/slcc_calc.html. Data was obtained using the web tool from the closest available gage which was 8772440 at Freeport which is located approximately 6 miles from the project site. The data was extracted 100 years from the project start date of 2025, to show the extent of sea level change beyond the project life of 50 years. Figure 9 shows the resulting relative sea level change over the project life (until 2075) and 100 years from the project start date (2125). Figure 10 displays the resulting inundation from the USACE high sea level change scenario in 2125, which is 100 years from project start.

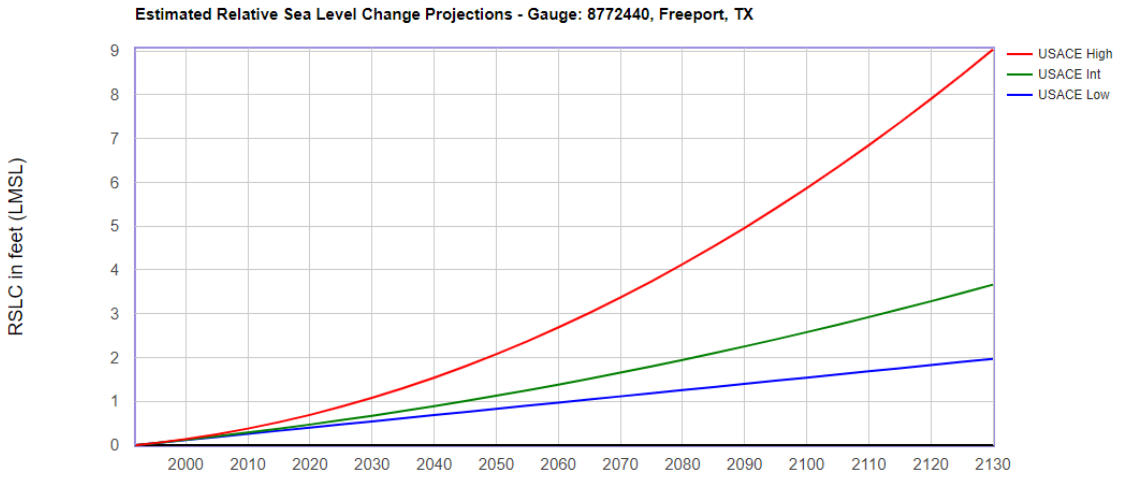

Figure 9. USACE projected RLSR, at NOAA gage 8772440, Freeport TX over 100-Year Period of Analysis (2025 Base Year/2075 End of 50-Year Project Economic Life, 2125 End of Project Planning Horizon).

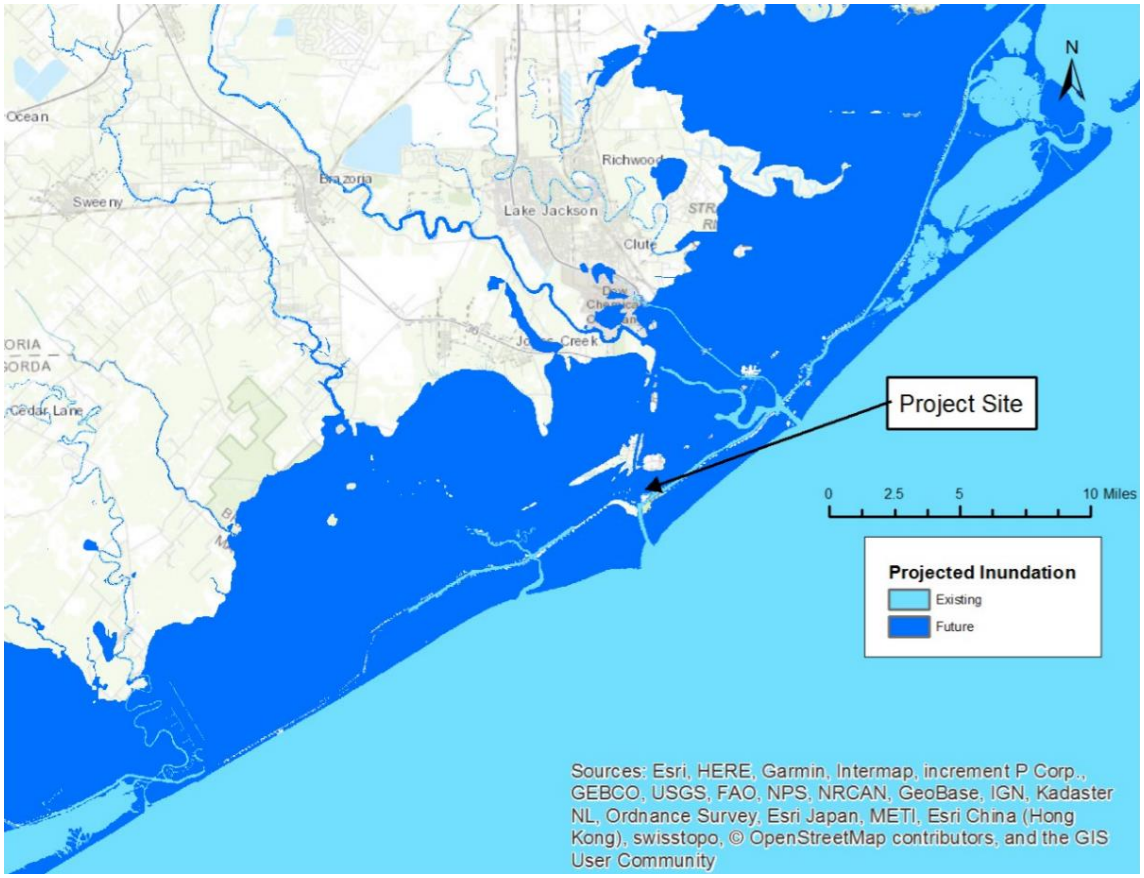

Figure 10. Project inundation map for mean sea level in the year 2125 under the high sea level rise scenario.

2.1.4.1 Analysis of Flow Gage Data Trends

To evaluate the long-term trends of climate change on river discharge, a trend analysis was conducted on the annual peak discharges at the Rosharon, Texas USGS gage for the Brazos River and at the Boling, Texas USGS gage for the San Bernard River. A trendline was fit to the annual peak discharges at each site. Figures showing the peak annual discharges, along with linear trendlines are shown below in Figure 11 and Figure 12 for the Brazos and San Bernard Rivers, respectively.

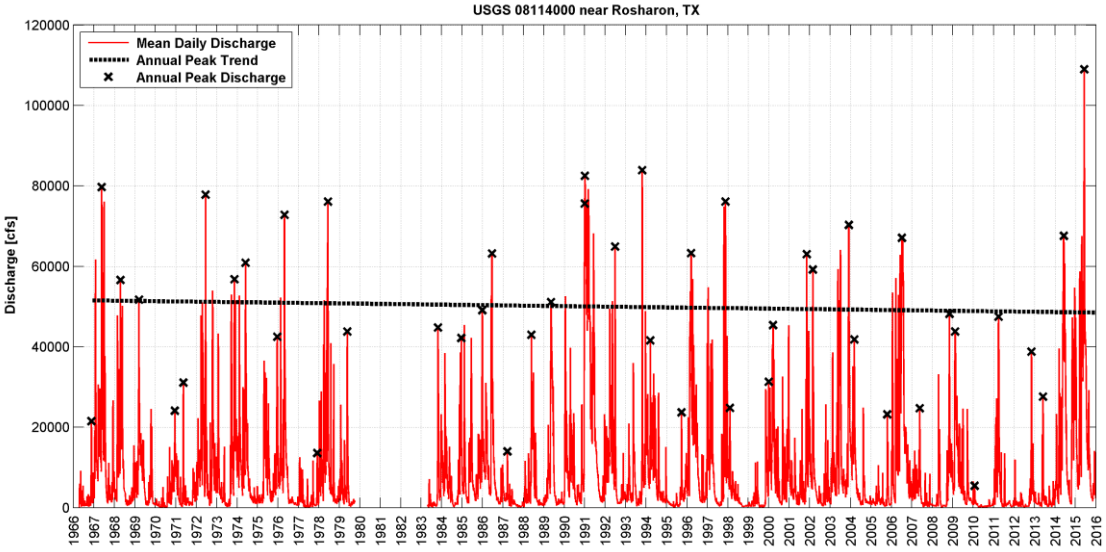

Figure 11. Annual peak discharges on the Brazos River near Rosharon, TX.

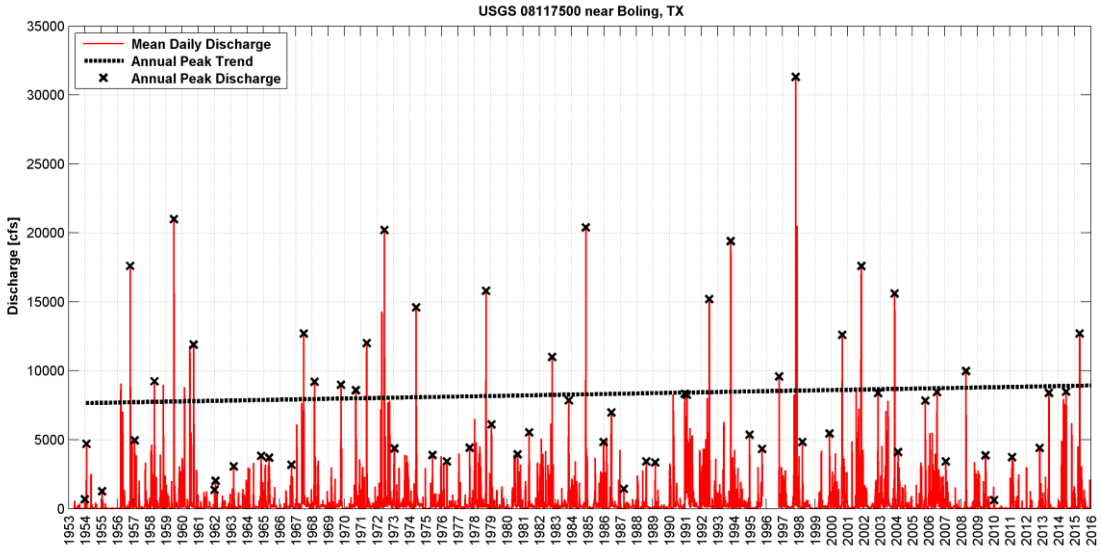

Figure 12. Annual peak discharges on the San Bernard River near Boling, TX.

The trendline fitted to the Brazos River data shows a slight decrease from 1966-2016. The trendline fitted to the San Bernard River data shows a slight increase from 1953-2016. The discrepancy between the two datasets could be attributed to very low flow years in the early 1960's which are present in the San Bernard dataset, but absent from the Brazos River dataset. Changes in discharge rate are expected to result in changes in the sedimentation, however the

amount of increased sedimentation due to increased discharge is assumed to be relatively small compared to the uncertainty associated with the sediment rating curve. The analysis conducted above is based on annual trends at the Brazos River was compared to the peak discharge trends produced by the USACE Climate hydrology assessment tool (see Figure 13). The trends developed by the USACE also show a slight decrease in peak annual discharge. However, the climate hydrology tool does not include data from 2016 and 2017, which were relatively wet years. As a result, the trendline developed by the USACE climate hydrology tool shows a steeper decrease in peak flow, while the revised analysis shown in Figure 11 shows a more gradual decrease in peak flow rates. However, note that the climate hydrology tool is missing the most recent data from 2015-present, which were relatively wet years. In addition, the tool shows a very weak trend with a P-value of only 0.41.

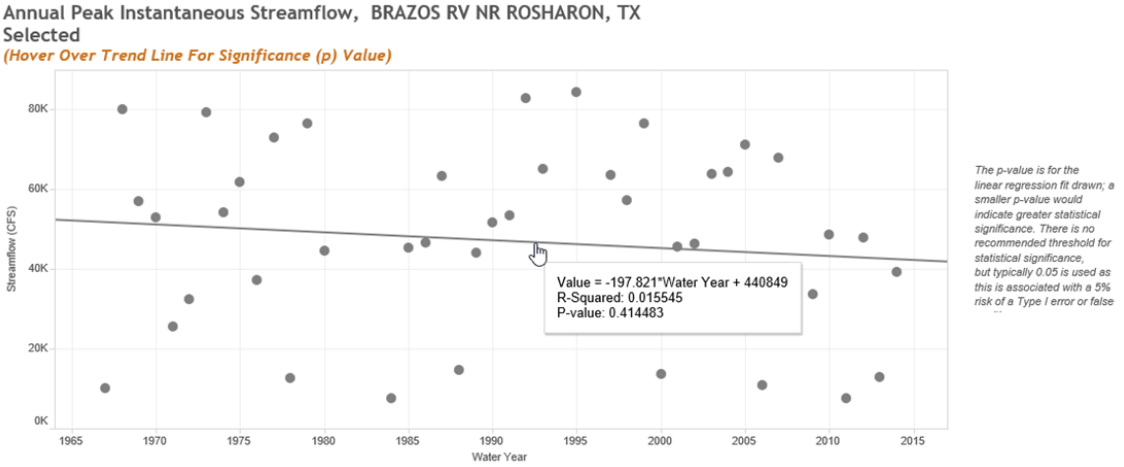

Figure 13. Annual peak instantaneous flow trends at the Brazos River near Rosharon, TX pulled from USACE Climate Hydrology Assessment Tool.

Further discussion of the sedimentation modeling, including modeling of sedimentation with sea level rise, is conducted in Section 3.

2.1.4.2 Climate Change Literature Review

As part of Responses to Climate Change Program, the Region 12 (Texas-Gulf Region) of the USACE climate change report were reviewed. The Region 12 report is located here: http://www.corpsclimate.us/rcccliareport.cfm (USACE, 2015). This report describes applicable climate change and hydrology literature for the project area. First, precipitation projections were reviewed to qualitatively analyze the effects on the project site. According to USACE 2015, precipitation in the southeastern United States may be expected to decrease slightly in a warmer climate, though intense rainfall events may increase in frequency (USACE, 2015). This means that mean rainfall may decrease while variance increases. See Figure 14 (extracted from USACE, 2015) showing the projected changes in seasonal precipitation in 2085 relative to a 30-year period (1971-2000) centered at 1985 (USACE, 2015).

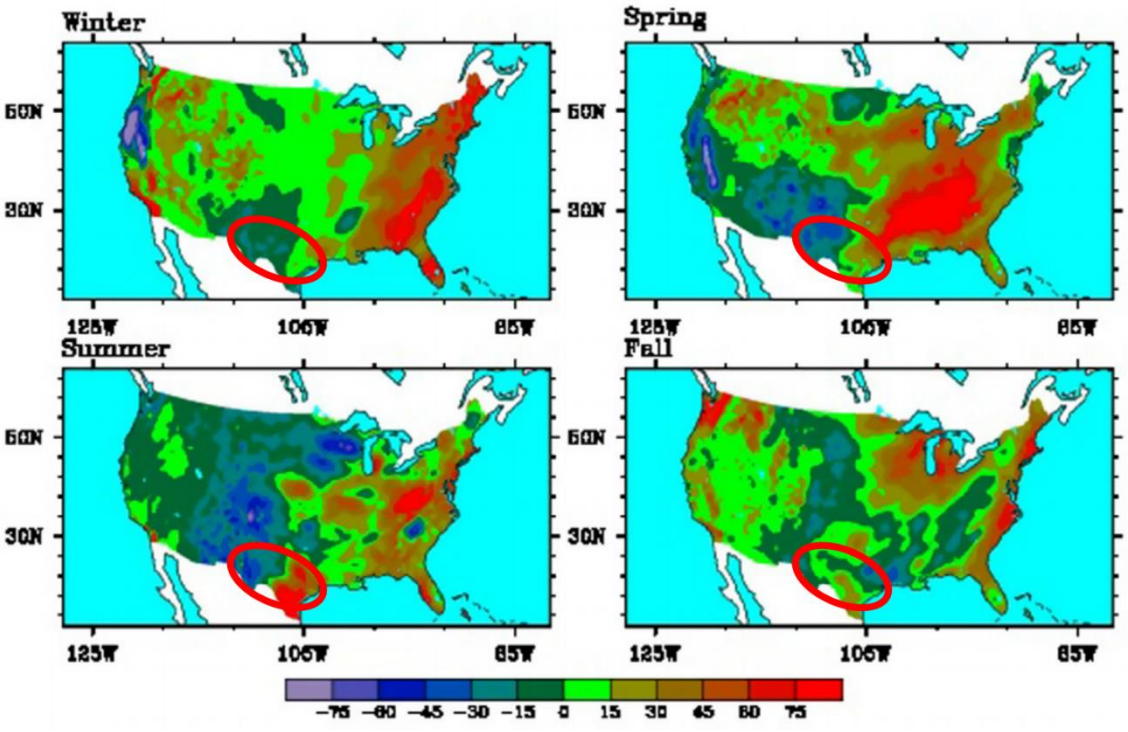

Figure 14. Projected changes in seasonal precipitation, 2085 vs. 1985 mm (from USACE, 2015). Texas region circled with red oval.

Although Figure 14 shows a slight decrease in precipitation at the project site, projections of future precipitation change are especially uncertain in this region because it is located in a transition zone between projected drier conditions to the south and projected wetter conditions to the north, which could have mixed effects on flows at the project site. Due to these uncertainties, the assumption that future precipitation in the project area will be roughly similar to past precipitation appears to be justified.

The USACE watershed vulnerability tool was used to examine the vulnerability of the project area to flooding under future conditions. For the Brazos River Watershed (HUC 1207), the projected future risk to navigation is expected to be low for the dry scenario, and moderate for the wet scenario. Figure 15 shows the vulnerability of the Brazos River watershed for 2050 and 2085 conditions.

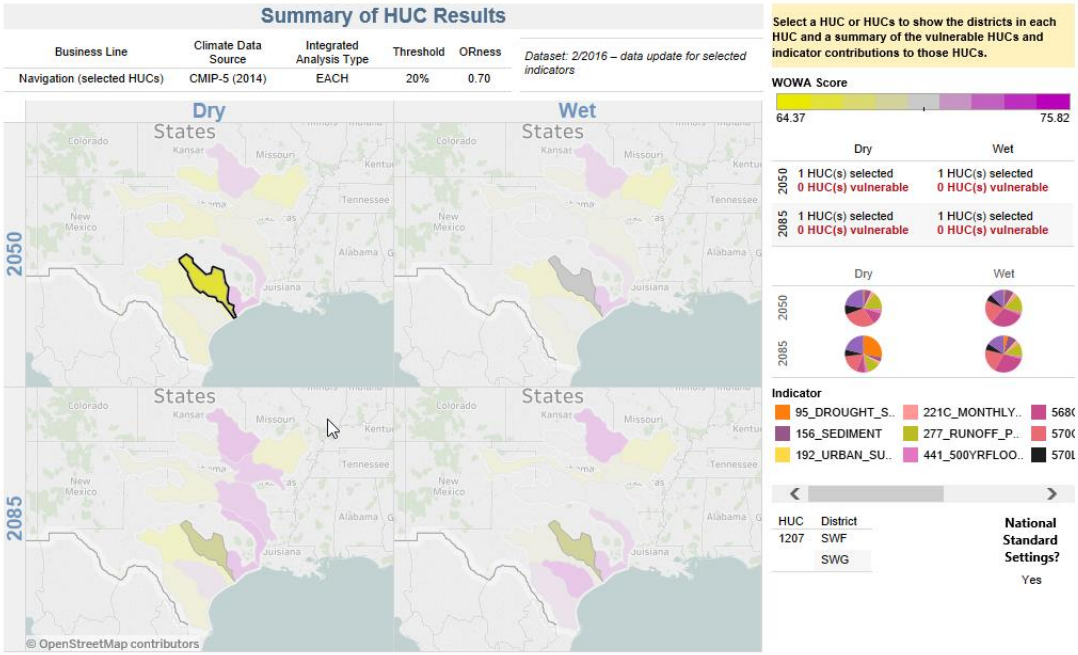

Figure 15. Watershed vulnerability for the Brazos River watershed (HUC 1207) from the USACE watershed vulnerability tool.

The climate hydrology assessment tool was also used to assess the predicted trends of the peak annual discharge for the Brazos River. Figure 16 shows the trends in projected peak annual flowrate, which represent the mean of 93 climate change hydrology models for the Brazos River watershed (HUC-1207). The projected annual maximum monthly streamflow for the Brazos River is expected to remain relatively constant, with the potential for a very small increase in flow rates in the future based on the climate hydrology model results shown in Figure 16. However, there is considerable uncertainty in making such specific predictions of future peak annual discharges. It is important to note that this data is not to be used for quantitative analysis.

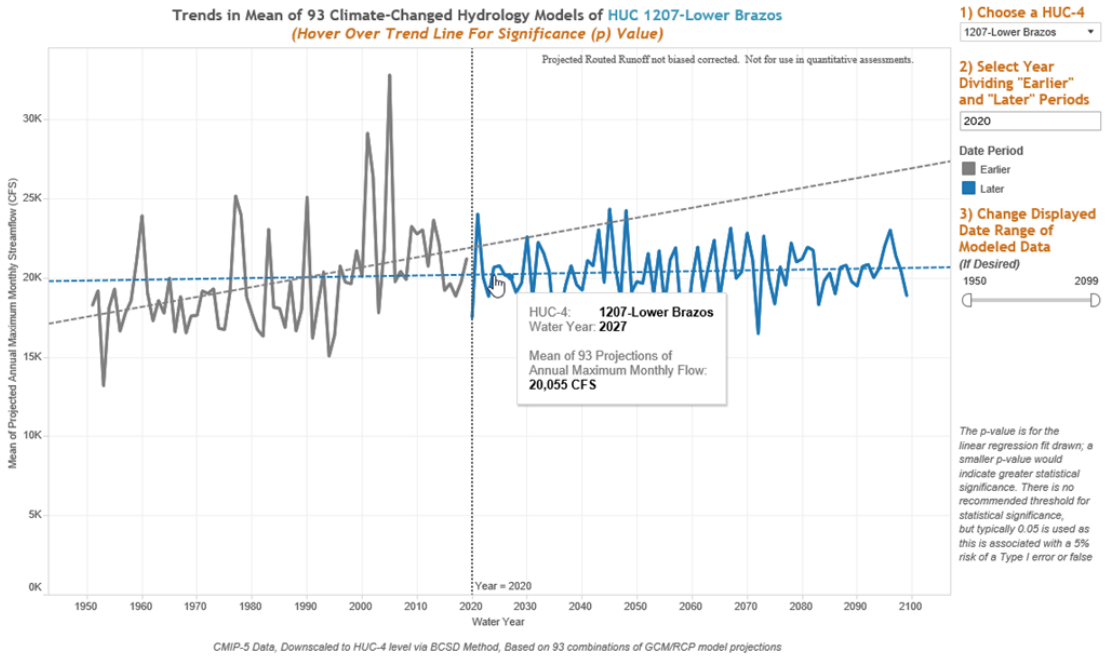

Figure 16. Trends in mean modeled annual maximum streamflow. The mean (blue line) is the average of 93 Climate-Change Hydrology Models of HUC 1207

The consensus in the recent literature points toward mild increases in annual precipitation and streamflow in the Texas-Gulf Region over the past century. In some studies, and some locations, statistically significant trends have been quantified however the trends at the Brazos project site remain insignificant or unclear. However, the discussion above should be used for qualitative analysis of the impacts of climate change on the project site.

2.1.4.3 Quantification of Climate Change Impacts on the proposed projects.

Relative sea level rise trends were analyzed from the USACE projections at Freeport gage 8772440. These relative sea level rise trends include water level changes, as well as general subsidence estimates for the Freeport gage.

Future conditions were modeled by adjusting the boundary conditions and re-running the AdH simulations for the open channel and existing alternatives. Given the uncertainty in projected sea level rise and subsidence, a range of relative sea-level rise (RSLR) scenarios was evaluated. For this project, 1.0 ft. and 2.0 ft. RSLR were evaluated. A RSLR higher than 2.0 ft. is possible, but that scenario was purposefully not evaluated in the hydraulic modeling for two reasons: First, at that level of inundation, the project would no longer function as designed, as the Gulf Intracoastal Waterway would be located seaward of the future coastline and would therefore cease to be “intracoastal.” Modeling additional sea level change beyond this level will not inform selection among alternatives. Second, a higher RSLR amount was not evaluated due to limitations of the AdH model – with the entire model domain inundated, the model will not run stably or reliably. In theory the model could be extended to allow additional sea level elevations to be evaluated, but the cost of this extension was not justified by the limited additional knowledge it would yield. Furthermore, the future condition modeling is not able to capture many of the processes that will impact project area hydraulics over the long term, including marsh accretion, coastal erosion, dredging and other anthropogenic effects such as changes to the watershed. If modeling were conducted for higher RSLR amounts, the uncertainty around the results due to these processes would likely dwarf any conclusions drawn

from the modeling. Therefore, 2.0ft was selected as the highest RSLR value for which the hydraulic model could provide reliable predictions.

Although not modeled in this study, a higher RSLR scenario would most likely be beneficial to navigation, as channel depths would increase and velocities at the crossings would slow. Sedimentation impacts are less clear, but sedimentation could also be reduced as velocities upstream would provide less transport capacity to bring sediment to the project site. Under higher RSLR scenarios, structures would be more likely to be removed or bypassed, which is consistent with the preferred alternative. As more structures are removed or spend more time in the open position, the differences between structural alternatives are reduced, further reducing the information to be gained from a higher RSLR modeling exercise. The projected changes in relative sea level rise were analyzed in the hydraulic modeling described in Sections 3-5 of this report. The impacts of sea level rise to velocities in the Brazos River, sedimentation, and salinity are further described in Sections 3-5 of this report

2.1.5 Winds

There are several wind data stations in the vicinity of the project. The wind stations available consisted of two onshore stations and three offshore stations. While the onshore stations give representation winds at the project site, the collected wind data at the offshore stations are more useful for the purpose of wind-wave generation modeling. The offshore wind data is available as Wave Information Studies (WIS) hindcast data at WIS stations 73060, 73062, and 73064, shown in Figure 17. WIS 73062 was chosen for wind data due to its location directly offshore of the project site.

Figure 17. WIS hindcast data stations near Brazos River Floodgates.

Statistics and extremal analysis of the wind data was calculated in order to characterize the winds just offshore of the project site. Rose plots were developed for the wind data at WIS 73062. Rose plots illustrate the frequency of occurrence of event over different directional bins for various magnitudes. Figure 18 shows the wind rose for all of the wind data at WIS 73062.This wind rose shows that the majority of the winds are from south-southeast to south east direction with wind speeds of 0 to 25 mph. The majority of the highest winds speeds (over 30 mph) tend to come from the north. Additionally, the seasonal variation in the winds was

explored by plotting the wave roses for summer (April to September) and winter (October to March) months. Summer winds are characterized primarily of low magnitude winds coming from south-southeast to southeast directions, whereas winter season experiences much stronger cold fronts coming dominantly from northern directions as shown in Figure 18.

The Gulf shoreline fronting the Brazos River Outlet is subject to extratropical storms (cold fronts), tropical storms, and hurricanes. The summary of hurricanes and tropical storms that made landfall within a 60-nautical mile radius near the project site in the last 50 years is listed in Table 8. A total of 19 storms have made landfall in the vicinity of the project site since 1959.

Toro et al. (2010) recommends against using point gauge data for extreme value analysis when the primary extreme events are tropical storms. In order to provide a more comprehensive analysis of wind speed, MM used an extreme value of wind based on methodology of the National Hurricane Center Risk Analysis Program (HURISK) (NOAA, 1987). The average Saffir-Simpson Hurricane Wind Scale velocity was used in combination with the NHC study to calculate the return period winds for these larger events. An extreme value distribution was fit to these max wind speeds; results are shown in Table 9.

Lower return period wind speeds, such as the 1, 2, and 5-year events are not accurately represented by the NHC methodology due to the infrequent nature of hurricanes making the landfall. These events are better represented by cold fronts and other extratropical storms that affect the project area. In order to form a complete extremal wind dataset, the wind data from WIS 73062 was used to generate extremal winds for the 1, 2 and 5-yr return period events while the NHC methodology was used to generate extremal winds for the 10-yr and greater return period events.

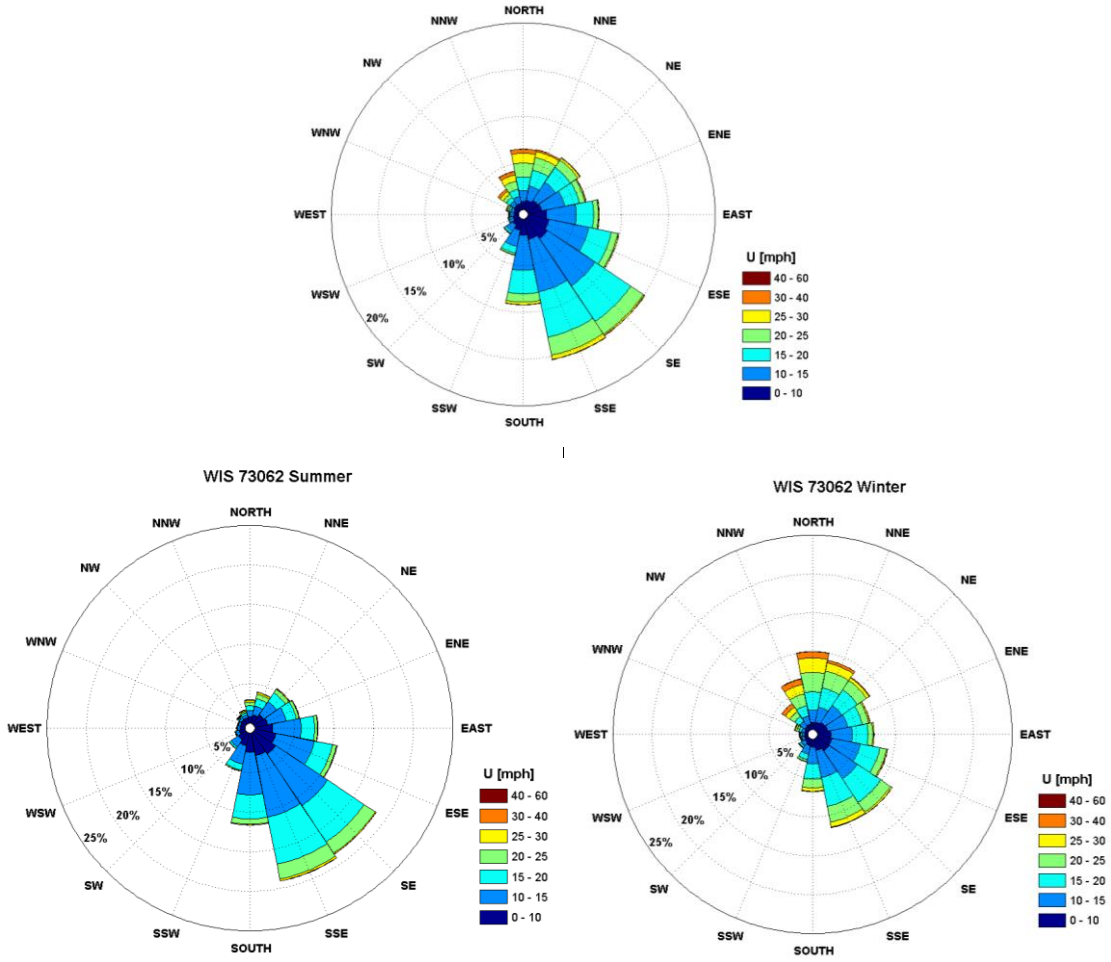

Figure 18. Wind Rose at WIS 73062 for overall (top), summer (left) and winter (right) months.

Table 8. Summary of storms that have made landfall near the project site.

Name	Year	Landfall location [mi from project site]	Landfall Pressure [mob]	Landfall Wind Speed [kts]	Landfall Intensity	Landfall Wind Speed [MPH]
Debra	1959	22	984	70	H1	81
Abby	1964	26	1000	55	TS	63
Fern	1971	80	979	60	TS	69
Edith	1979	160	978	85	H2	98
Delia	1973	8	N/A	50	TS	58
Elana	1979	29	1008	35	TS	40
Danielle	1980	53	1004	40	TS	46
Alicia	1983	24	962	100	H3	115
Unnamed	1987	68	1009	40	TS	46
Allison	1989	23	1001	45	TS	52
Jerry	1989	31	983	75	H1	86
Dean	1995	21	999	40	TS	46
Allison	2001	4	1003	45	TS	52
Fay	2002	61	999	50	TS	58
Claudette	2003	70	979	80	H1	92
Grace	2003	25	1007	35	TS	40
Humberto	2007	80	985	80	H1	92
Ike	2008	52	950	95	H2	109
Harvey	2017	127	938	113	H3	130

Table 9. Return period of extreme winds.

Return Period [yrs]	Wind Speed [mph]
1	39
2	42
5	47
10	91 (Cat 1)
15	112 (Cat 3)
20	120 (Cat 3)
25	129 (Cat 3)
50	141 (Cat 4)
75	146 (Cat 4)
100	150 (Cat 4)

2.1.6 Waves

In addition to wind data, the WIS station also contains hindcast wave data. As described in Section 2.1.5, the location of WIS 73062 (shown in Figure 17) is closest in relation to the project site being directly offshore. Wave statistics and extreme values were calculated to gain perspective of the wave conditions within the project vicinity. Similar to the wind rose, Figure 19 shows the wave rose for WIS station 73062 identifying a predominant wave direction from the

south east. This wave direction correlates to shore normal direction as the shoreline near the project site runs approximately from the north east to the south west. Seasonality of the waves was also analyzed by plotting wave roses for the summer and winter months, shown in Figure 19. During the summer months, a majority of the waves come from the south-south east to south east direction. Wave directions during the winter months are more equally distributed from south to north east directions, influenced by the winter cold fronts from the north as described in Section 2.1.5.

Wave statistics were developed for WIS Station 73062, which is shown in Table 10. Waves are generally from southeast with a mean wave height and period of 2.9 ft. and 5.5 seconds respectively. Table 11 shows the percent occurrence of wave height and wave period and demonstrates that 90% of the waves are less than 7 ft. and 99.5% are less than 9 ft. in height.

Table 12 contains the extreme wave height and peak wave period for the wave data at WIS station 73062 and gives the associated return period. The wave height values were developed using the peak over threshold method. The peak wave period was approximated using a calculated linear relationship between the wave heights and associated wave periods at the WIS station 73062.

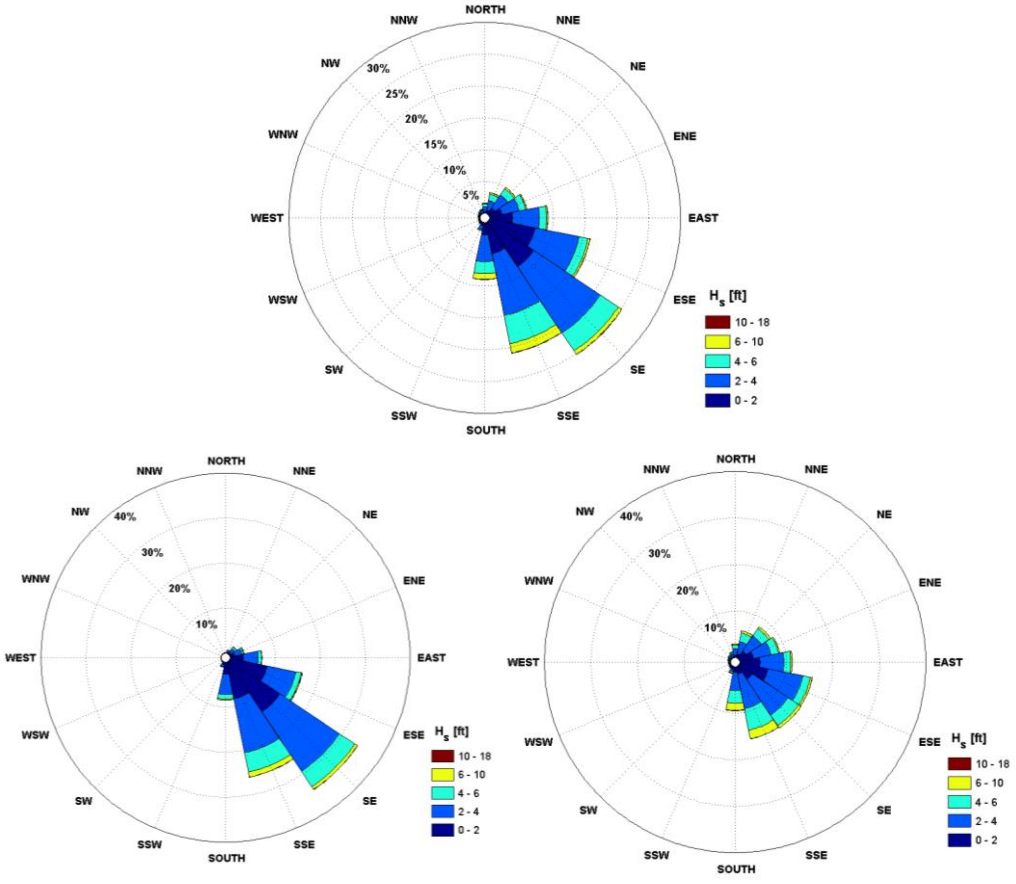

Figure 19. Wave Rose as WIS 73062 for overall (top), summer (left) and winter (right) months.

Table 10. General statistics computed for WIS Station 73062 from 1980-2013.

Parameter	Max	Mean	Std
Depth (ft.)	--	66	--
H_s (ft.)	19.4	2.9	1.6
T_p (sec)	16.4	5.5	1.4
W_θ (TN)	--	126	52

Table 11. Percent occurrence of wave height and wave period at WIS station 73062.

Tp [s]	2 - 4	4.1 - 5	5.1 - 6	6.1 - 7	7.1 - 8	8.1 - 9	9.1 - 10	10.1 - 12	12.1 - 14	14.1 - 16	Sum
Hs [ft.]											
0.0 - 1	2.8	2.0	1.2	1.2	0.4	0.2	0.1	0.2	0.02	0.006	**8.2**
1.1 - 2	6.3	7.5	7.7	2.7	0.4	0.2	0.05	0.04	0.02	0.001	**24.7**
2.1 - 3	3.3	8.2	8.6	5.6	0.7	0.2	0.08	0.06	0.04	0.003	**26.8**
3.1 - 4	0.4	5.0	7.2	5.2	1.1	0.3	0.1	0.06	0.03	0.007	**19.5**
4.1 - 5	0.0	1.4	4.2	3.5	0.9	0.3	0.1	0.05	0.02	0.012	**10.6**
5.1 - 6	0.0	0.3	1.6	2.7	0.7	0.3	0.05	0.03	0.01	0.009	**5.7**
6.1 - 8		0.02	0.6	1.6	0.8	0.4	0.1	0.06	0.01	0.009	**3.6**
8.1 - 12			0.03	0.2	0.3	0.3	0.1	0.02	0.01	0.004	**0.9**
12.1 - 16				0.001	0.002	0.003	0.008	0.01	0.00	0.002	**0.03**
Sum	**12.8**	**24.5**	**31.1**	**22.6**	**5.2**	**2.3**	**0.7**	**0.5**	**0.2**	**0.1**	**100**

Table 12. Extreme Values of Wave Heights at WIS 73062.

Return Period [yrs]	Wave Height [ft.]	Peak Wave Period [s]
1	10.3	9.7
2	11.6	10.5
5	13.6	11.7
7.5	14.6	12.3
10	15.4	12.7
15	16.5	13.4
20	17.3	13.9
25	17.9	14.2
50	19.9	15.5
75	21.2	16.2
100	22.1	16.7

3 Hydrodynamic Analysis

3.1 Hydrodynamic Processes Modeling

The combined influences of tidal circulation and river hydraulics was simulated in the project vicinity to evaluate the influence of tidal currents and the Brazos and San Bernard River discharges on flow velocities and water surface elevations at the Brazos River Floodgates. Following the guidance on quality assurance for engineering models contained on ER 1110-2-1150 (USACE, 1999), the modeling was conducted using an adaptive two-dimensional finite-element model of flow and transport Adaptive Hydraulics (ADH) (USACE, 2014). The model domain development and calibration are discussed in the following sections.

3.1.1 Model Description

The Adaptive Hydraulics Model (ADH) is a modular, parallel, adaptive finite-element model for one-, two- and three-dimensional flow and transport developed by the Engineering Research and Development Center Coastal and Hydraulics Laboratory (ERDC-CHL). ADH has several integrated modules to supplement the shallow water wave module including SEDLIB (a multiple grain size mixed sediment library), and a sediment transport module for dynamically coupling sediment transport with hydrodynamics. One unique function of ADH is mesh adaption, where the model will automatically refine the mesh resolution in areas where higher resolution is required. This allows for the original mesh to be much coarser, leading ultimately to better computation efficiency. ADH also uses an implicit adaptive time step which can be automatically calculated to control stability and convergence.

3.1.2 Mesh & Bathymetric Surface Development

The computational grid for the ADH circulation model is shown on Figure 20. The area around Brazos River Floodgates was refined to 5 m (16 ft.) resolution to better capture the flows; the resolution decreases to 3500 m (11,500 ft.) in the offshore. Based on prior experience in modeling this region, the mesh was created to include both Galveston Bay and the eastern Matagorda Bay. The Brazos River was extended approximately 50 miles upstream to the USGS Gage at Rosharon (08116650) and the San Bernard River was extended about 50 miles upstream to the USGS Gage at Boling (08117500) to ensure accurate boundary conditions at the river boundaries. Smaller tributaries and estuaries that are connected to the GIWW were also included in the mesh, as retention of water in these estuaries has an influence on circulation locally within the GIWW.

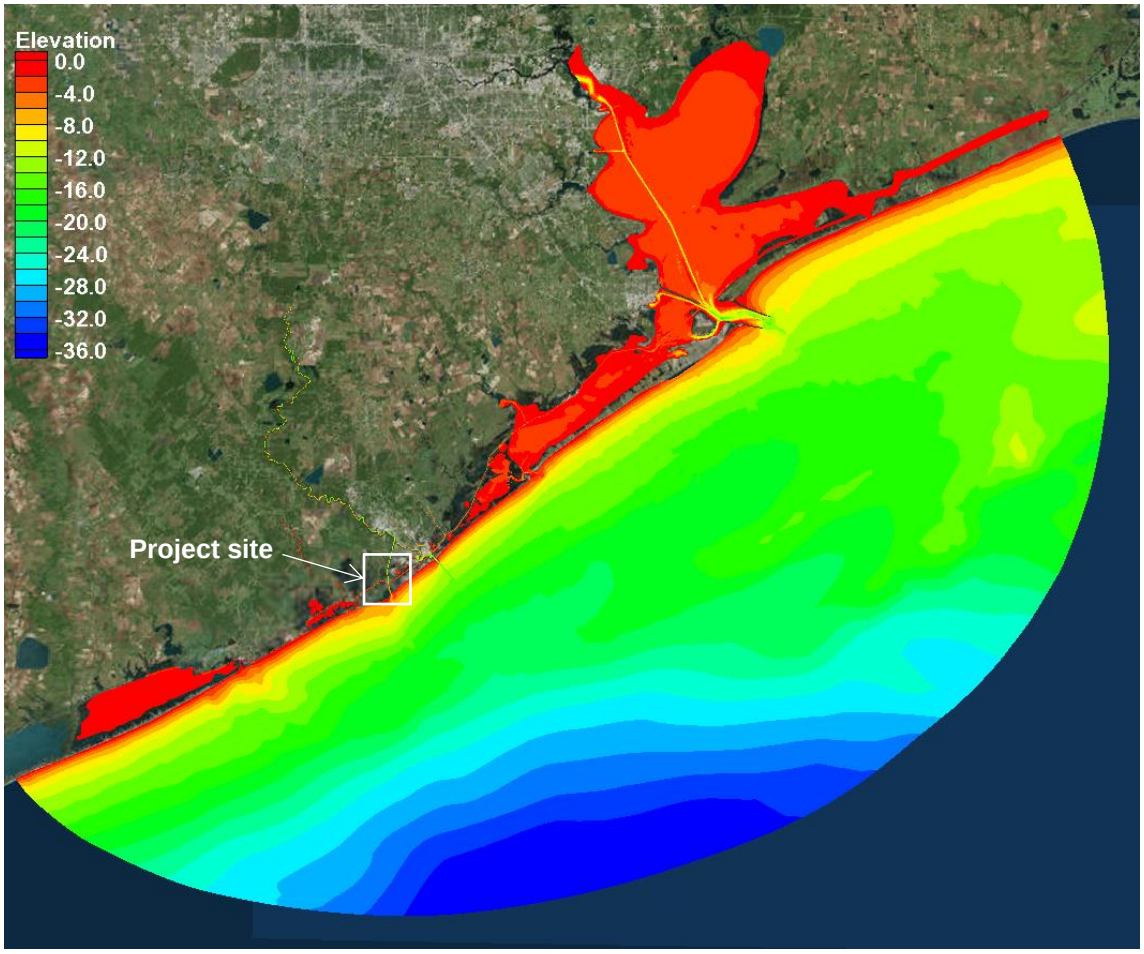

Figure 20. Brazos River Floodgates ADH circulation model mesh.

The base of the model bathymetry was taken from previous models that Mott MacDonald constructed in the region, with bathymetry sourced from the NOAA Coastal Relief Model, local and USACE surveys. The bathymetry in the GIWW and the Brazos Locks was updated using more recent bathymetric surveys where appropriate, as discussed in Section 2.1.1.3.

Bathymetric survey transects of the Brazos River were taken in April 2017 at 400-ft increments for approximately 2.5 miles upstream of the Brazos River inlet to the Gulf, and at 0.5-mile increments for approximately 50 miles upstream to Rosharon, TX. In the absence of available survey data, the depth of the San Bernard River was assumed to be constant at -10.5 ft. MLLW, with side slopes of 8H:1V. The assumption of depth in any hydrodynamic model could introduce uncertainty, and in the San Bernard River, this results in uncertainty regarding the routing of flow from the model boundary at Boling, TX to the San Bernard's intersection with the GIWW. The model calibrated well at measurement gages near the San Bernard River and GIWW intersection, which reduces uncertainty attributed to the assumed depth, however there is still uncertainty in this assumption outside the calibration period.

The bathymetry of the Brazos River between the Gulf of Mexico and the BRFG was artificially lowered to -18 ft. NAVD88 (Figure 21). This was required since the hydrodynamic model does not have a way to account for intermittent erosion and accretion of the due to flood and drought events, as was evident through model calibration (Section 3.1.4). As shown in Figure 71, the Brazos River can experience significant event-driven bed change, which in turn would affect the hydrodynamics. It was found through sensitivity testing that a bed level of -18 ft. NAVD88

significantly improved the model validation. Like the assumed depth along the San Bernard River, the bathymetry correction downstream of the Brazos River-GIWW is a potential source of uncertainty in the model. The model calibrates well with water surface elevations and velocities at the project site over the simulation period (as further described in Section 3.1.5), which reduces the uncertainty, however the absence of a dynamic bed in this stretch of the Brazos River still introduces uncertainty around the seasonal changes in hydrodynamics at the project site. It is not believed that this uncertainty could result in a plan selection change.

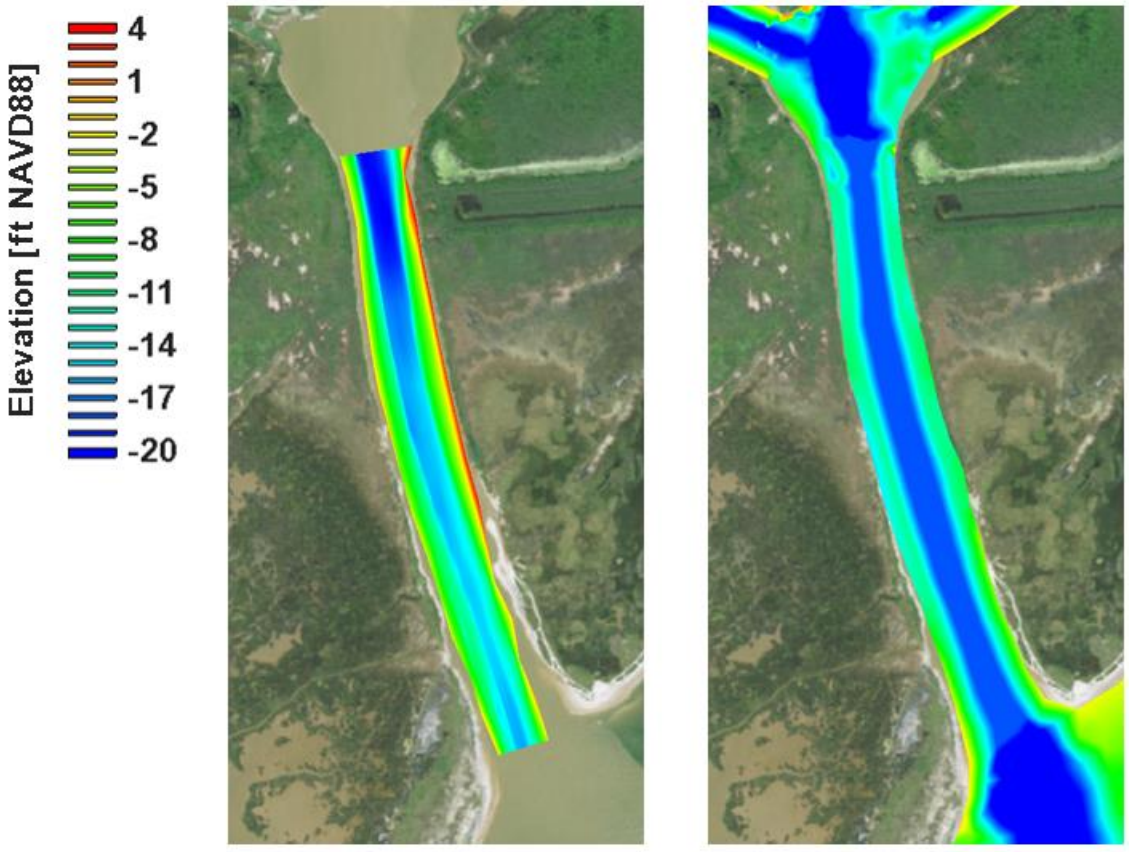

Figure 21. Bathymetry correction between the BRFG and the Gulf of Mexico.

3.1.3 Hydrodynamic Model Setup

The offshore model boundary is a natural boundary condition forced by a uniform time series of water surface elevation that is constant in phase extracted from the Tidal Model Driver (TMD), a product of the Earth and Space Research Institute (ESR). A uniform timeseries on the offshore boundary was selected given the spatial unknowns in the meteorological component of water level, and the boundary instabilities in the ADH model when using varying phase. The harmonic tides were then adjusted based on the residual difference between predicted and measured tide at the Freeport tide gage (8772447) to account for meteorological effects at the model boundary. By using this methodology, relevant wind-driven processes, such as set-down from northerly winds, are accounted for in the model simulations. For simulations involving sedimentation, the offshore boundary was assumed to have a constant sediment concentration of zero parts-per-thousand for all sediment constituents. Furthermore, for simulations involving salinity, the salinity concentration was assumed to be spatially constant along the offshore boundary.

The river boundaries are natural boundary conditions forced by a measured time series of discharge extracted from the Rosharon Gage (08116550) and the Boling Gage (08117500) for the Brazos River boundary and the San Bernard River boundary respectively. The model domain was extended in both rivers to the gage locations to ensure the appropriate routing of flows and timing of the flow hydrographs. For simulations involving sediment transport, the river inflow was applied with a specified time-varying concentration of each sediment constituent as described in Section 5. For simulations involving salinity, the river inflow was assumed to be completely fresh water with a salinity concentration of zero parts-per-thousand.

The side boundary locations were selected to minimize the uncaptured volume transfer into, and out of the model domain. The model domain is terminated in the GIWW at the East Matagorda Bay for the western boundary, where volume flux is limited by the Colorado Locks (See Figure 20 for model bounds). The model domain is terminated in the GIWW at the East Galveston Bay for the eastern boundary, where the distance to the nearest significant water body, Sabine Lake, exceeds 40 miles; thus, any volume flux through this boundary will be small. For both side boundaries, a zero-flow boundary condition is applied.

For the free surface boundary condition, a constant atmospheric pressure was applied. A wind boundary condition was not explicitly applied to the model domain, as it is assumed that on this spatial scale the impact of wind on hydrodynamics within the model domain are negligible. However, meteorological effects of wind and varying pressure were incorporated into the offshore boundary condition via the residual water level offset described above. Furthermore, rainfall was not included as a free surface boundary condition since, as discussed in Section 2.1.1, the local hydrology has a relatively small contribution to the total inflow volume.. Finally, a spatially uniform Manning's roughness coefficient of 0.015 was applied to the bottom boundary.

3.1.4 Sensitivity Testing and Calibration

The data analysis in Section 2.1.1 indicates the USGS gaging stations have an overlapping time period between July 2004 and January 2005 (Table 13). Within that window, a two-week calibration period of July 20 – Aug 2 was selected due to the moderate flow rate in the Brazos River and good agreement between predicted and recorded tide elevation at the Freeport Gage (8772440), meaning that meteorological forces potentially influencing hydrodynamics is negligible.

Table 13. Available overlapping data between July 2004 and January 2005 among all USGS stations to be used in calibration and validation.

USGS Gage	Discharge	Stage	Velocity
San Bernard Upstream of GIWW	✓	✓	✓
GIWW at San Bernard	✓	✓	✓
San Bernard Downstream at GIWW	✓	✓	✓
San Bernard at Boling	✓	✓	N/A
Brazos at Richmond	✓	✓	N/A
Brazos at Rosharon	✓	✓	N/A
Brazos at GIWW	N/A	✓	✓

The hydrodynamics and hydraulics were simulated during this period using the default parameters to create a base case. The overall modeling required assessment of a variety of parameters as site specific data was not available, including detailed gate operations and bathymetry at the San Bernard river and river outlet. Therefore, the following parameters were modified and compared to the base case to determine sensitivity of the model to each parameter:

- Friction coefficient

- River discharge rate
- Gate operations
- Opening of the San Bernard River inlet.

As sector gate function is not explicitly included in the ADH model, the gate operations were simulated by rapidly raising and lowering the bed elevation of an assigned set of gate nodes to allow and restrict flow. No record of actual gate opening, and closing is available from the Brazos Floodgates (George, 2016). Therefore, an artificial gate operational scheme was developed based on input from the lockmaster. The frequency of gate operations was based on an assumed 50 openings and closings a day, an opening time of 5 minutes, a closing time of 2 minutes and an open gate duration of 15 minutes. This gate operation was cycled at uniformly spaced events to produce 50 operations a day. Model sensitivity was analyzed at the San Bernard Upstream Gage (08117730) since this gage presented the most reliable data at a high sampling frequency. Figure 22 shows the results of the sensitivity analysis on water surface elevation at this gage. The model was found to be sensitive to gate operations and the opening of the San Bernard River inlet.

The sensitivity analysis concluded that the model friction coefficient over a reasonable range of values and a 20% variation in river discharge does not significantly influence velocities at the intersection of the San Bernard and the GIWW. However, the gate operations have a large influence in the hydraulics in the GIWW, and when combined with an approximated San Bernard connection with the Gulf of Mexico (which was present during the calibration time period) the model was able to reasonably represent the hydraulics in the system. Important conclusions from this sensitivity testing is that the hydraulics are very sensitive to the gate operations, and the exact gate operations (exact timing and duration of opening and closing) are unknown. Therefore, there will always exist some inaccuracies in the model results as it is impossible to simulate correct hydraulics without operational data. Results match well using the artificial scheme, but further model refinement is not warranted with the lack of this data set.

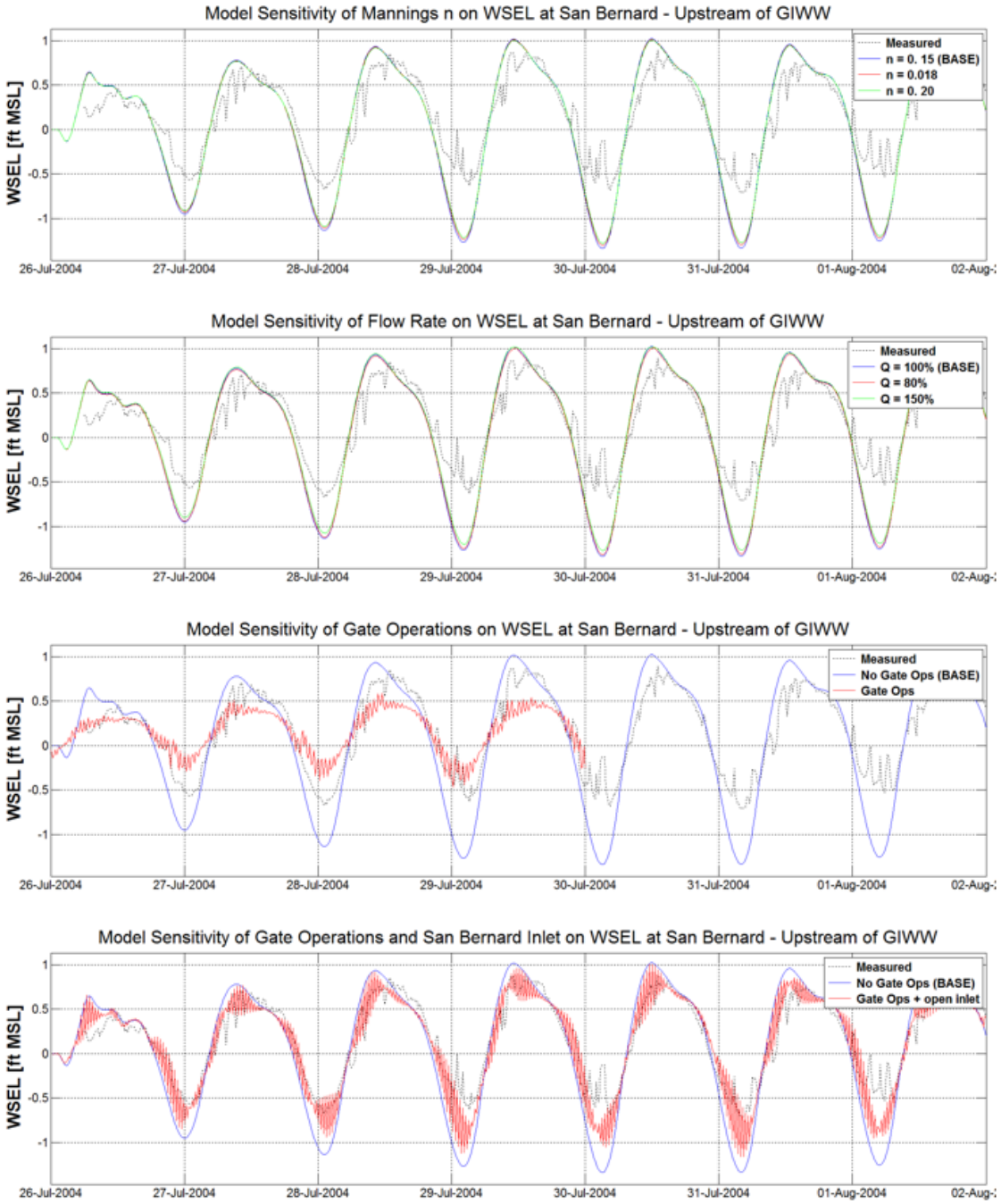

Figure 22. Time series of water surface elevation showing the model sensitivity to friction coefficient (top), river flow rate (mid-top), gate operations (mid-bottom) and the combined effect of gate operations and an open San Bernard River inlet (bottom).

3.1.5 Validation of Calibrated Model

The calibrated model was validated using a 13-month period between March 1, 2015 and April 1, 2016. This period is a relatively high-flow year and covers a large range of high and low flow conditions, with the following hydrodynamic and hydraulic conditions:

- An approximately 4-year flood event in the Brazos river
- An approximately 5-year flood event in the San Bernard River

- 186 days with reported limited navigation and 23 days of reported restricted navigation
- 3 flood events in the Brazos River greater than the 1-year event
- 4 flood events in the San Bernard River greater than the 1- year event
- An approximately 2-month period having low river flows in both rivers

Note that the time period selected includes high flow cases in the Brazos combined with low flow events in the San Bernard, as well as the opposite scenario. The time series of river discharge for the Brazos and San Bernard Rivers is shown in Figure 23.

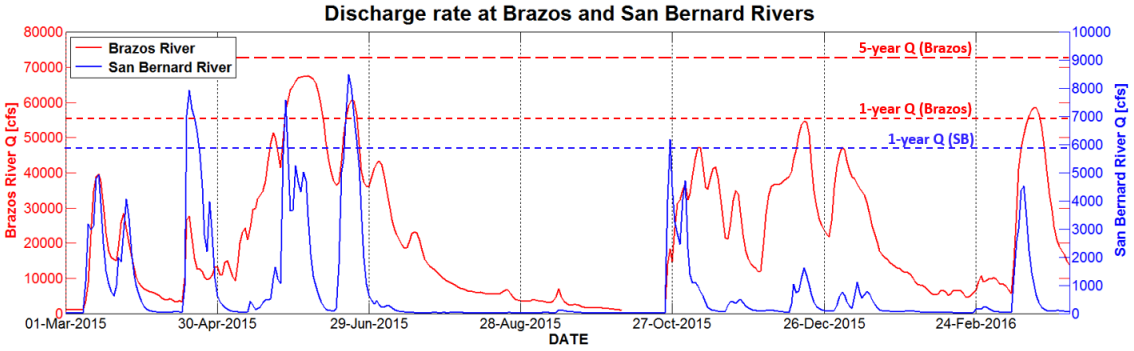

Figure 23: River discharges during the model validation period.

A comparison time series of modeled vs. measured water surface elevations and velocities is shown in Figure 24. As discussed in Section 2.1.3, water level and velocity data are available immediately adjacent to each gate. Gate operations cause high frequency oscillations in the water surface and velocity signals in both the measured and modeled data. Model data can be extracted at frequency to resolve the gate operations and their influence, but the measured data does not. Therefore, for validating the model, these high frequency signals were filtered using a low-pass filter with a frequency cutoff of 3-hours in an attempt to extract a meaningful signal. The 3-hr cutoff was determined through sensitivity testing of the modeled data sampled at the same sampling interval as the measured data to produce as close to a real signal without the noise of gate opening and closing, however, as previously discussed, the real gate operations are at a random, inconsistent frequency while modeled gate operations are at a set, cyclical frequency, and therefore it is not possible to know how well the filtered data represents actual measured conditions. Given these limitations, model results shown in Figure 24 match the measured data with reasonable accuracy.

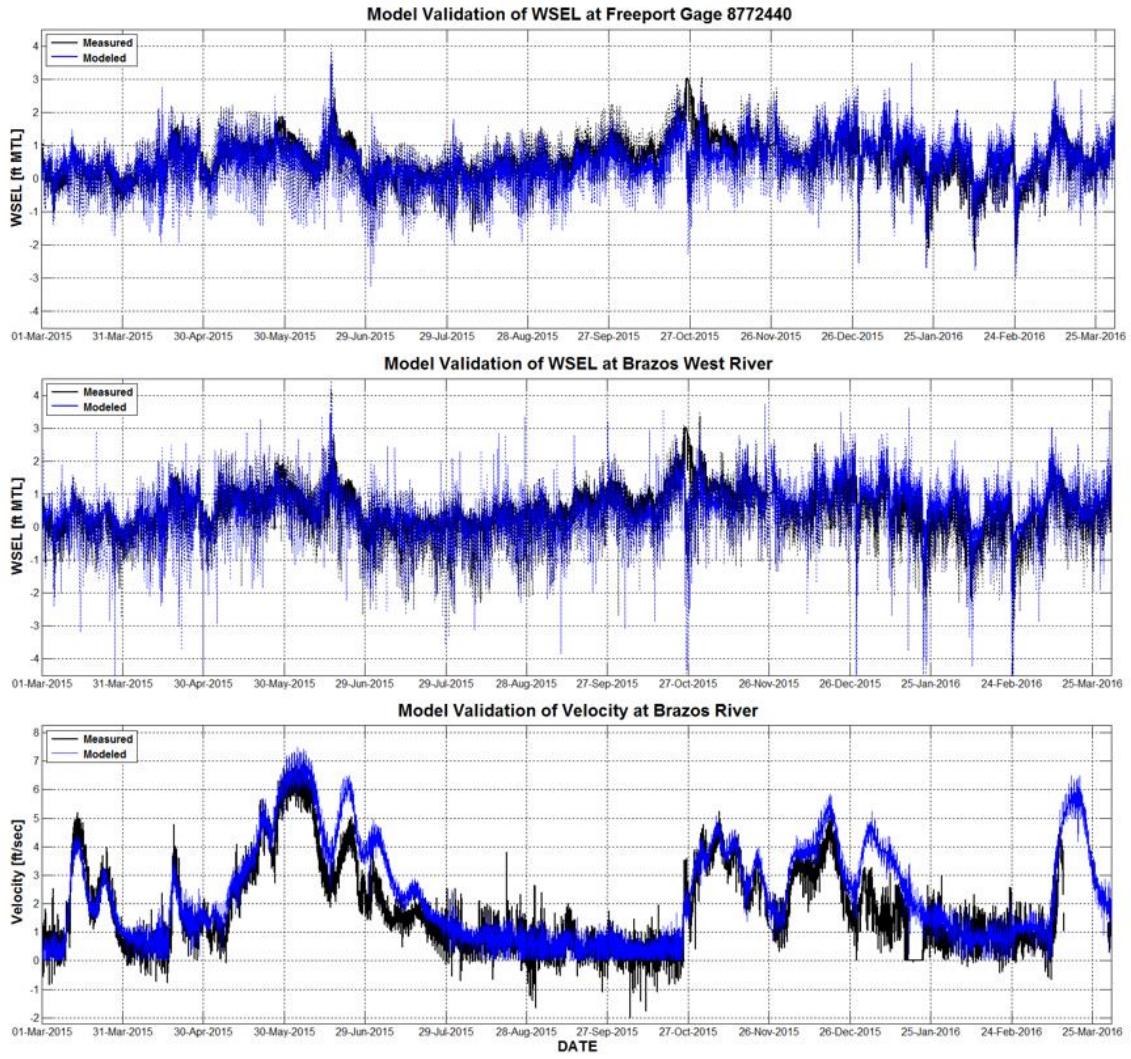

Figure 24: Time series comparison of water surface elevation at the Freeport Gage (top) and the river side of the West Gate (middle) and of velocity at the Brazos River Gage (bottom)

Figure 25 shows a scatter plot of the measured vs. modeled water surface elevation of every time step at every available gage in the model domain. Using these data, the model index of agreement (IA) was calculated based on the following equation (Willmott *et al.* 1985):

$$IA = 1 - \frac{\langle (x_c - x_m)^2 \rangle}{\langle (|x_c - \langle x_m \rangle| + |x_m - \langle x_m \rangle|)^2 \rangle}$$

Where x_m represents the measured values and x_c represents the calculated values. An IA equal to 1 represents perfect agreement, and an IA of 0 indicates no agreement. For the purposes of this study, an IA greater than 0.9 is considered good agreement.

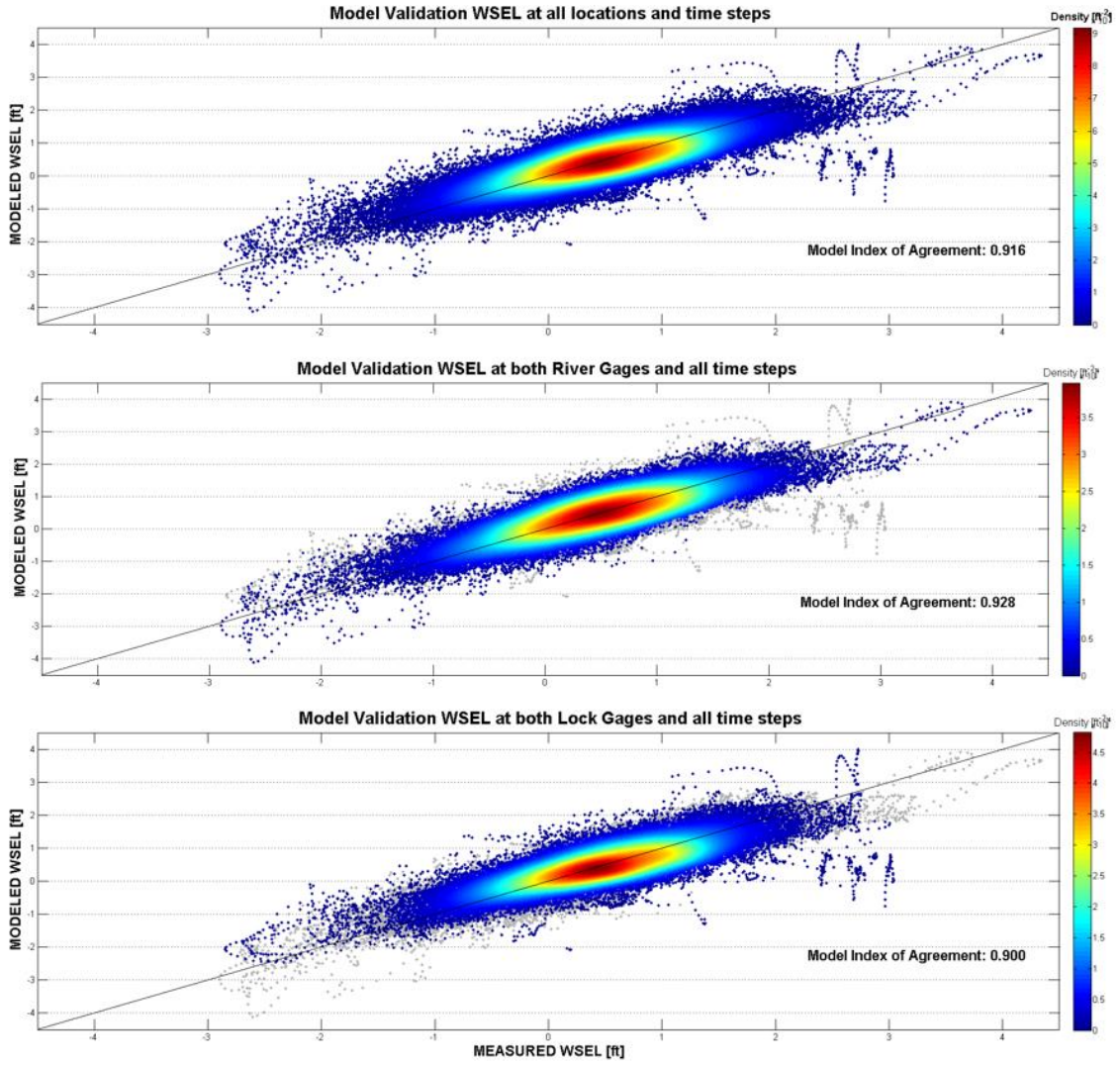

Figure 25: (top) measured vs. modeled water surface elevation at every gage in the domain and for every time step in the model period. (Middle) measured vs. modeled water surface elevation at the east and west river gages for every time step in the model period. (Bottom) measured vs. modeled water surface elevation at the east and west lock gages for every time step in the model period. Color bar indicates point density calculated as the number of points within a 0.25 ft. radius of the point specified.

The hydrodynamic model validated well with observed conditions at six tide stations and one velocity station as shown in Figures Figure 24 and Figure 25, with a combined index of agreement of 0.916. The model performs slightly better on the river-side of the gates, which is expected since the direct connection to the Gulf makes the water level less sensitive to gate operations.

River velocity was reasonably represented by the model. In some instances,, the model tended to over-estimate velocities on the trailing edge. Since model boundary condition discharges are based on daily rates from USGS gages, the model's tendency to over-estimate velocities on the trailing edge of a flood could be attributed to the loop effect. The loop effect is simply the errors in a stage-discharge curve attributed to the hydraulic differences between a rising and falling hydrograph. As a result of the loop effect, discharge rates and velocities on the trailing end of an

event hydrograph tend to be overestimated. Based on these results, the model is considered validated and can adequately represent the system's hydraulics to conclude meaningful results.

3.2 Hydrodynamic Alternatives Analysis

The proposed alternatives were modeled using the same 13-month period as the validation period described in Section 3.1.5. For analysis of alternatives performance, the project region was separated into five zones of influence: West GIWW, Brazos Basin, East GIWW, Freeport, Brazos Delta, and Freeport Offshore as shown in Figure 26. These zones of influence were used to identify relative changes as discussed in Section 3.3 and Section 5.

Figure 26. Project zones of influence.

For Alternative 2a, or the "no-build" alternative, no changes were made to the existing mesh or bathymetry. This alternative is henceforth referred to as "Existing Conditions." The model alignment and bathymetry for Existing Conditions is shown in Figure 28. This alternative represents the standard by which the other alternatives are analyzed. Figure 27 shows the model mesh resolution and populated bathymetry for each TSP alternative.

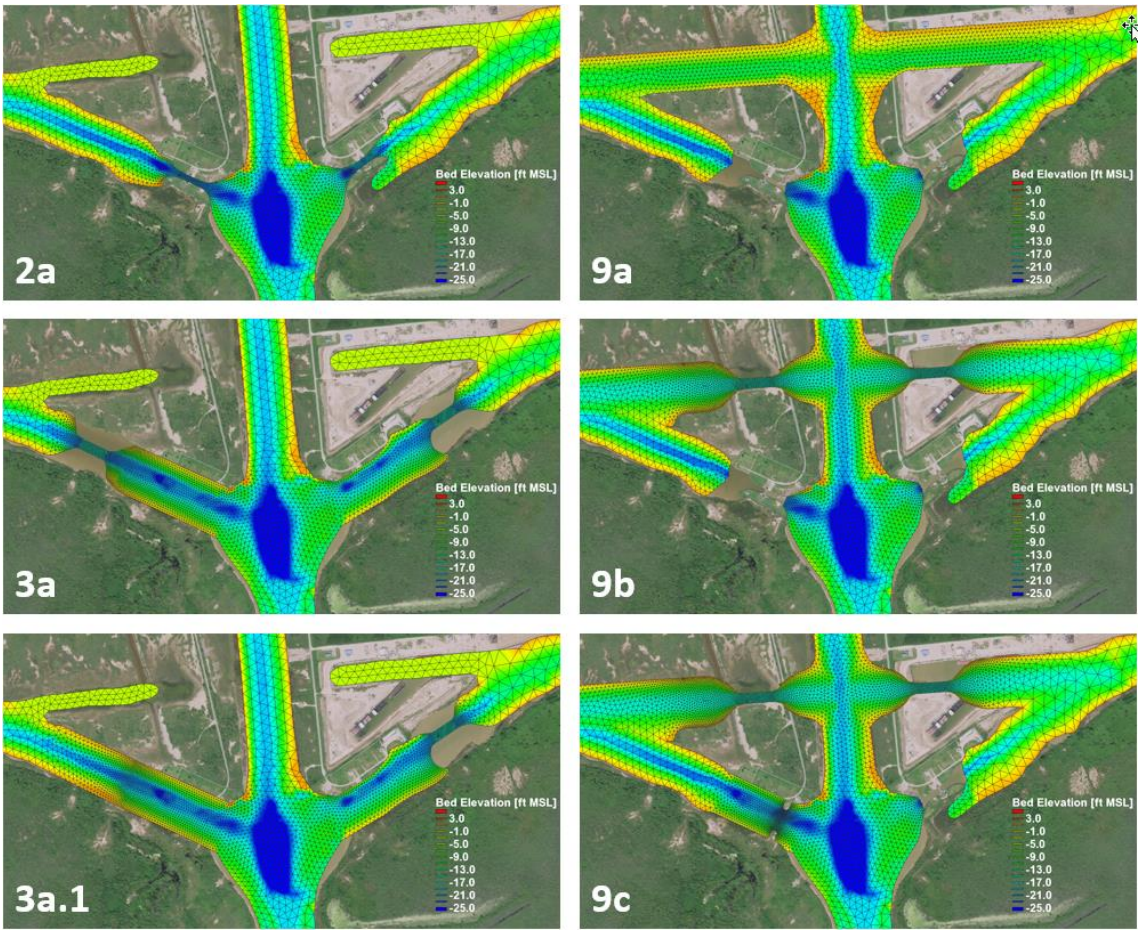

Figure 27. Model mesh resolution and bathymetry for all proposed TSP alternatives

A snapshot of velocity during peak ebb conditions (combination of tide and river discharge) and peak flood conditions is shown in Figure 29. The peak ebb velocity reaches a maximum of about 12 ft./s just north of the Brazos Basin, and eddying is observed on either side of the Brazos River channel. During flood tide, the velocity through the west gate is often more than double that through the east gate.

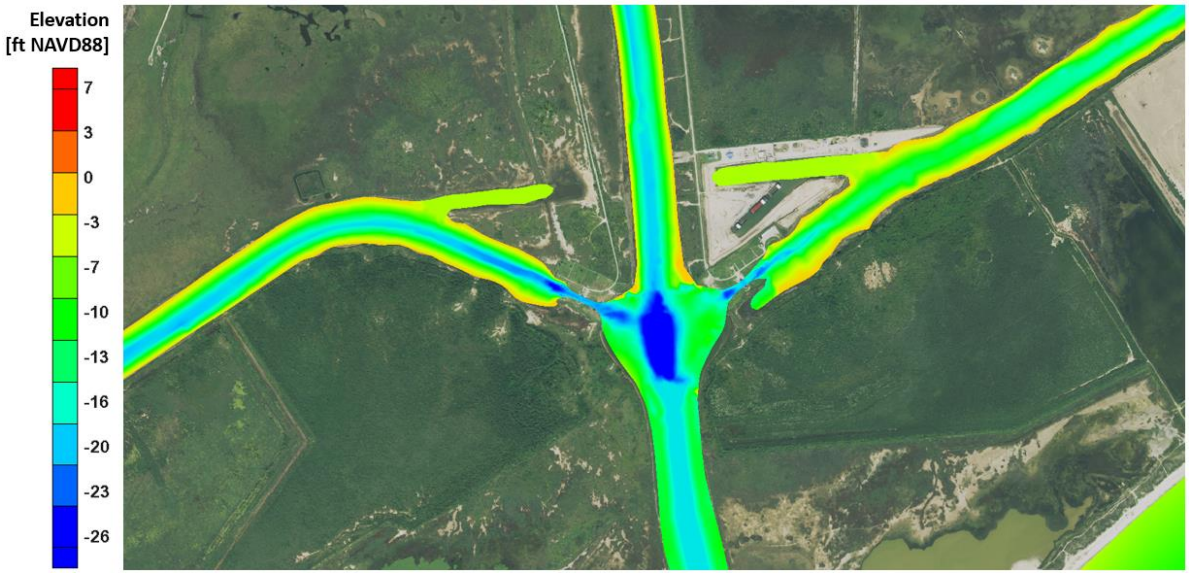

Figure 28. Existing conditions model alignment and bathymetry.

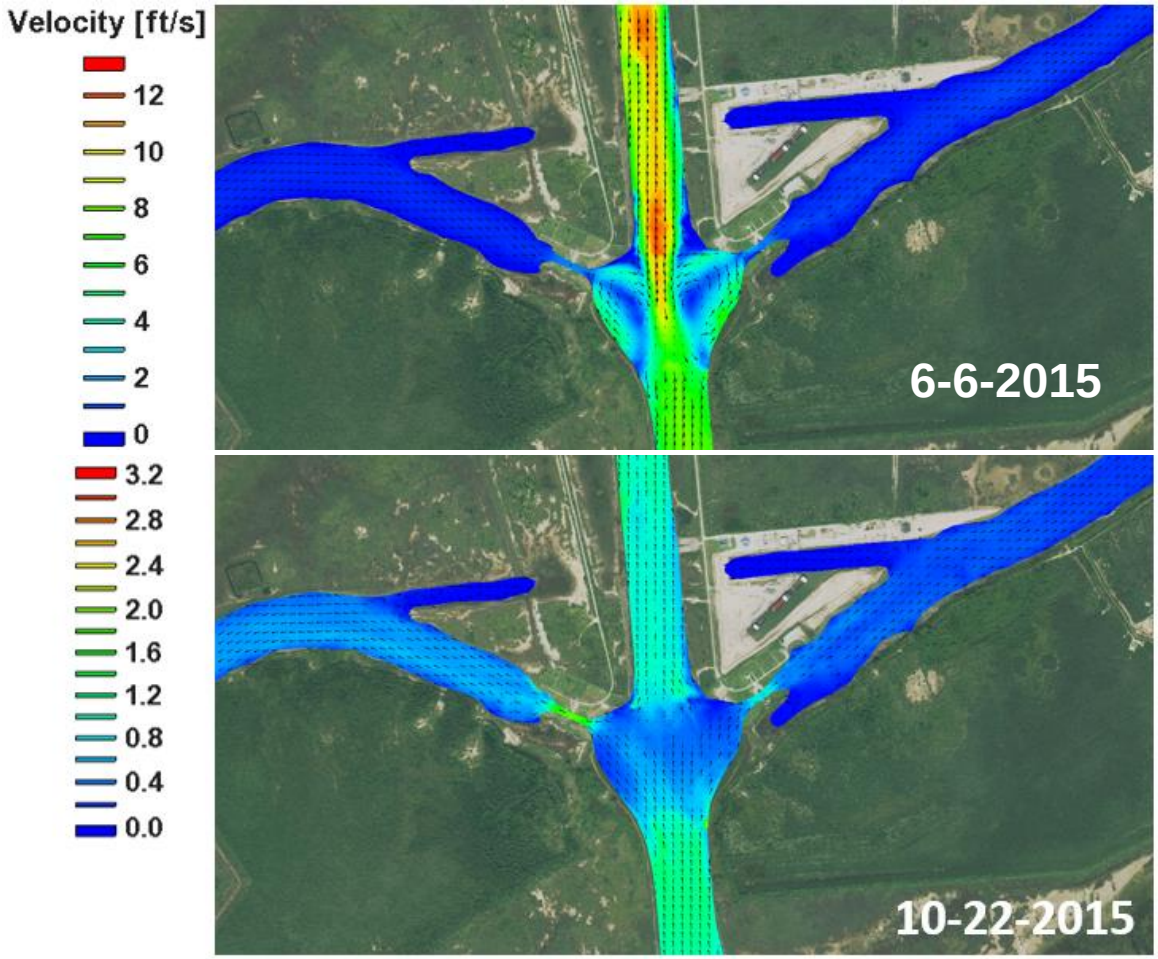

Figure 29. Existing Conditions peak ebb velocity (top) and flood velocity (bottom) at the Brazos River - GIWW intersection.

For Alternative 3a, the flood gates are moved back from the Brazos River by approximately 1,300 ft. and the gates are widened from 75 ft. to 125 ft., while maintaining the same channel alignment (Figure 30). The land surrounding the existing gates is removed to create a straight GIWW alignment approximately 500 ft. wide. While the depth of the channel near the existing gates has been scoured to approximately -21 ft. NAVD88, the elevation of the new gates will be limited to -16 ft. NAVD88. A snapshot of velocity during peak ebb conditions (combination of tide and river discharge) and peak flood conditions is shown in Figure 31. The peak ebb velocity reaches a maximum of about 12 ft./s, and no significant difference in velocity from Existing Conditions is evident. The eddies on either side of the Brazos Basin are approximately the same scale as Existing Conditions. During flood, the velocity through both gates is reduced, likely because of the gate widening.

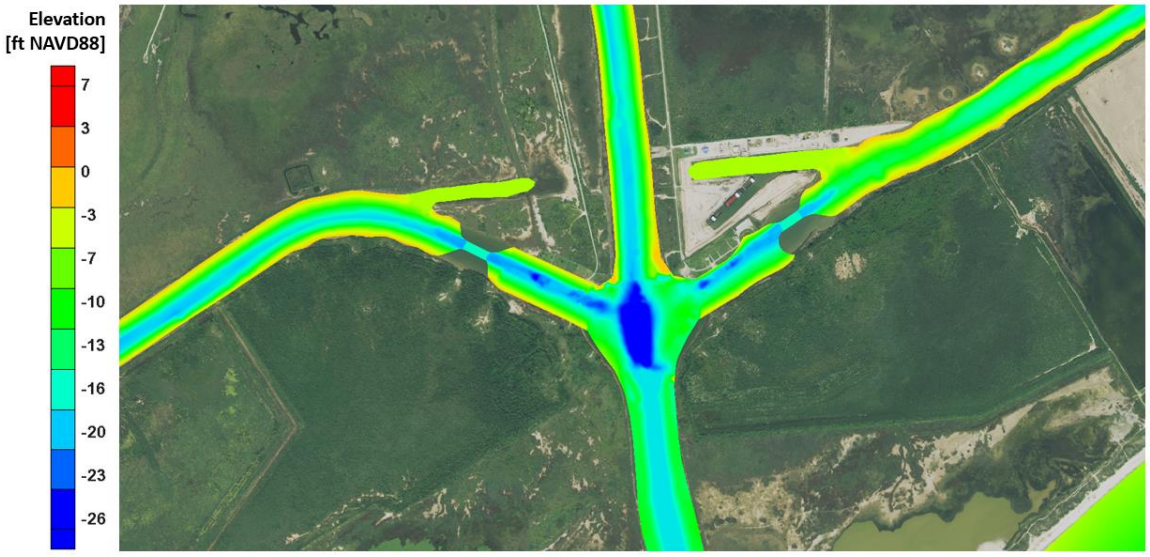

Figure 30. Alternative 3a model alignment and bathymetry.

Alternative 3a.1 has the same gate alignment as Alternative 3a on the East side and an open channel along the existing alignment on the west side (Figure 32). A snapshot of velocity during peak ebb conditions (combination of tide and river discharge) and peak flood conditions is shown in Figure 33. The peak ebb velocity reaches a maximum of about 12 ft./s in the Brazos River channel. The eddy on the east side of the Brazos Basin is approximately the same scale as Existing Conditions, while on the west side of the Brazos Basin, the eddy has reduced in magnitude. During peak ebb, the velocities in both the East and West GIWW are slightly increased, while during peak flood, the velocity in the West GIWW is significantly increased to about 2 to 3 ft./sec.

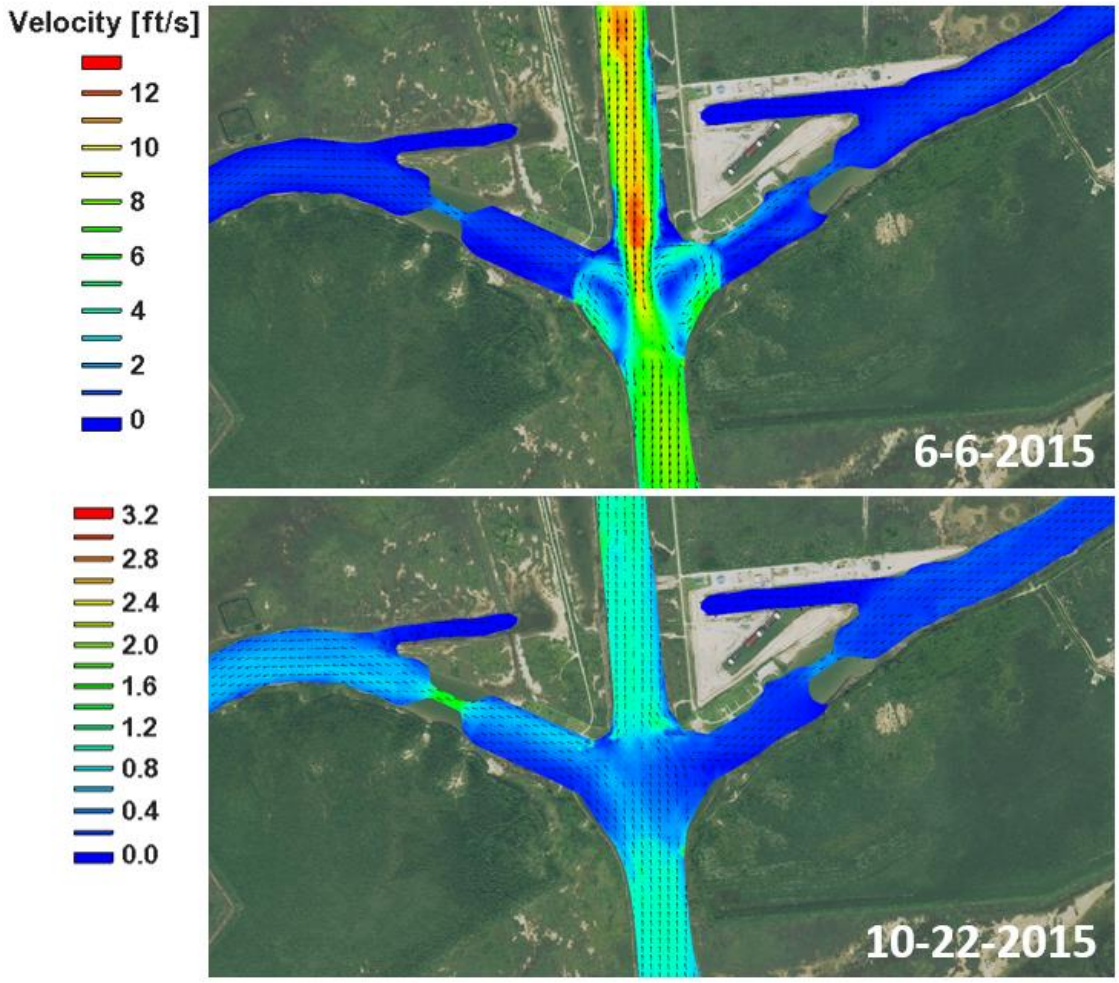

Figure 31. Alternative 3a peak ebb velocity (top) and flood velocity (bottom) at the Brazos River - GIWW intersection.

Figure 32. Alternative 3a.1 model alignment and bathymetry.

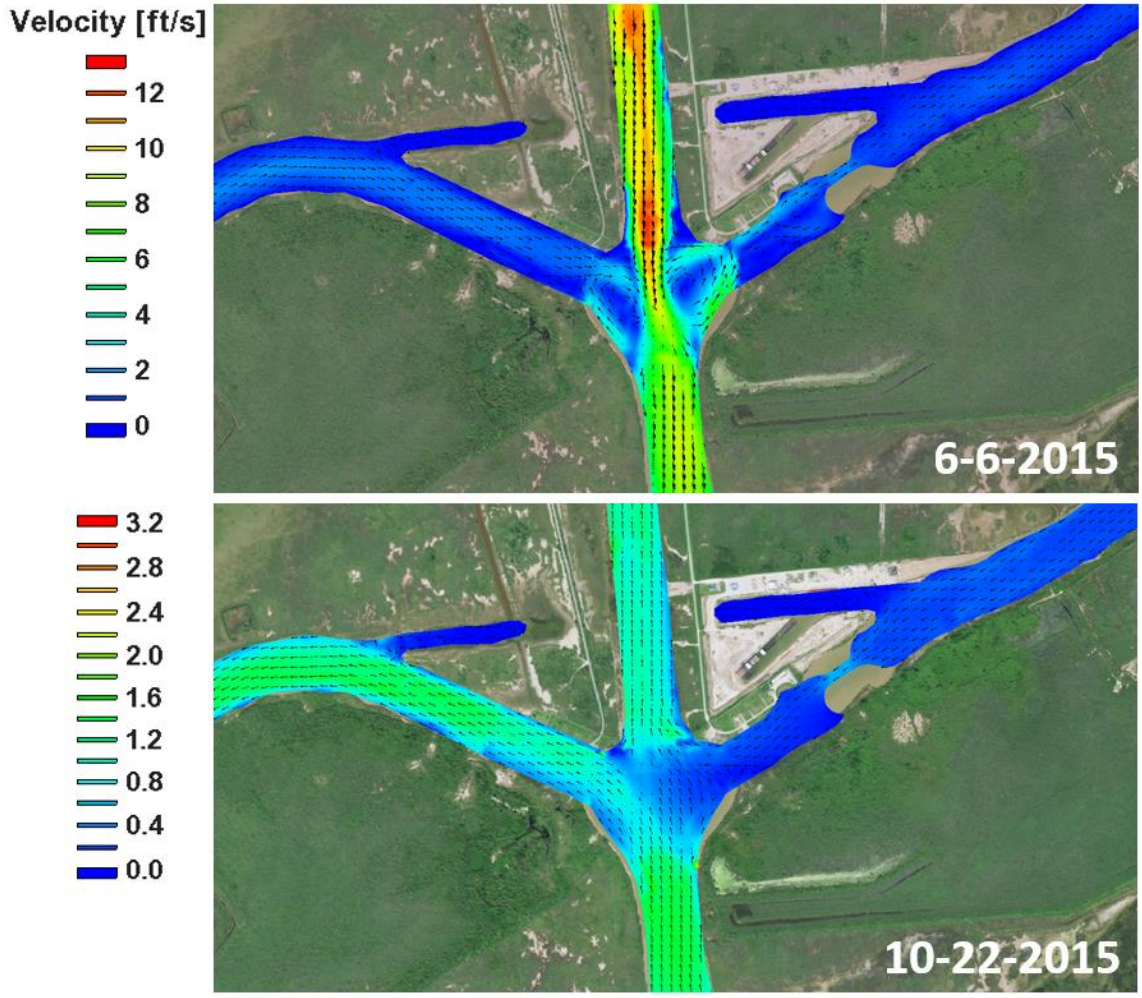

Figure 33. Alternative 3a.1 peak ebb velocity (top) and flood velocity (bottom) at the Brazos River - GIWW intersection.

Alternative 9a is defined by a straight, open channel whose alignment roughly reflects a straight line between GIWW Stations 588+000 and 597+000 (Figure 34). The new channel has a depth of -12 ft. NAVD88 and a bank-to-bank width of approximately 500 ft. There are no gates controlling flow between the Brazos River and the GIWW. The site of the existing gates has been infilled on both the east and west sides to prevent flow. A snapshot of velocity during peak ebb conditions (combination of tide and river discharge) and peak flood conditions is shown in Figure 35. The peak ebb velocity reaches a maximum of nearly 14 ft./s, on the north side of the Brazos River – GIWW intersection. Interestingly, there's also a strong eastward current on the south side of the east channel connection, and a return current on the north side of the east channel connection. There is also a very high velocity of about 12 ft./s south of the Brazos River – GIWW intersection and eddying in the previous Brazos Basin consistent with Existing Conditions and Alternative 3a. During flood, the velocity in both the West and East GIWW has increased, possibly because of the new channel alignment and shallower channel depth.

Figure 34. Alternative 9a model alignment and bathymetry.

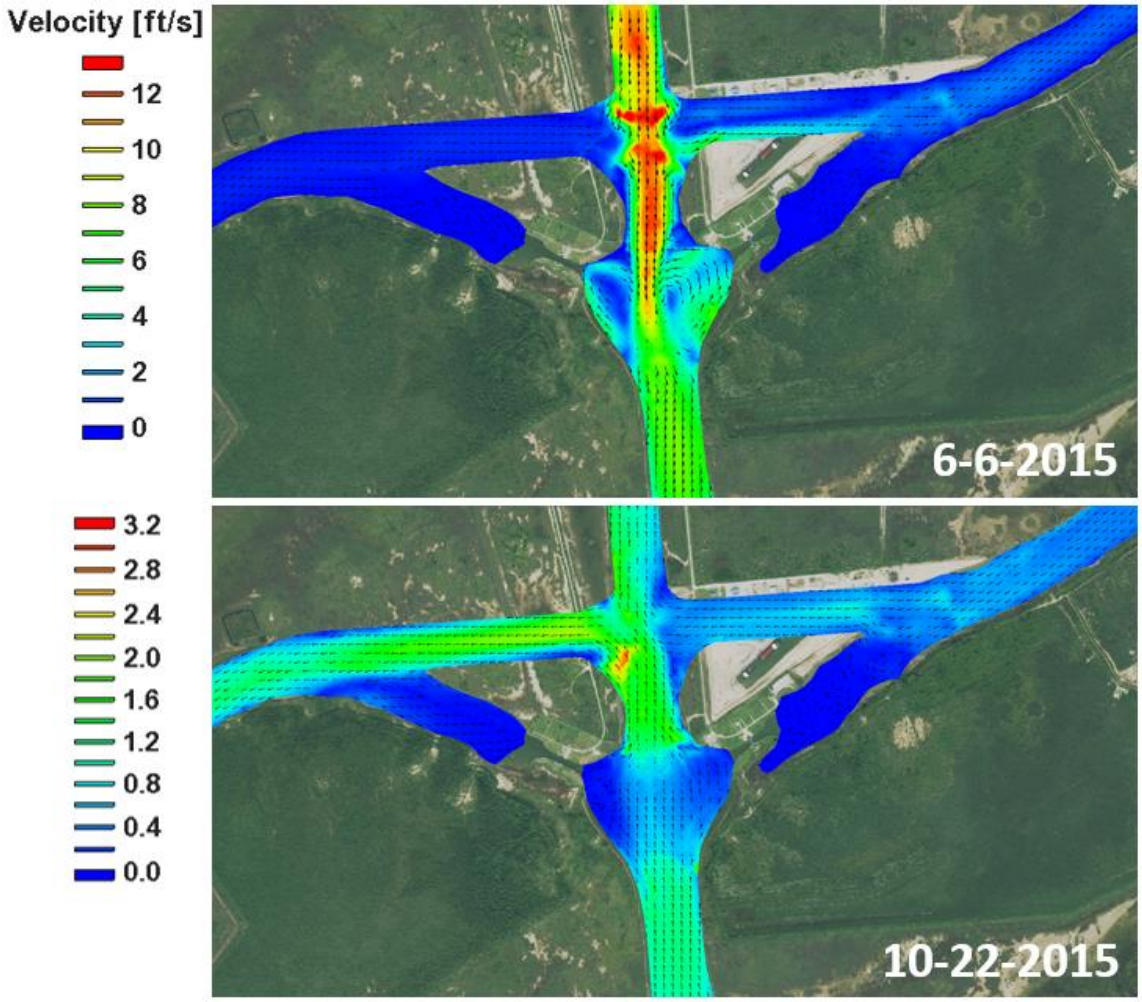

Figure 35. Alternative 9a peak ebb velocity (top) and flood velocity (bottom) at the Brazos River - GIWW intersection.

Alternative 9b has the same channel alignment as Alternative 9a, but with 125 ft. wide flood gates set back about 800 ft. from the Brazos River (Figure 36). For this alternative, the new channel alignment has a constant depth of -16 ft. NAVD88. A snapshot of velocity during peak ebb conditions (combination of tide and river discharge) and peak flood conditions is shown in Figure 37. The peak ebb velocity reaches a maximum of about 12.5 ft./s both north and south of the Brazos River – GIWW intersection. A similar return flow pattern seen in Alternative 9a can also occurs in 9b, however is it restricted in size by the gate. Minimal eddying occurs on the west side of the new Brazos basin, while eddying still occurs on both sides of the previous Brazos Basin. During flood, the velocity in the West GIWW is slightly lower than for Alternative 9a at the gates, but significantly lower west of the gates.

Figure 36. Alternative 9b model alignment and bathymetry.

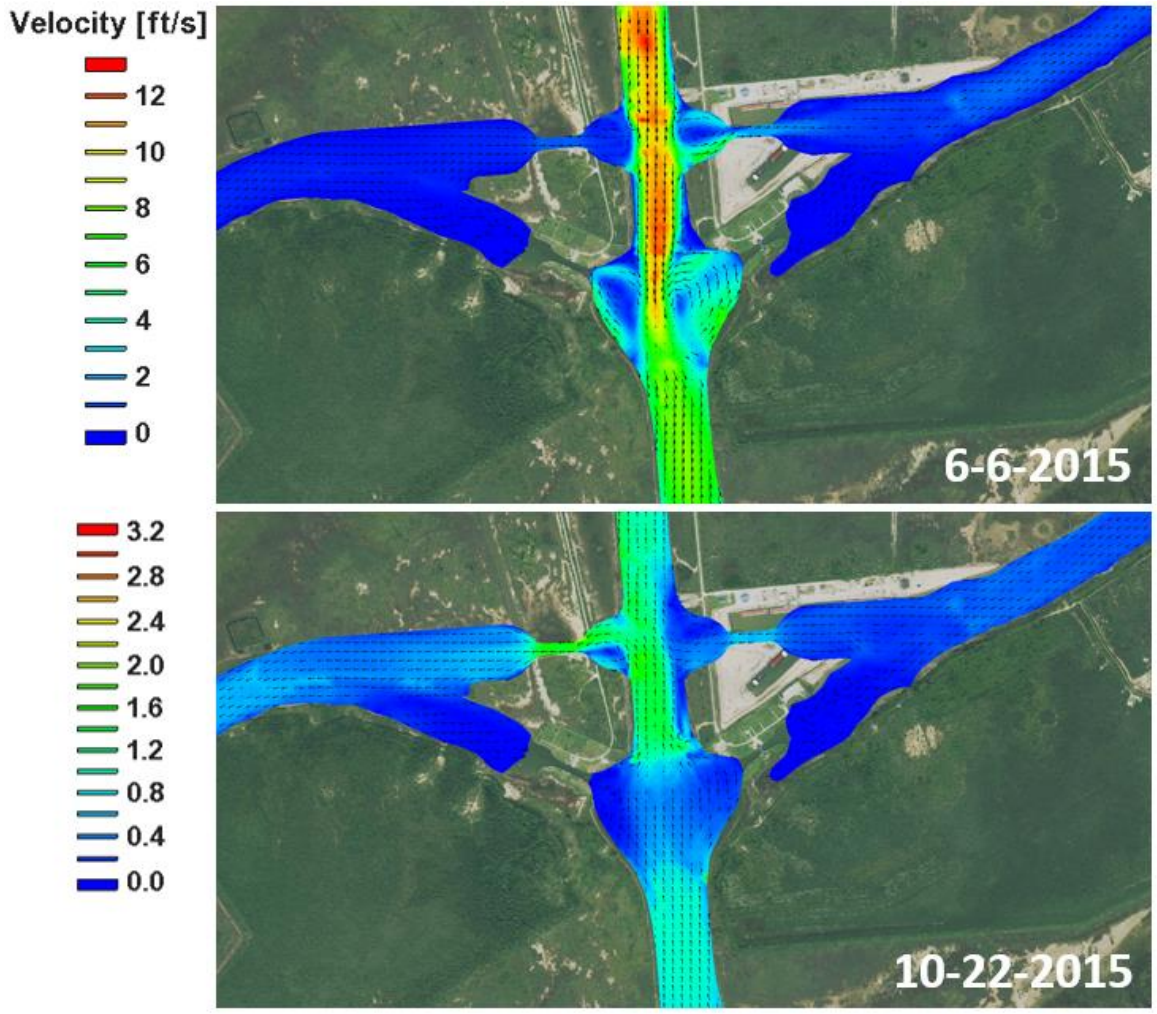

Figure 37. Alternative 9b peak ebb velocity (top) and flood velocity (bottom) at the Brazos River - GIWW intersection.

Alternative 9c is identical to Alternative 9b, but instead of completely filling in the existing channel alignment, flow was restricted through the west side of the existing channel via a sluice gate (Figure 38). The goal of this sluice gate feature is to allow for head relief when the head difference across the west gate restricts safe navigation. The sluice gate was modeled by the same concept of raising and lowering the bed elevation at the gate to allow and restrict flow. The sluice gate operations were determined based on the head differences from the Alternative 9b simulation. A snapshot of velocity during peak ebb conditions (combination of tide and river discharge) and peak flood conditions is shown in Figure 39. There are no distinguishable differences from Alternative 9b in the peak flood or ebb flow pattern, as the sluice gates are not open during these times.

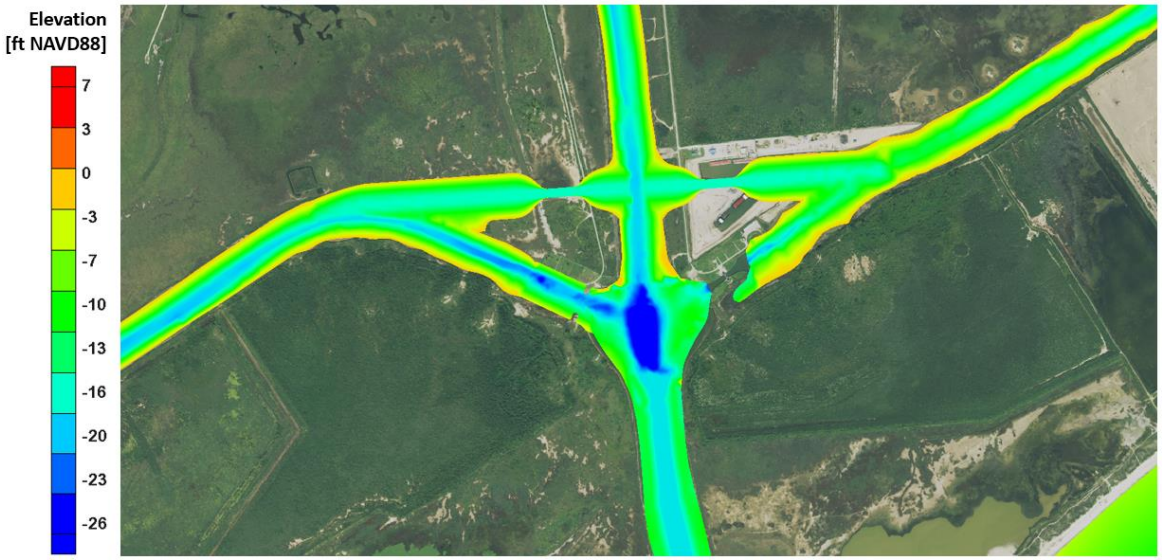

Figure 38. Alternative 9c model alignment and bathymetry.

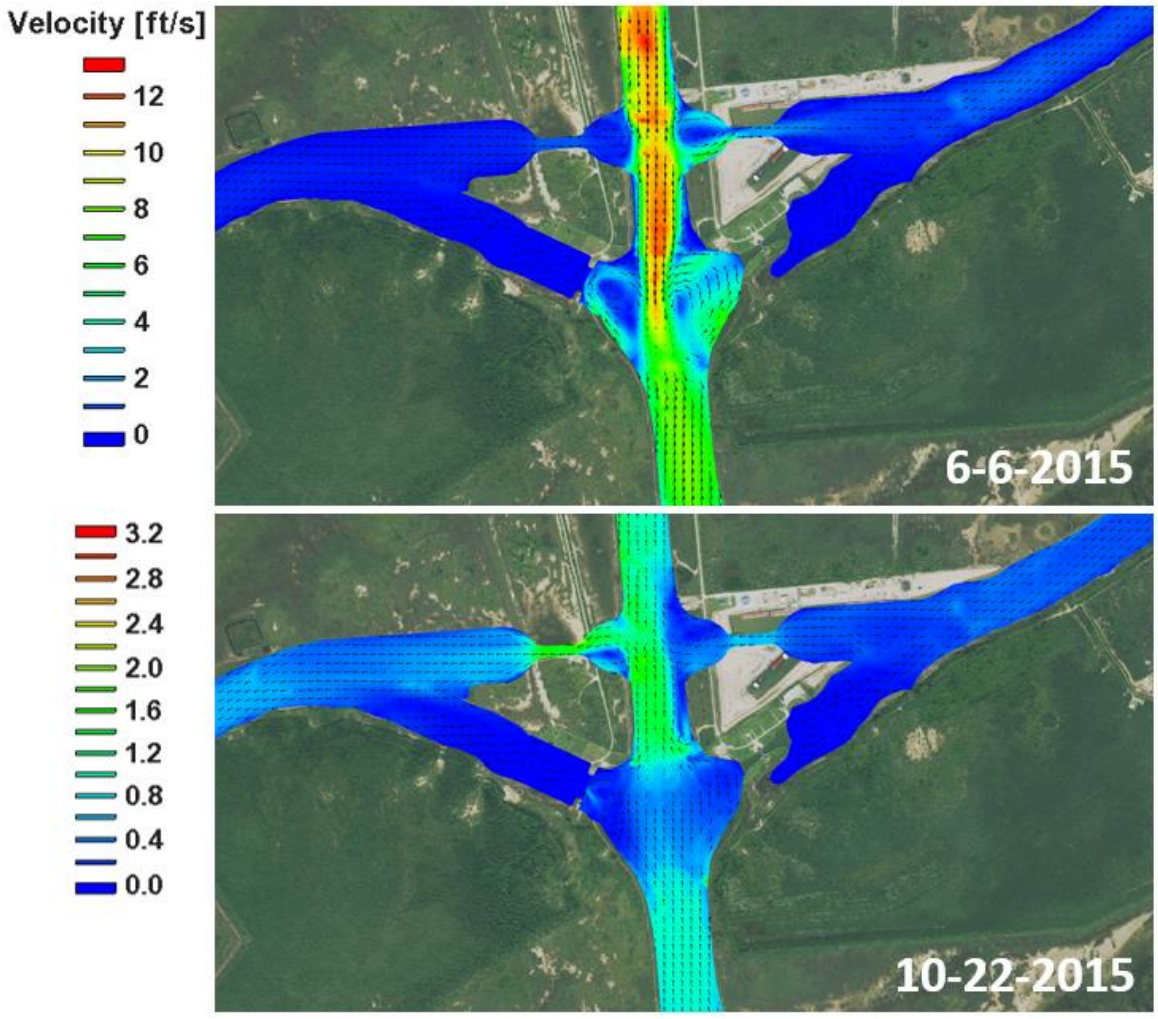

Figure 39. Alternative 9c peak ebb velocity (top) and flood velocity (bottom) at the Brazos River - GIWW intersection.

Since the West GIWW does not have an alternate nearby connection to the Gulf other than through the west gate, there was some concern that the alternate alignment could lead to elevated water levels in the GIWW during high river flow events, causing a risk of flooding the adjacent land areas. Time series of water levels in the West GIWW were analyzed at an approximately 1/3 mile spacing between the Brazos River and the San Bernard River for each alternative. The probability of water level non-exceedance for each extraction point was computed and compared to existing conditions. Figure 40 through Figure 43 show the probability of non-exceedance curves for all alternatives compared with the Existing Conditions (Alternative 2a); the color blending on these curves show the general change in water level along the West GIWW.

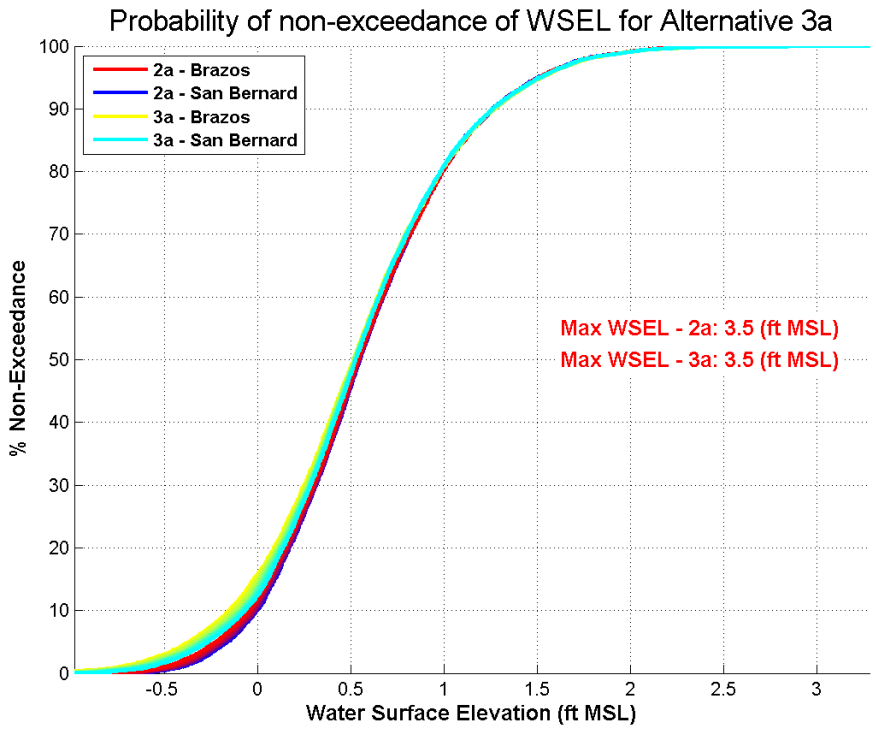

Figure 40. Probability of water level non-exceedance in West GIWW for Alternative 3a.

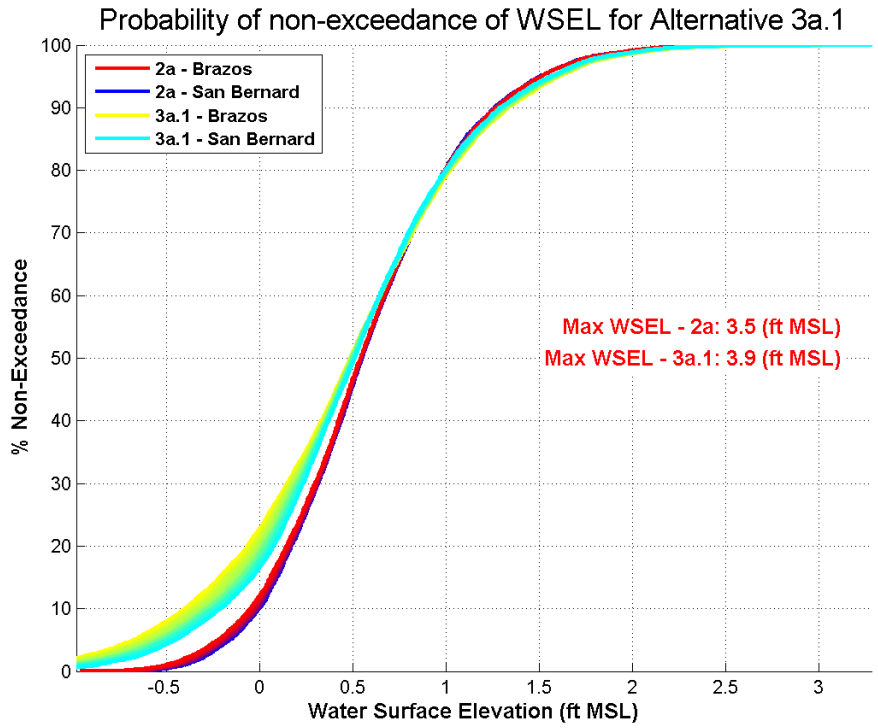

Figure 41. Probability of water level non-exceedance in West GIWW for Alternative 3a.1.

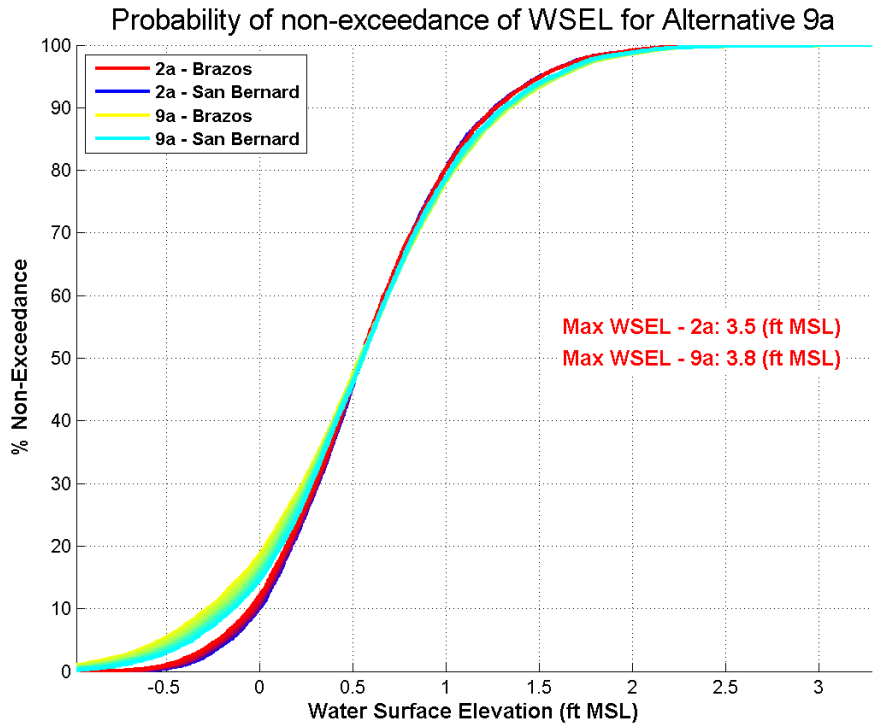

Figure 42. Probability of water level non-exceedance in West GIWW for Alternative 9a.

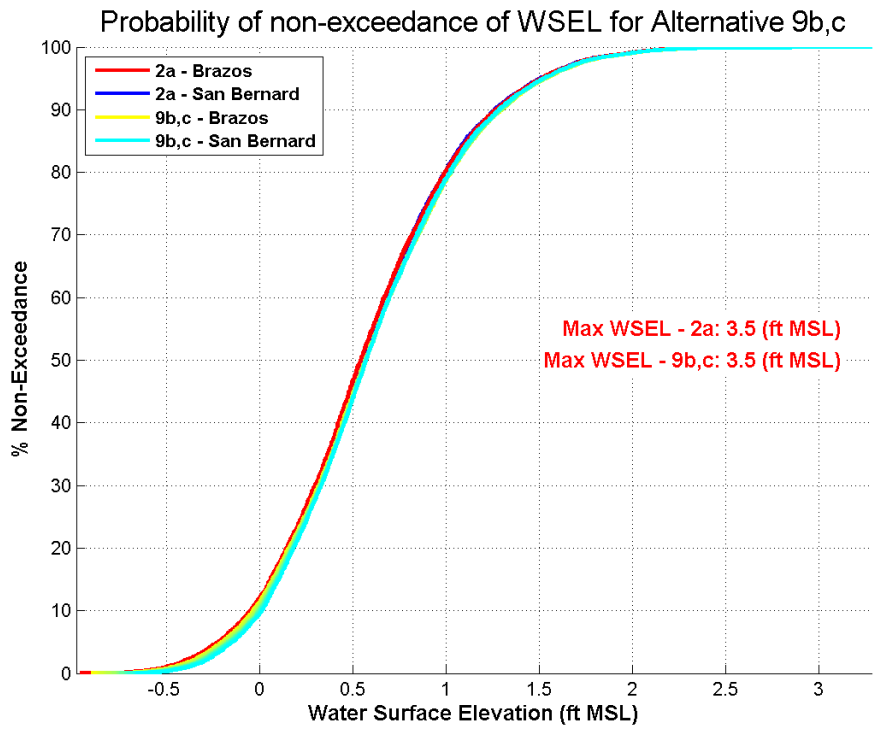

Figure 43. Probability of water level non-exceedance in West GIWW for Alternatives 9b and 9c (negligible difference).

For alternatives that have an open channel connection to the Brazos River at the West GIWW (Alternative 3a.1 and Alternative 9a), the low water levels in the West GIWW are reduced while high water levels are slightly increased. Despite the slight increase in the highest 10% of water levels, the absolute peak water level for both these alternatives is only increased by 0.3-0.4 ft. Furthermore, these open channel alignments tend to cause an increased attenuation of low water levels from east to west as shown by the thickness of the non-exceedance curve. For Alternatives 3a, 9b, and 9c, the change in water level non-exceedance from Existing Conditions is negligible, and the absolute peak water level is unchanged. LiDAR data was examined along the west GIWW to determine whether this change could result in additional overtopping of the banks of the GIWW Bank elevations ranged from 3.5-4.0 ft. NAVD88, so the minor increase in peak water level is not expected increase overtopping of the GIWW banks.

There was additional concern that the open connection between the west GIWW and the Brazos River (i.e. Alternatives 9a and 3a.1) could cause elevated water levels in communities along the San Bernard River. Water levels were extracted near the communities of Rivers End and Sanders Road, which are approximately 1 mile and 5 miles upstream of the GIWW San Bernard River intersection respectively. Figure 44 and Figure 45 show the probability of non-exceedance curves for Alternative 3.a.1 and Alternative 9a compared with the Existing Conditions.

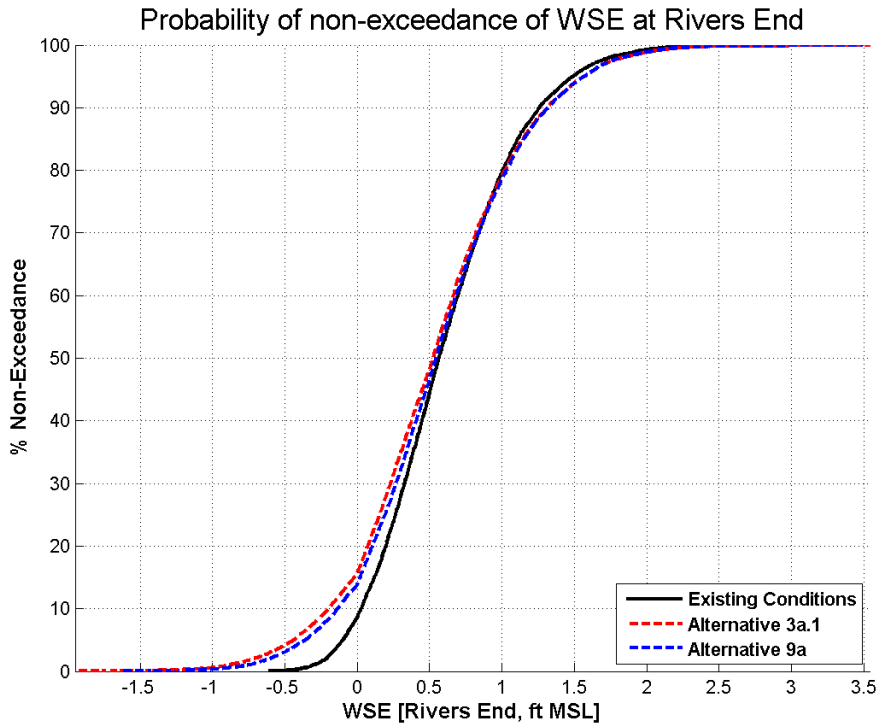

Figure 44. Probability of Non-Exceedance (PNE) for WSE [ft. MSL] at Rivers End.

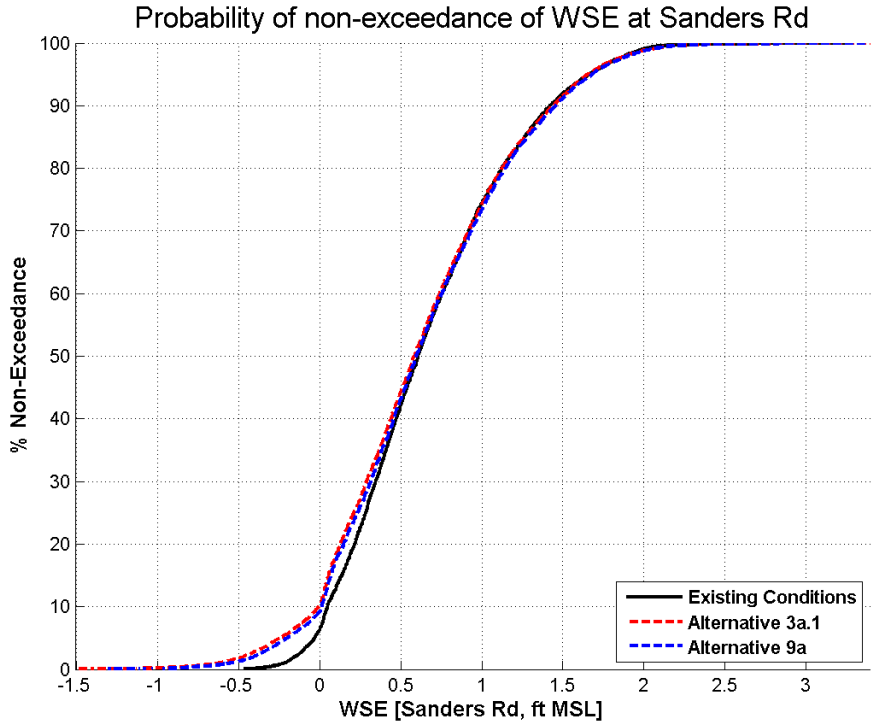

Figure 45. Probability of Non-Exceedance (PNE) for WSE [ft. MSL] at Sanders Rd.

Figure 44 and Figure 45 show reduced water levels for the lower 40% and similar water levels for the upper 60% at both communities along the San Bernard River. The San Bernard Rivers connection to the Gulf has silted in in recent years. The reduction of water surface elevations observed at low tide for Alternatives 3a.1 and 9a along the San Bernard River likely occurs due to the proposed open channel at the intersection of the west GIWW and Brazos River, which allows increased drainage of San Bernard flows, thereby reducing water surface elevations along the San Bernard. FEMA DFIRMS were also investigated to determine the base flood elevations of communities along the San Bernard River. DFIRMS indicate the areas of River's End and other communities up the river several miles are in the AE zone with Base Flood Elevations ranging from 12 to 14 ft. NAVDD88. Based on the above analysis, it is unlikely that Alternatives 3a.1 or 9a would have any adverse impacts to flooding and may to improve mitigate along the San Bernard River from fluvial events. It should be cautioned that the AdH circulation model was not calibrated or developed as a flood model, and the modeling was not conducted to determine flooding impacts.

3.2.1 Impacts on Relative Sea Level Rise on River Velocity

The impacts of Relative Sea Level Rise (RSLR) on river velocity are important to consider when analyzing the performance of the proposed alternatives. As later discussed in Section 6, the river velocity impacts navigability across the Brazos River and high river velocities can result in closures of the Brazos River Floodgates system. Therefore, the velocity for all alternatives for a RSLR scenario of +1.00 and +2.00 feet from existing conditions was extracted from the model results. Figure 46 shows probability of non-exceedance curves for river velocity in ft./s for all proposed alternatives. All alternatives show similar trends for the RSLR scenarios, with reduced velocities compared to existing conditions. Since the changes in river velocity appear to be uniform across all alternatives, it is unlikely that the outcome of a TSP selection will change based on RSLR.

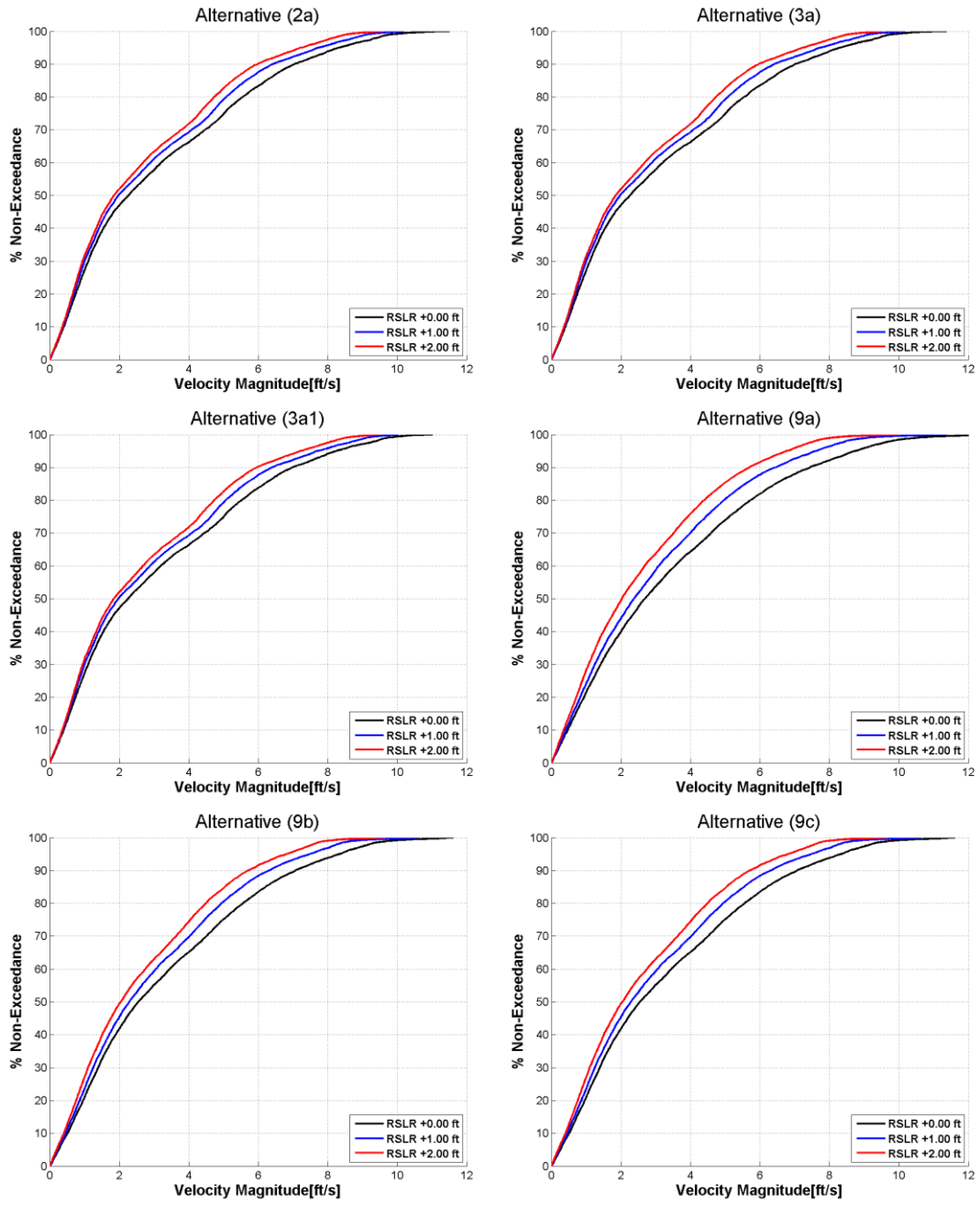

Figure 46. PNE of velocities extracted just north of the Brazos River Crossing for Existing Conditions/2a (top left) and all proposed alternatives for existing conditions, +1.0 ft. RSLR and +2.0 ft. RSLR.

3.3 Storm Surge Analysis

A Level 1 storm surge analysis was conducted using a design storm methodology. A Design storm needs to be developed based on the understanding of project site conditions for the 100-yr event. Storm surge modeling involved developing a model representative of the hydrodynamics. This model was then calibrated and validated to the historical data described in Section 2.1.1.3. Once calibration and validation simulations were conducted, a Design storm simulation was developed that provides a storm surge elevation equal to the 100-yr water

surface elevation in the project vicinity. This same Design storm was then simulated to evaluate potential changes to storm surge at the project vicinity and to generate design conditions for the alternative gate structures.

3.3.1 Mesh Development & Model Setup

It was determined that utilizing existing validated meshes would be the most efficient procedure to develop a working mesh. However, none of the existing meshes collected were completely suitable for the project's need. The existing meshes would either require extensive computation time due to the resolution or didn't include enough resolution within the project area. In order to gain the most accurate results for storm surge for the project site, high resolution is required in the upland area surrounding the project site. Therefore, the unstructured mesh used for the storm surge modeling for this study was creating using a combination of two validated meshes - EC95d mesh and the TX2008 mesh. The overall mesh is shown in Figure 47, which displays the variation in resolution (the highest being near the project site). As seen in Figure 48 the resolution becomes more refined closer to the project area. The open ocean resolution is as high as approximately 98 km. The mesh at the project site has a resolution of approximately 65 m or 213 ft. The resolution was refined to approximately 35 ft for analyzing alternative designs in order to resolve the various designs of the flood gates. The final merged mesh contains 525,332 nodes.

The current bathymetry of the modeling mesh has been extracted from the TX2008 mesh. The bathymetric surface was updated with the latest bathymetric and topographic data available near the project site, as described in Section 2.1.1.3.

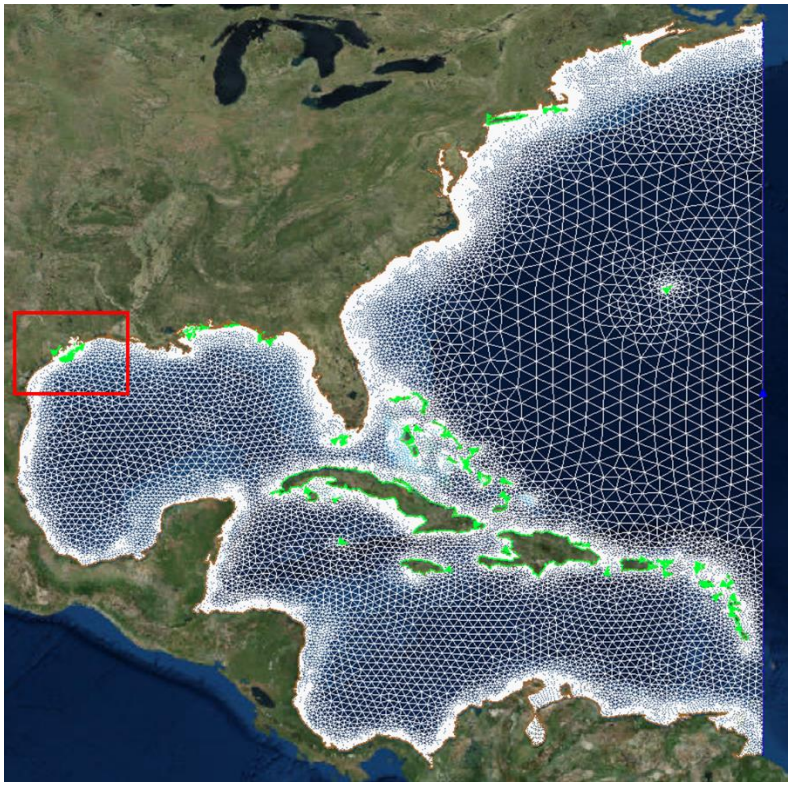

Figure 47. Full mesh domain.

Figure 48: Resolution of Mesh at Project Site (approximately 65 m or 213 ft)

3.3.2 Model Calibration & Validation

A hindcast of Hurricane Claudette was simulated in order to calibrate the model. The wind field for the model was an asymmetric Holland vortex model created using the BestTrack data that the National Hurricane Center stores for each hurricane. The parameters used in the model include location of the eye of the storm, distance to the 34 knot winds in each of the 4 quadrants of the storm, max wind velocity, and radius to the maximum winds. The length of the model was 7 days, which allowed the storm to enter the Gulf from the Atlantic and lasts until after the storm made landfall. The maximum water surface elevation near the project site is shown Figure 49. The figure shows Hurricane Claudette cause significant overland flooding in the project area.

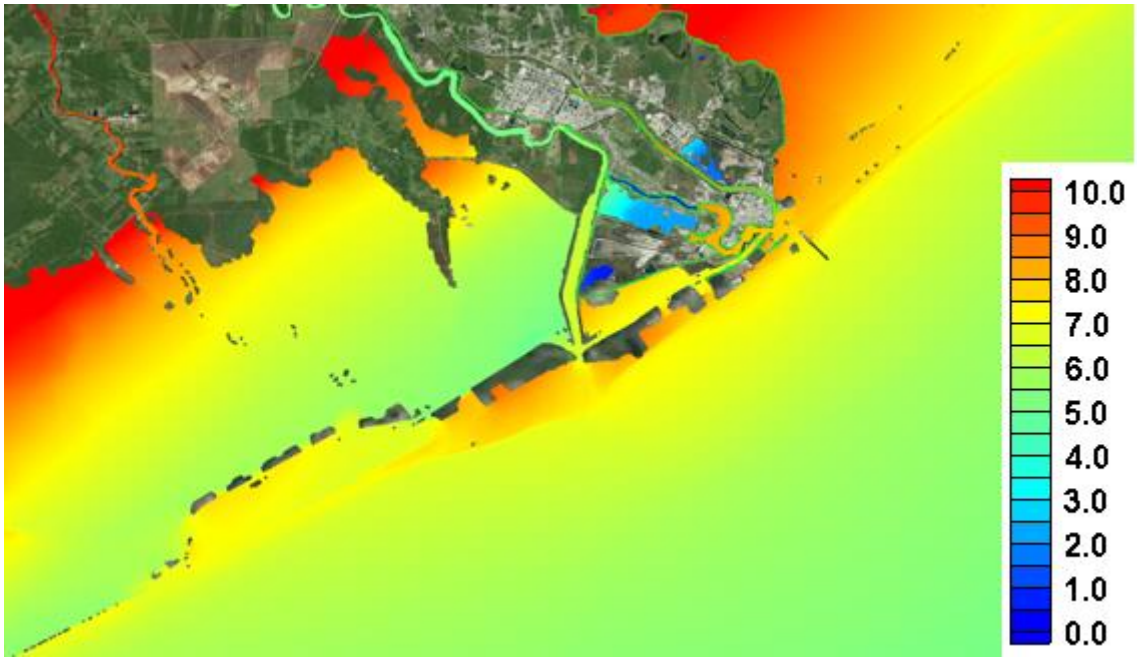

Figure 49. Maximum modeled water surface elevation from Hurricane Claudette (ft MSL)

To quantify the accuracy of the model, the maximum water level was extracted at the same location of the high-water marks as discussed in Section 2.1.1.3. A comparison of the measured vs modeled high water marks are show below in Table 14.

Table 14: High Water Mark Comparison (Modeled vs. Measured)

Gage	Lat.	Long.	Measured (ft MLLW)	Modelled (ft MLLW)	Difference (ft)	% difference
Clear Lake	29.5633	-95.0667	5.63	5.78	-0.15	-3%
Galveston South Jetty	29.3267	-94.6917	8.74	5.33	3.41	39%
West Bay	29.1443	-95.1596	5.23	6.41	-1.18	-22%
Colorado River Bypass	28.68444	-95.9689	5.56	4.54	1.02	18%
Freeport	28.95083	-95.3386	9.15	8.60	0.55	6%
Moses Lake/Galveston Bay	29.44722	-94.92	4.9	4.26	0.64	13%
Highland Bayou	29.36	-95.0394	5.77	7.01	-1.24	-21%
Bob Hall Pier Corpus Christi	27.58	-97.2167	2.75	2.49	0.26	9%
Eagle Point	29.48	-94.9183	4.22	4.15	0.07	2%
Freeport Jetty	28.94333	-95.3017	5.14	7.47	-2.33	-45%
Galveston North Jetty	29.35667	-94.725	4	4.92	-0.92	-23%
Galveston Pier 21	29.31	-94.7933	3.71	3.81	-0.10	-3%
Galveston Pleasure Pier	29.285	-94.7883	5.28	5.59	-0.31	-6%
Morgans Point	29.68167	-94.985	4.96	5.53	-0.57	-11%

For the most part, the model calibrated very well (within 20%) when compared to the measured data. The two biggest trouble areas are at the Freeport and Galveston South Jetty inlets where. The differences of the values at these two points could possibly be attributed to a varied bathymetry from the time of the storm, which occurred in 2003 and the model bathymetry which was created in 2008. Sedimentation and erosional forces are the highest in the inlets themselves during storm events, which lead to highly varying bathymetry from one year to the next. While the water levels at the inlet did not produce good calibration, overland water elevations generally matched quite well. These inland elevations are the focus of the work and considered the most important. Based on the results from the other points compared the grid looks to be reasonably calibrated for future use in the project as modeled surge elevations match measured to a similar degree as published flood studies.

A hindcast of Hurricane Carla was run to validate the model. The wind field developed for the Hurricane Carla model was an asymmetric Holland vortex model. The comparison of the measured vs modelled high water marks is shown in Table 15. The model validates very well (within 10%) near the project area. The Galveston Pleasure Pier and Pier 21 did not validate well, but this area was also poor in the calibration of the model. The results of the validation at the project site indicate that the model is validated for use in future simulations.

The hurricane modeling effort was performed to analyze extremal water surface elevations at the project site and did not include calculation of extremal wave conditions. Therefore, the coupled ADCIRC-SWAN model was not calibrated for offshore wave heights. The model reasonably simulates water surface elevations near the project site, however the model is limited in its ability to predict offshore water surface elevations or wave heights. Any results in this area should be applied with caution.

Table 15: High Water Mark Comparison (Modeled vs. Measured)

Gage	Latitude	Longitude	Measured (ft MSL)	Modelled (ft MSL)	Difference (ft)	% difference
Rollover Pass	29.515	-94.5133	9.6	9.3	-0.3	-3%
Colorado River Bypass	28.68444	-95.96889	15.2	16.0	0.8	5%
Freeport	28.94333	-95.30167	13.4	13.7	0.3	2%
Galveston Pier 21	29.31	-94.79333	8.8	10.5	1.7	19%
Galveston Pleasure Pier	29.285	-94.78833	9.3	12.8	3.5	38%
Morgans Point	29.68167	-94.985	13.8	12.5	-1.3	-9%
Brazos flood gates west			10.9	10.9	0.0	0%
Brazos flood gates east			10.9	11.3	0.4	4%

3.3.3 Storm Surge Alternatives Analysis

The calibrated storm surge model described in the previous Section was used to simulate velocity and water surface elevation for each of proposed alternative alignments. Any increase in water elevation for each alternative will be used to show where the potential for additional flooding may occur.

To determine the impacts of the proposed alternatives, a synthetic storm was developed that represented the 100-yr. surge event at the project location, based on FEMA base flood elevations. The FEMA base flood elevation for the project site was used to determine the 100-yr. surge level, which is approximately 11 ft. MSL. The modeled maximum water surface elevation for the design storm is shown in Figure 50. Note the water surface elevations at the project site, which are approximately 11 ft. MSL.

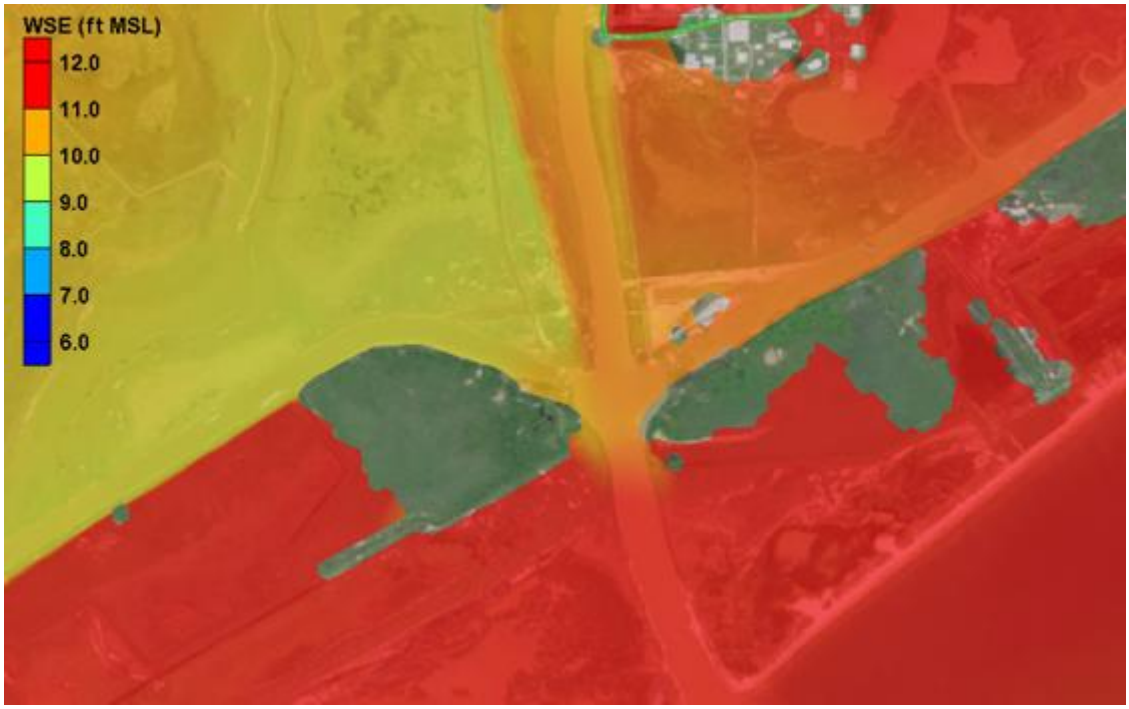

Figure 50: Maximum Water Surface Elevation (ft MSL) for design storm.

The maximum velocities resulting from the design storm are shown in Figure 51. The maximum velocity for each alternative is shown in Table 16. The higher velocities are along the elevated levees that surround the project area and through the proposed floodgate structures. Alt 3a.1 has lowest velocity on the West side of the Brazos while Alt 2a has the lowest velocity on the East side of the Brazos. In general, the velocities are higher for the proposed alternative when compared to the existing conditions, with Alts 2a and 3a.1 having the closes velocities to

existing conditions. Alts 3a and 9b have the highest velocities at the structures.

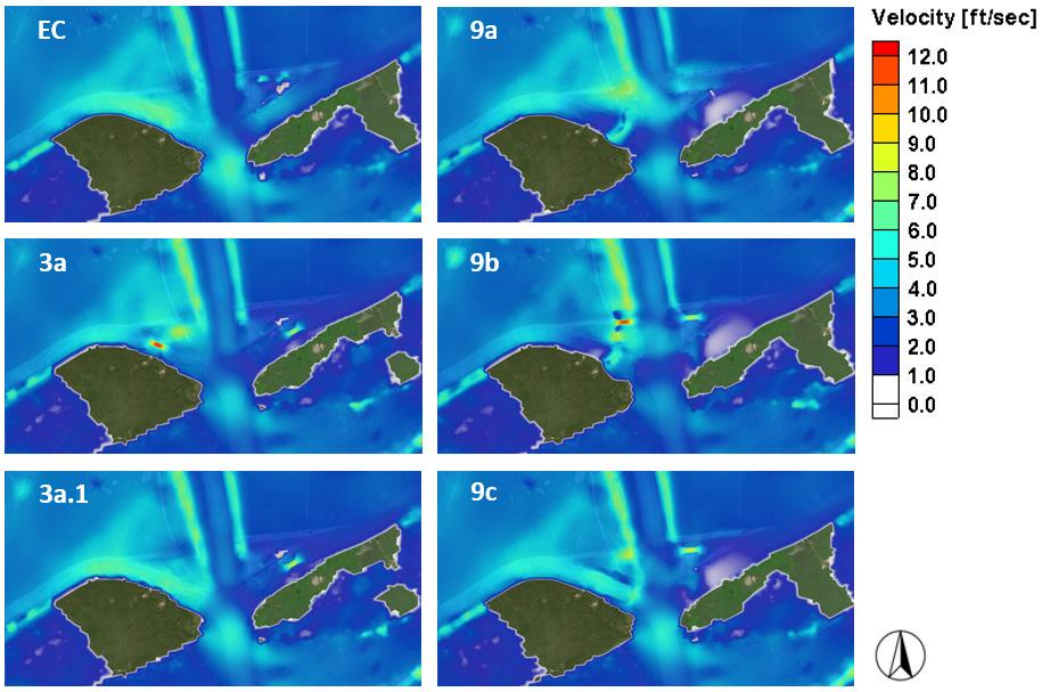

Figure 51: Maximum velocity [ft/sec] at the Brazos River from Storm surge runs.

Table 16: Maximum velocity at proposed or existing structures

	West GIWW Vel. [ft/s]	East GIWW Vel. [ft/s]
EC/2a	6.2	3.6
3a	11.5	7.0
3a.1	5.9	7.7
9a	6.9	4.3
9b	11.1	7.4
9c	7.6	8.2

Any increase in the maximum water level compared to existing conditions are shown in Figure 52. The largest increases in surge occur in the alternatives where the gate structures were moved. This is cause by the buildup of water around the structures behind the design storms. Alternatives 3a and 9b cause a larger increase in water elevation than the other alternatives. These alternatives increase the surge near the South of the GIWW near Freeport inlet. All the other alternatives do not cause an increase in surge in any inhabited areas. Alts 3a.1 and 9c performed the best out of the alternatives by limiting the increase of water elevation in surrounding areas.

Figure 52: Increase in Water Surface Elevation [ft] from Existing conditions.

The maximum change that occurs due to the implementation of the TSP is 1.3 feet. This change is located at the edge the new gate 125' gate structure monolith in the GIWW east of the Brazos river crossing. The increase in WSE here is due to water piling against the monolith, which was previously open water. This change is expected and does not change the conclusion that the TSP has very minimal impacts to storm surge inundation. Outside of this point, the average increase in water surface elevation over the shaded area shown in Figure 52 is 0.2 feet, and the maximum increase is approximately 0.9 feet. The maximum increase occurs on the southern edge of the GIWW abutting the placement areas. The design storm analysis shows that the proposed TSP (Alternative 3a.1) has minimal impacts during storm surge events.

4 Salinity Analysis

4.1 Introduction

Salinity was modeled for Existing Conditions all alternatives to assess potential impacts of the project on the possible changes to salinity in the system resulting from the proposed alternatives. Salinity was modeled using ADH for the same 13-month validation period described in Section 3.1.5.

A 2-D model was selected for salinity analysis at the project site. A 2-D approach was selected as a reasonable approximation of the system that would be sufficient for supporting plan selection. A review of a review of Carlin et al., 2015, was conducted to determine whether a 3-D model would be necessary to accurately capture salinity, and salinity driven hydrodynamics at the project site. Carlin et al., 2015 study focused on the influence of a salt wedge on sedimentation in the Brazos River itself rather than on sedimentation in the adjacent GIWW. Carlin (2015) states that the salt wedge does not exist when the Brazos River Flow is more than 405 m3/sec (approximately 14,000 cfs). Analysis of the behavior of sedimentation in the Brazos River and GIWW as a function of Brazos River flow rate is shown in Figure 78. The Brazos Basin shows increasing sedimentation with flow up to approximately 10,000 cfs and decreasing sedimentation into erosion as the flow increases from there, which match the trends described in the Brazos River described by Carlin (2015). Conversely, the GIWW east and west show a linear increase in sedimentation approximately proportional to the increase in flow rate, so that increasing flow rate continues to increase sedimentation in the GIWW. Further, as shown in Figure 62, when the flow rate in the Brazos River is low (a prerequisite for salt wedge intrusion), the sediment load is also low and thus plays less of a role in the total long-term sedimentation rate. It is likely that the absence of a salt wedge in the model will make for more conservative results since sediment which would otherwise settle in the Brazos River due to the salt wedge can instead settle in the GIWW. Therefore, it is unlikely that capturing the salt wedge via 3-D salinity modeling would affect plan selection. For these reasons the team chose to develop a 2-D salinity model, as described in this Section.

4.2 Data Collection

Salinity is recorded at a 15-minute frequency at a location east of the east gate at USGS Station 08117300. These measured data were used to validate the salinity model.

4.3 Model Setup

A 1-year spinup simulation was run to determine the initial salinity distribution for the 13-month simulation. The spinup run was initiated with a salinity concentration of 0 ppt in the Brazos and San Bernard Rivers, 20 ppt in the GIWW and attached estuaries, and 33 ppt in the Gulf. The salinity distribution at the end of the spinup run is shown in Figure 53, and this distribution was used as an initial condition for the 13-month simulation.

The model was run with a boundary concentration of 0 ppt at both river boundaries and 33 ppt at the offshore boundary.

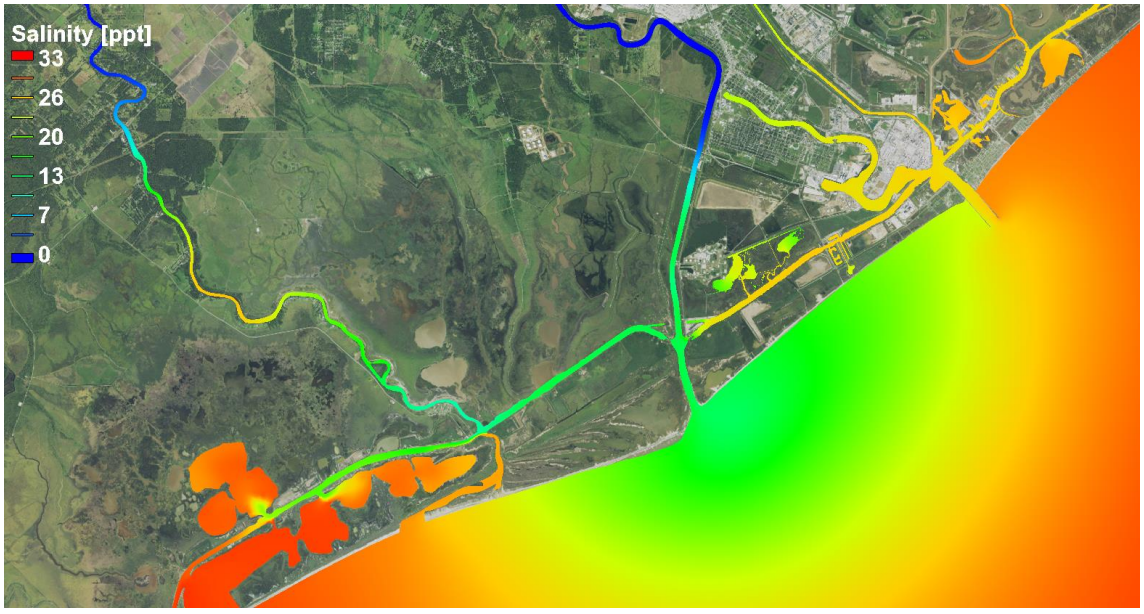

Figure 53. Initial salinity concentration in the model domain.

4.4 Results

The salinity model was validated with the measured data at USGS Gage 08117300 (Figure 54). The model captures the trends associated with the flow rates in the Brazos River (e.g. Salinity drops abruptly during a flood event and gradually recovers during low flow conditions). Inaccuracies in the salinity model are likely due to assumptions in modeling gate operations, which controls the flow of fresh water into the GIWW from the Brazos River. The model is considered validated to sufficiently explain salinity variations in the system.

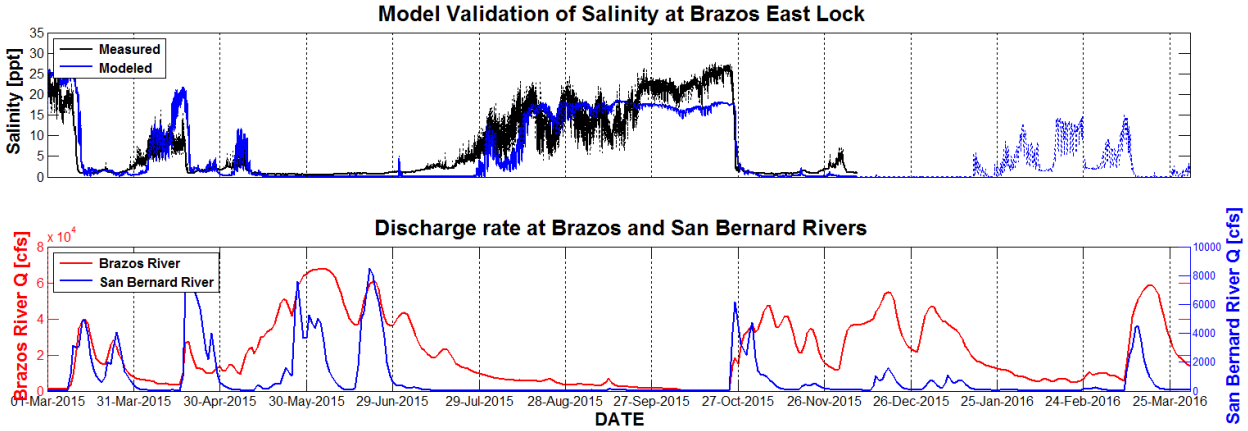

Figure 54. Validation of Salinity at USGS gage 08117300 (top) and flow rates in the Brazos and San Bernard Rivers (bottom).

Table 17 and Table 18 show the average salinity in each of the impact zones for low freshwater flow (summer: June – August) and high freshwater flow (late fall: October – December) respectively. In general, Alternatives 3a.1, 9a, 9b, and 9c tend to reduce the salinity in all zones of influence, while alternative 3a causes minimal changes to salinity. Figure 55 through Figure 59 show the difference in mean salinity between Existing Conditions and Alternatives 3a, 3a.1, 9a, 9b and 9c respectively for both summer and late fall time periods. This is due to larger gates

(or lack of gates for Alt 9a) which leads to greater exchange from the Brazos River into the GIWW.

Table 17. Mean salinity (and change for alt-existing) [ppt], October – December

Alternative	West GIWW	Brazos Basin	East GIWW	Freeport Channel
Existing	5.7	1.7	5.0	15.0
3a	6.1 (0.4)	2.2 (0.6)	3.9 (-1.1)	14.6 (-0.4)
3a.1	3.9 (-1.8)	2.1 (0.4)	5.2 (0.3)	15.2 (0.2)
9a	3.7 (-2.0)	2.3 (0.6)	3.9 (-1.0)	9.7 (-5.3)
9b	4.2 (-1.5)	1.9 (0.2)	3.7 (-1.2)	12.8 (-2.3)
9c	4.2 (-1.5)	2.1 (0.4)	3.6 (-1.4)	12.7 (-2.3)

Table 18. Mean salinity (and change for alt-existing), June – August.

Alternative	West GIWW	Brazos Basin	East GIWW	Freeport Channel
Existing	3.1	0.4	3.8	15.0
3a	3.0 (-0.2)	0.6 (0.2)	2.5 (-1.2)	14.6 (-0.4)
3a.1	0.9 (-2.2)	0.2 (-0.2)	2.6 (-1.1)	15.1 (0.1)
9a	1.5 (-1.6)	0.2 (-0.2)	0.3 (-3.4)	9.9 (-5.1)
9b	2.3 (-0.8)	0.4 (-0.0)	1.7 (-2.1)	12.1 (-2.9)
9c	2.2 (-0.9)	0.5 (0.0)	1.7 (-2.1)	12.1 (-2.8)

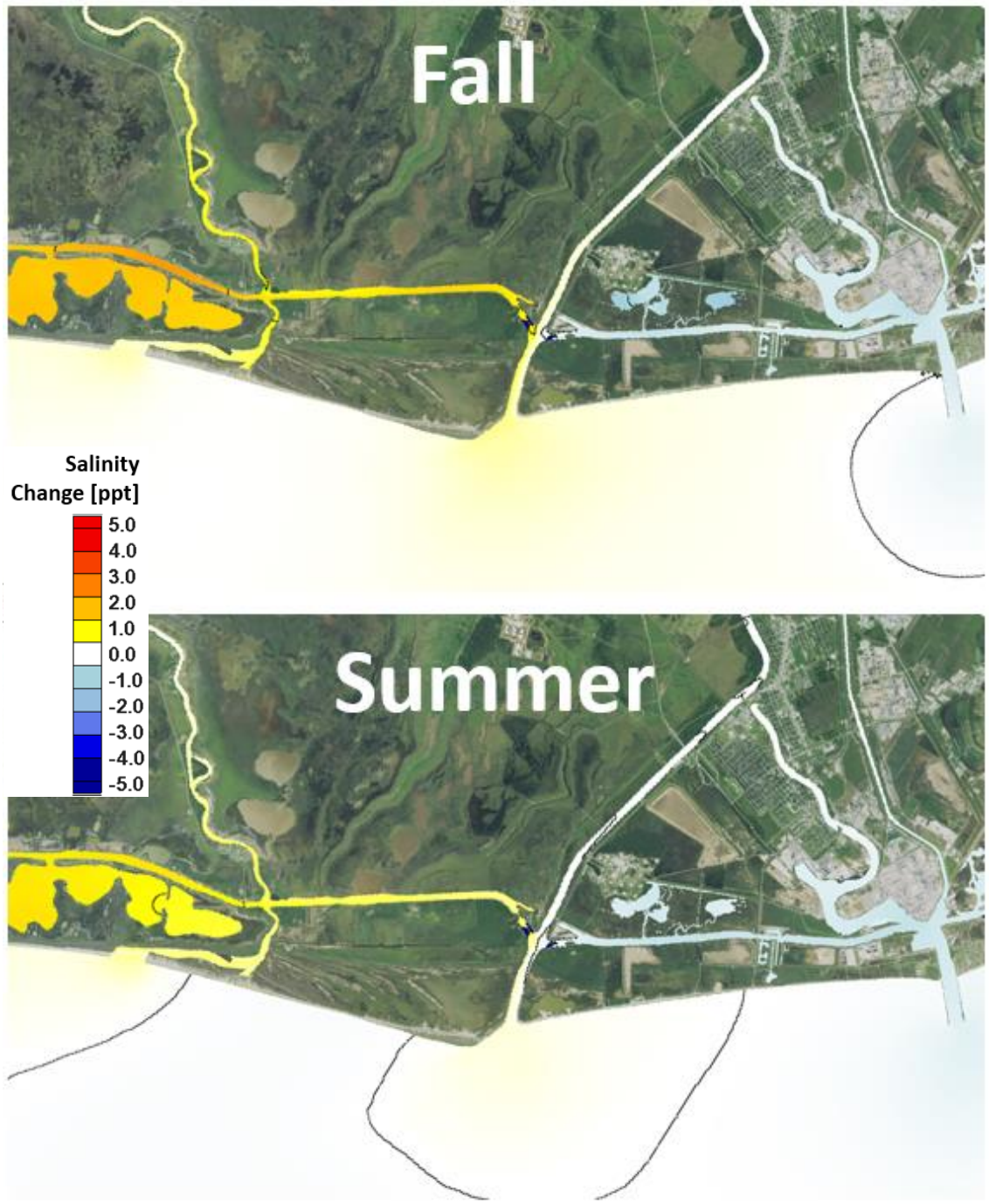

Figure 55. Change in mean salinity for summer and late-fall between Existing Conditions and Alternative 3a.

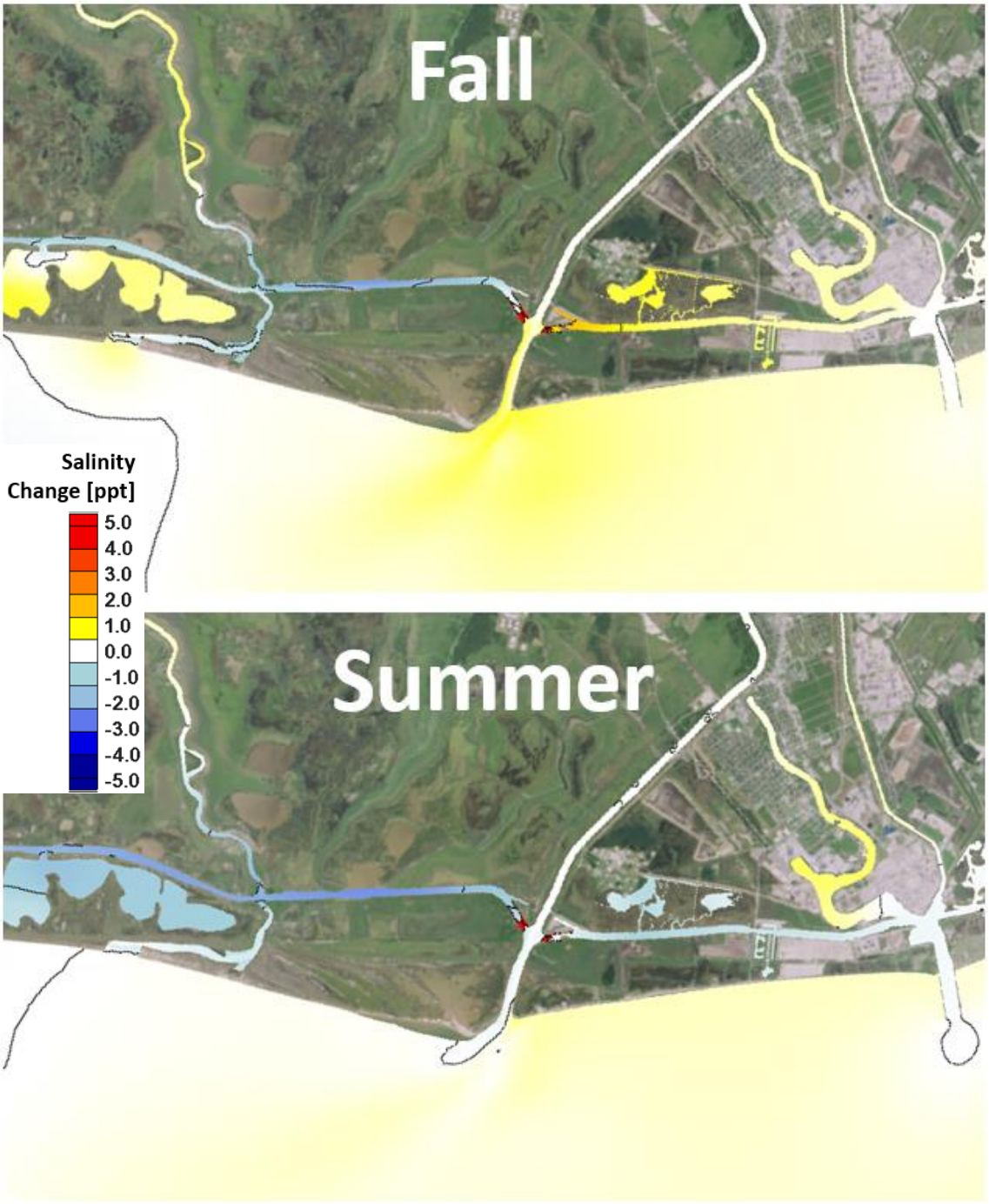

Figure 56. Change in mean salinity for summer and late-fall between Existing Conditions and Alternative 3a.1.

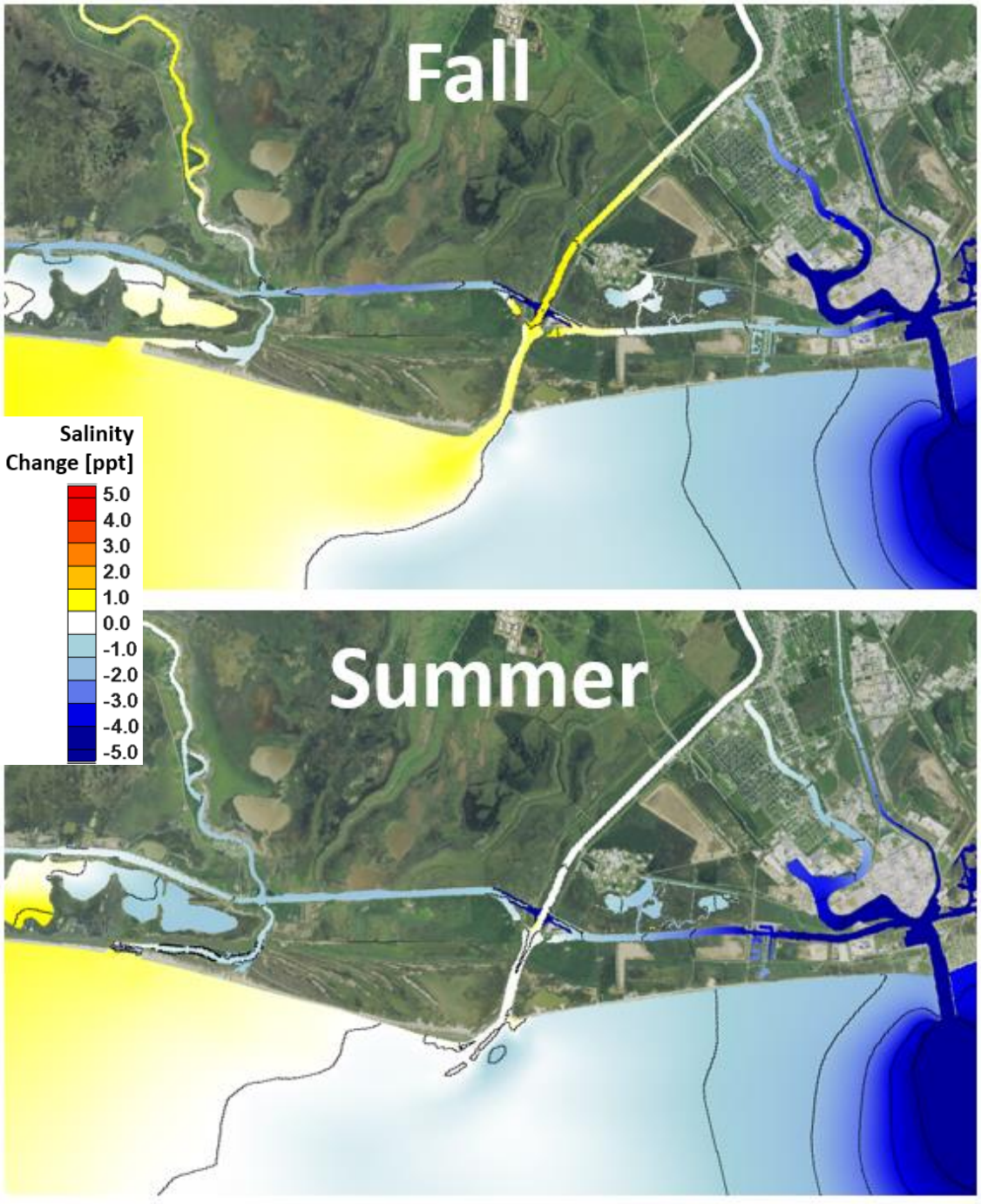

Figure 57. Change in mean salinity for summer and late-fall between Existing Conditions and Alternative 9a.

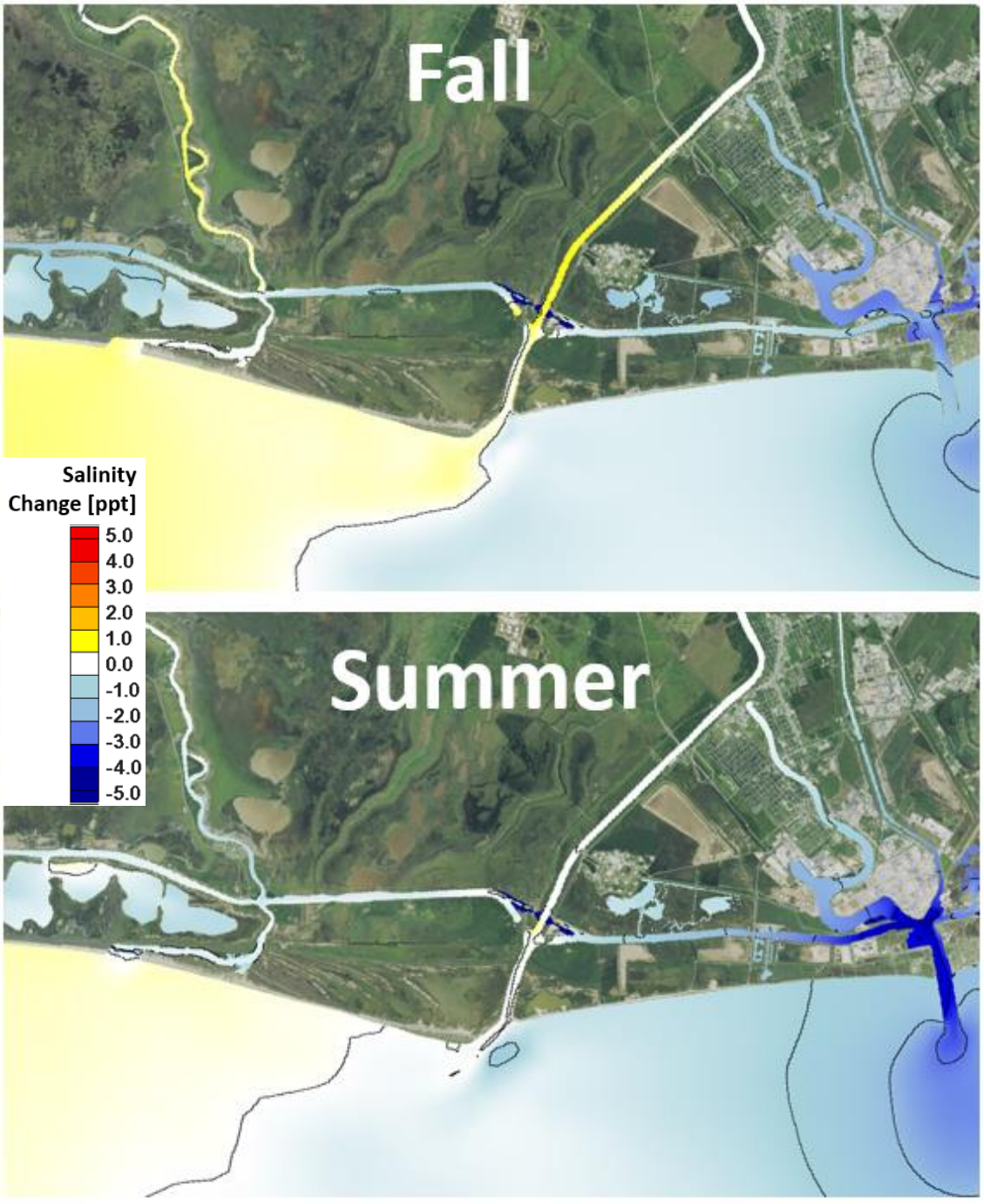

Figure 58. Change in mean salinity for summer and late-fall between Existing Conditions and Alternative 9b.

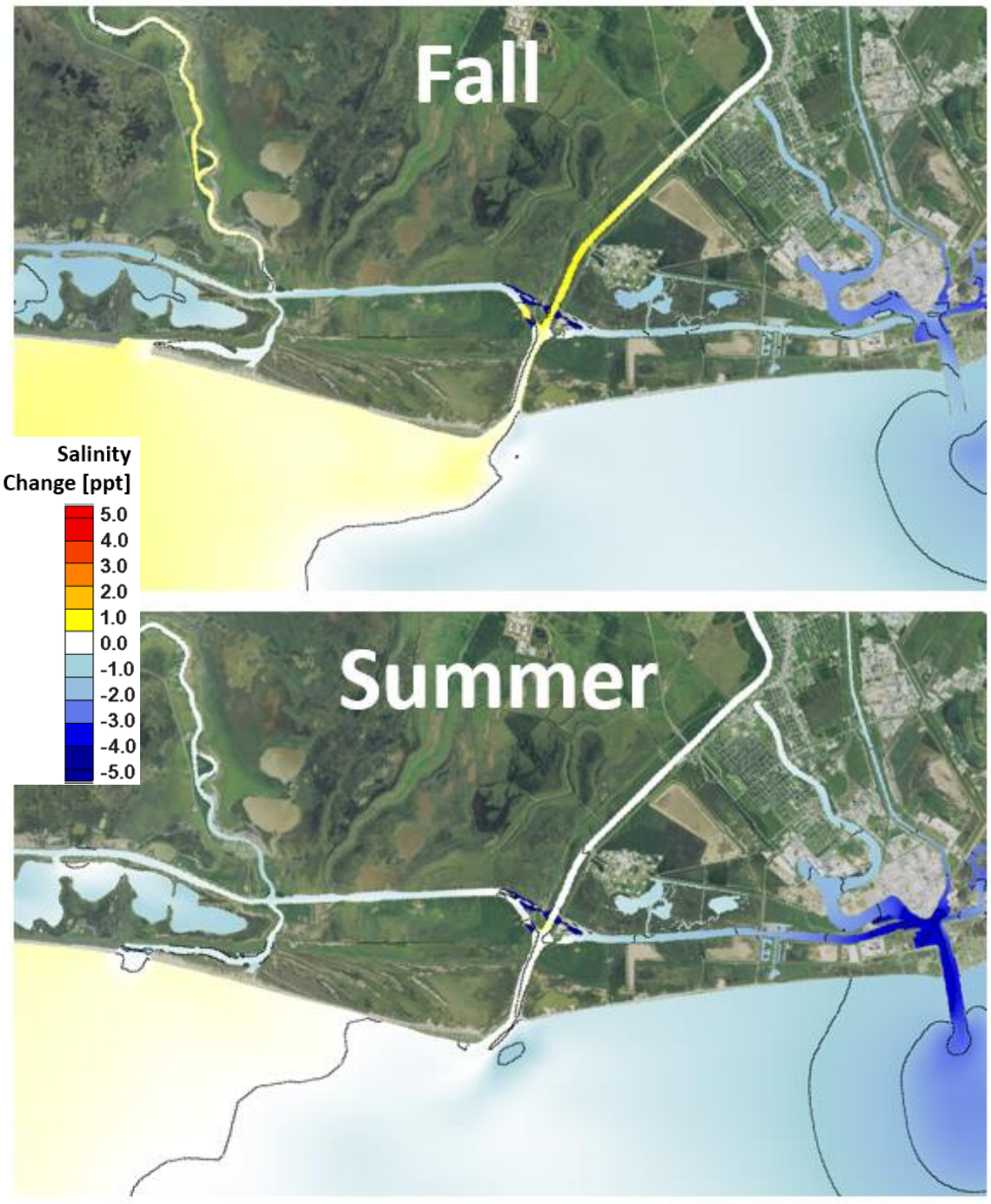

Figure 59. Change in mean salinity for summer and late-fall between Existing Conditions and Alternative 9c.

4.5 RSLR Salinity Results

Additional salinity simulations were run with potential relative sea level rise conditions of +1 ft. and +2 ft. for each proposed alternative. The results of the simulations are summarized in Table 19.

Table 19. Influence of relative sea level rise (RSLR) on seasonal average salinity in each zone of influence for all proposed alternatives. Salinity concentrations in ppt.

		Fall			Summer		
		RSLR=0	RSLR=1	RSLR=2	RSLR=0	RSLR=1	RSLR=2
Existing Conditions	West GIWW	5.7	5.3	4.5	3.1	4.7	4.2
	Brazos Basin	1.7	1.1	0.6	0.4	0.4	0.3
	East GIWW	5.0	4.2	2.9	3.8	2.8	2.5
	Freeport	15.0	16.4	16.4	15.0	17.0	17.7
Alternative 3a	West GIWW	6.1	5.1	4.0	3.0	4.1	4.2
	Brazos Basin	2.2	1.5	0.9	0.6	0.7	0.5
	East GIWW	3.9	3.8	1.5	2.5	2.1	1.2
	Freeport	14.6	15.4	15.2	14.6	15.9	16.3
Alternative 3a.1	West GIWW	3.9	-	2.5	0.9	-	1.6
	Brazos Basin	2.1	-	1.2	0.2	-	0.3
	East GIWW	5.2	-	3.2	2.6	-	2.0
	Freeport	15.2	-	15.4	15.1	-	16.3
Alternative 9a	West GIWW	3.7	3.5	2.7	1.5	3.6	1.8
	Brazos Basin	2.3	2.0	1.5	0.2	0.9	0.3
	East GIWW	3.9	3.6	3.3	0.3	0.2	0.2
	Freeport	9.7	9.2	9.1	9.9	9.3	8.8
Alternative 9b	West GIWW	4.2	4.2	3.9	2.3	3.8	3.3
	Brazos Basin	1.9	1.4	0.9	0.4	0.8	0.5
	East GIWW	3.7	2.9	1.3	1.7	0.8	0.4
	Freeport	12.8	13.1	13.2	12.1	12.8	13.2
Alternative 9c	West GIWW	4.2	4.3	2.4	2.2	3.5	2.3
	Brazos Basin	2.1	1.7	1.0	0.5	0.9	0.3
	East GIWW	3.6	2.8	1.5	1.7	0.9	0.5
	Freeport	12.7	13.2	13.5	12.1	12.9	13.6

*Due to time constraints, the RSLR=1 condition was not simulated for Alternative 3a.1

In general, the average salinity in the West GIWW tends to decrease with rising sea level during the fall, but increase with rising sea level in the summer. In the Brazos Basin, the average salinity also tends to decrease with rising sea level during the fall, but in the summer the salinity is mostly unchanged. In the East GIWW there is a significant decrease in salinity for all alternatives, while in Freeport, except for Alternative 9a, there is an increase in salinity with rising sea level for both the fall and summer months. The decrease in salinity in Freeport for Alternative 9a is likely due to the open channel connection between the Brazos River and the East GIWW.

5 Sedimentation Analysis

To determine the potential impacts of the project on sedimentation patterns and volumes in the GIWW, a thorough sedimentation study was carried out. This study included review of available surveys and dredge records, analyzing sediment grab samples, generating suspended sediment rating curves from available measured data, and developing a calibrated sedimentation model.

5.1 Site Conditions

5.1.1 Sediment Sampling

Sediment grab samples were collected and analyzed at ten locations near the project site, identified as BR-01 – BR-10 in Figure 60. The grab sample locations span from approximately 4.5 miles west of the San Bernard River – GIWW intersection to the intersection of the GIWW with the Freeport Harbor. The grab samples were analyzed for grain size distribution and liquid/plastic limits. The average sediment class distributions, as well as the median grain size diameter is shows in Table 20.

Figure 60. Locations of sediment grab samples.

Table 20. Grab sample sediment class distributions and median grain size.

Sample	% Silt	% Clay	% Sand	D50 [mm]
BR-01	37.9	60.1	2.1	0.0021
BR-02	36.0	60.0	4.0	0.0028
BR-03	42.9	51.1	6.0	0.0046
BR-04	51.1	43.2	5.8	0.0089
BR-05	55.0	29.4	15.7	0.0347
BR-06	71.4	21.3	7.4	0.0369
BR-07	62.3	31.5	6.2	0.0234
BR-08	64.0	26.9	9.1	0.0345
BR-09	50.7	44.3	5.1	0.0077
BR-10	49.6	47.1	3.3	0.0061

As shown in Figure 61, the fraction of clay in the grab sample tends to increase farther away from the Brazos River. This is logical, as clay particles have a lower settling velocity, and thus can travel farther from the source (the Brazos River) before depositing. By the same reasoning, the fraction of sand is greatest near the Brazos River – GIWW intersection, and peaks at 15% just to the west of the west gate. Most of the sediment in the GIWW contains less than 7% sand

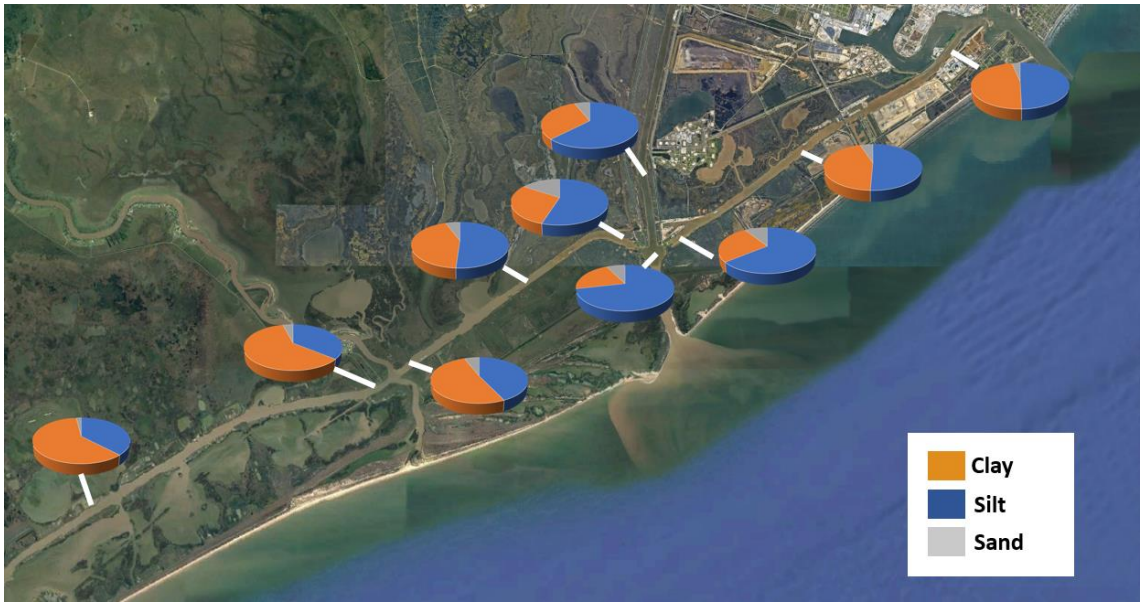

Figure 61. Grab sample sediment class distributions.

5.1.2 Suspended Sediment Concentrations

Historical suspended sediment concentration (SSC) was recorded in the Brazos River at USGS Station 08116650 at an approximately monthly frequency between 1973 and 1981, and again between 2008 and 2015. Historical SSC was also recorded in the San Bernard River at USGS Station 08117500 at approximately the same frequency between 1978 and 1987. Each measured sediment concentration was compared with its corresponding average river discharge, and the data were fit to an exponential regression curve. Figure 62 and Figure 63, show the sediment load curves for the Brazos and San Bernard Rivers respectively. These

curves were used to determine suspended sediment concentrations at the model boundary in Section 5.1.5. Note the scatter in the data spans at least an order of magnitude in concentration.

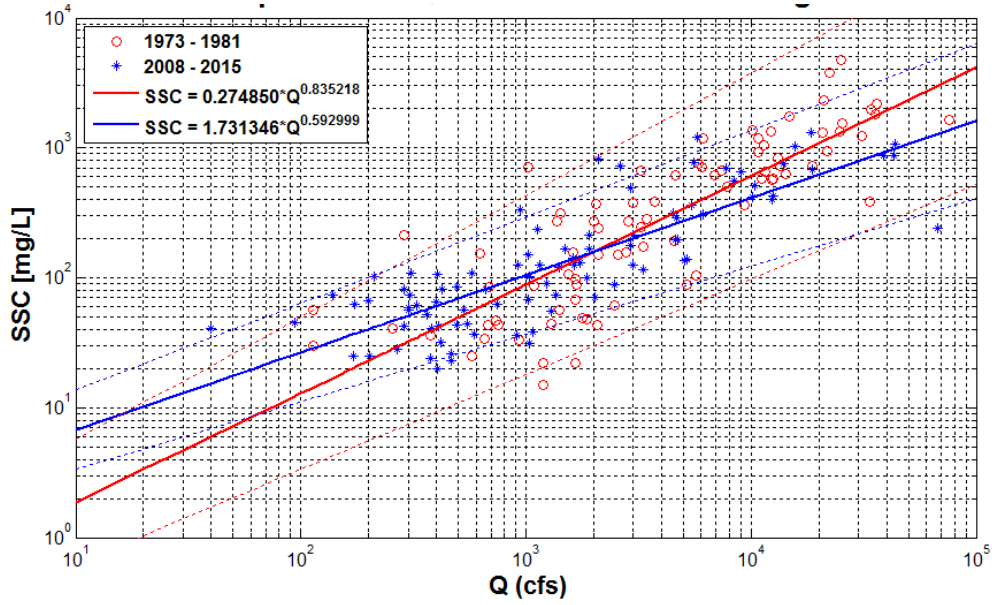

Figure 62. Sediment load curve at Brazos River, Rosharon gage based on measured data. 95% confidence intervals shown as dotted lines.

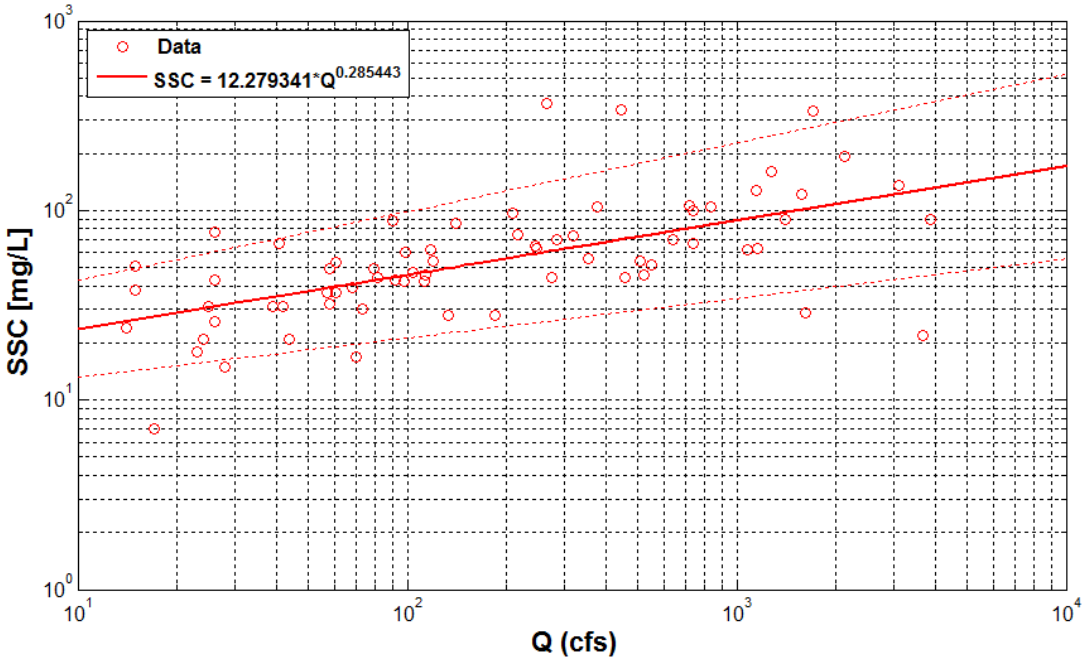

Figure 63. Sediment load curve at San Bernard Boling gage based on measured data. 95% confidence intervals shown as dotted lines.

5.1.3 Dredging History

To develop an understanding of sedimentation in the project vicinity, both historical bathymetric surveys and corresponding dredging history is required. Bathymetric surveys of the GIWW channel were obtained from the USACE within the project area (USACE, 2016). The surveys provided by the USACE document either existing (EX) conditions, before dredging (BD)

conditions, or after dredging (AD) conditions. Thus, dredging activities within the GIWW channel occurred during the duration between each BD and AD survey sets. Sedimentation rate can be inferred by comparing surveys where no dredging occurred between them (for example, comparing the BD survey to the preceding AD survey). The survey data from 2012 through 2016 was investigated along the stretch of the GIWW extending from Station 566+000 to Station 615+000. See Figure 64 for the location of these Stations. Figure 65 displays the temporal and spatial coverage of all documented surveys within this section of the GIWW. In Figure 65, blue indicates EX surveys, green indicates BD surveys, and red indicates AD surveys. Most dredging activities within this section of the GIWW occurred during August – November in 2012, with localized dredging in 2015 and 2016. Based on these data sets provided by the USACE, it is assumed that no dredging was conducted from December 2012 to August 2016, except for a small dredging event in August 2015 between Station 587+500 and 588+500.

Figure 64. Station numbers along the GIWW channel alignment; survey and dredging data was investigated for the reach of channel extending from Station 566+000 to Station 615+000.

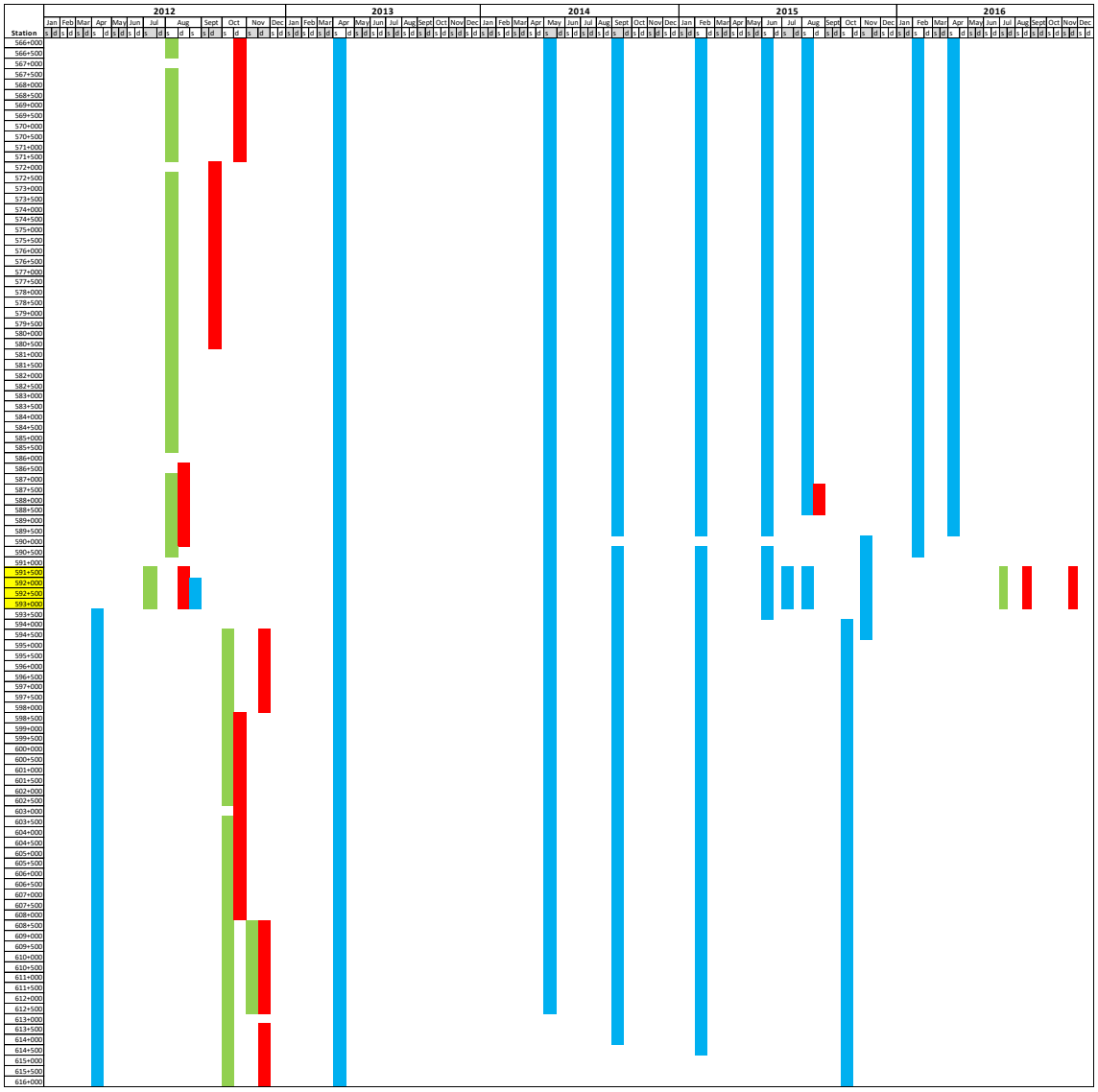

Figure 65. Summary of surveys and dredging activities from 2012 through 2016 along the reach of the GIWW channel from Station 566+000 to Station 615+000. Blue indicates surveys documenting existing conditions (EX); red indicates surveys documenting post-dredging conditions (AD); and green indicates surveys documenting pre-dredging conditions (BD).

5.1.4 Historical Sedimentation Analysis

To estimate the sedimentation rates within the project area, a preliminary analysis of historical sedimentation within the GIWW was performed using the available channel surveys documented in above. The most accurate sedimentation rates can be estimated by comparing AD surveys to their next consecutive BD surveys, as this comparison captures sedimentation that occurs after the channel is dredged to a known and measured dimension. However, due to the limited available AD to BD survey comparisons, consecutive AD to EX and EX to EX surveys were compared as well. Based on the available dredging history and discussions with the USACE Galveston District, it is assumed that no dredging activities occurred between consecutive EX surveys.

From Station 566+000 through Station 615+000, sedimentation rates were estimated in 1,000 LF segments, except in the region of the Brazos River Locks, between Stations 590+000 and 596+000, where the rates were estimated in 500 LF segments. Figure 66 displays a plot of the calculated average sedimentation rates along each Station, and the second column in Table 21 provides the sedimentation rate values. The third column in Table 21 shows sedimentation rates over a specified one-year period from March 2015 to April 2016; these sedimentation rates were used in the model calibration.

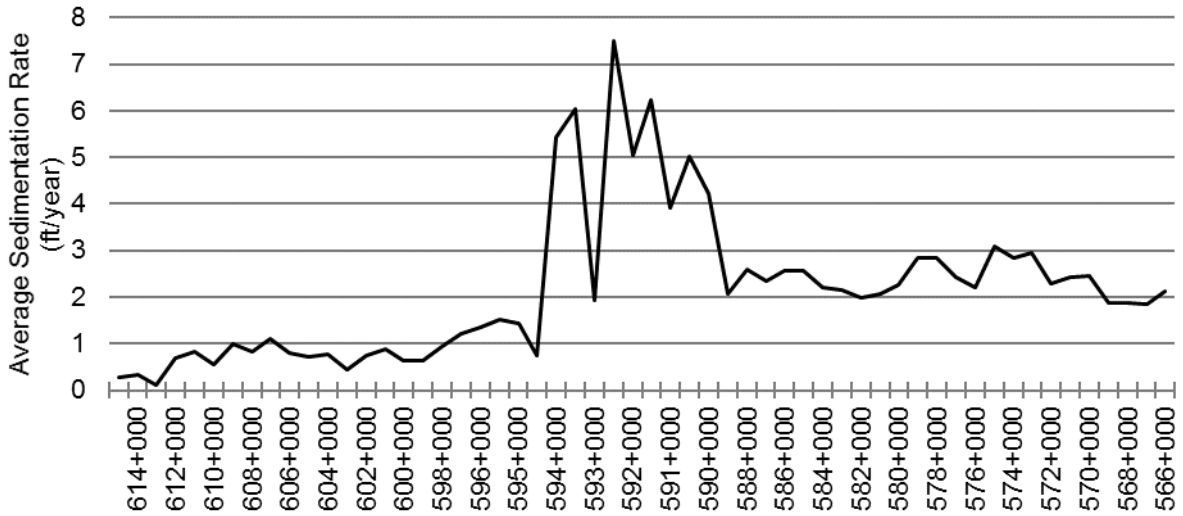

Figure 66. Sedimentation rates within the GIWW from Station 566+000 to Station 615+000 based on surveys from 2012 to 2016.

Table 21. Average sedimentation rates from Station 566+000 to Station 615+000 using survey data from 2012 through 2016. Note that cells stating No Data indicate areas where there were no consecutive surveys for the specified time period.

Start Station	2012 to 2016: Average Sedimentation Rate (ft./year)	March 2015 to April 2016: Average Sedimentation Rate (ft./year)
566+000	2.1	3
567+000	1.8	2.5
568+000	1.9	2.8
569+000	1.9	2.9
570+000	2.5	3.2
571+000	2.4	3.1
572+000	2.3	2.9
573+000	3	3.3
574+000	2.8	2.9
575+000	3.1	2.7
576+000	2.2	2.5
577+000	2.4	2.4
578+000	2.8	2.6
579+000	2.8	2.5
580+000	2.3	2.6
581+000	2.1	1.9
582+000	2	2.5
583+000	2.1	2.7
584+000	2.2	2.4
585+000	2.6	2.2
586+000	2.6	2.4
587+000	2.3	2.6
588+000	2.6	No Data
589+000	2.1	4.1
590+000	4.2	No Data
590+500	5	2.1
591+000	3.9	0.1
591+500	6.2	3.6
592+000	5	2.1
592+500	7.5	-5.6
593+000	1.9	2.8
593+500	6	1.9
594+000	5.4	0.6
594+500	0.8	2.9
595+000	1.4	4.2
595+500	1.5	3.6
596+000	1.4	2.7
597+000	1.2	2.3
598+000	1	2.3
599+000	0.6	1.7
600+000	0.7	1.9
601+000	0.9	1.3
602+000	0.8	0.8
603+000	0.5	0.3
604+000	0.8	0.3
605+000	0.7	0.5
606+000	0.8	0.1
607+000	1.1	0.6
608+000	0.8	0
609+000	1	-0.1
610+000	0.6	0.5
611+000	0.8	0.3
612+000	0.7	0
613+000	0.1	No Data
614+000	0.3	No Data
615+000	0.3	No Data

5.1.5 Hurricane Harvey

Hurricane Harvey made landfall in southern Texas on August 25, 2017 and then stalled inland of Matagorda for two days dumping heavy rainfall into the Brazos River floodplain. On August 29, the flow rate in the Brazos River reached 133,000 cfs at Rosharon, TX, the highest ever recorded at that location. Multibeam bathymetric surveys were made on June-1 2017, and post-

storm surveys were made on September-29, 2017. Sedimentation volumes were calculated based on the overlapping area of these two surveys and are summarized in Table 22.

Table 22. Calculated sedimentation volumes based on pre- and post-storm surveys.

W-GIWW	Erosion Volume [cu.yd.]	Sedimentation Volume [cu.yd.]	Average Sedimentation Depth [ft]
W-GIWW	0	150,000	1.0
Brazos Basin	-174,000	71,000	4.2*
E-GIWW	0	344,000	1.7
Total	-174,000	565,000	1.5

* Average sedimentation depth includes only the shoal on the east Brazos Basin forebay and does not include the eroded Brazos River Channel.

The sedimentation patterns for the West GIWW, Brazos Basin and East GIWW are shown in Figure 67 to Figure 69. Figure 68 shows the Sedimentation pattern at the Brazos Basin, where the most pronounced erosion and sedimentation occurs. The Brazos River channel has been scoured by about 6.9 ft., and a large shoal has been created in the forebay of the East Gate. Sedimentation in the West GIWW is less severe than in the East GIWW, which is consistent with the observations made in Section 5.1.4.

Figure 67. Sedimentation pattern in the W-GIWW due to Hurricane Harvey.

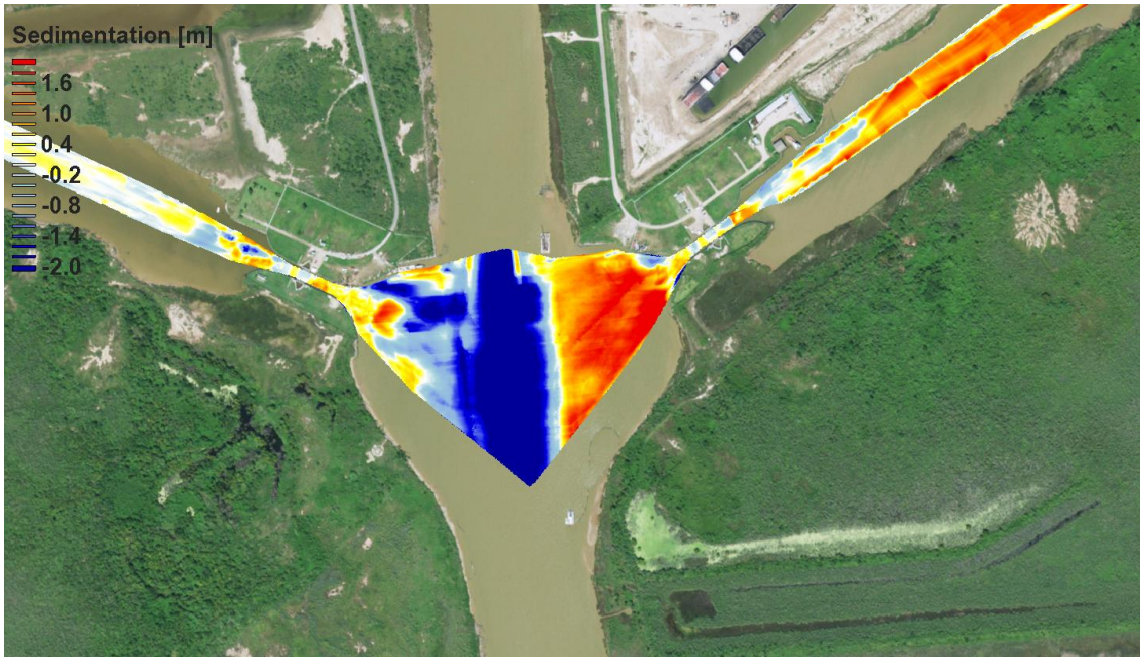

Figure 68. Sedimentation pattern in the Brazos Basin due to Hurricane Harvey.

Figure 69. Sedimentation pattern in the E-GIWW due to Hurricane Harvey.

Post-storm sediment samples were collected from the shoal at the east forebay, as well as on either side of the East and West Gate. The post-storm sediment composition in the shoal consists primarily of very fine silt with some sand, with the samples nearest to the south and north banks having a higher proportion of very fine sand, and the sample closer to the channel consisting primarily of fine silt and clay. The samples on either side of the East and West Gates were primarily very fine silt and clay. These post-storm sediment samples are consistent with the samples collected under typical conditions (Section 5.1.1) with a slightly higher proportion of sand in the Brazos Basin.

5.2 Sedimentation Modeling

To simulate the changes in sedimentation patterns and volumes associated with the proposed alternatives, a calibrated sediment transport and sedimentation model was required. Sedimentation was modeled using ADH for the same 13-month validation period described in Section 3.1.5.

5.2.1 Model setup

The sedimentation model was built using the same mesh and hydrodynamic forcing conditions as the hydrodynamic and salinity models. Sediment boundary conditions were determined using the sediment rating curves shown in Figure 62 and Figure 63 based on the boundary flow rates shown in Figure 23. Sensitivity testing was performed on the boundary constituent proportions and it was found that varying the Silt-Clay proportion between 60%-40% and 40%-60% did not have a significant impact on the overall sedimentation rates in each zone of influence. Furthermore, the sediment size distributions of measured grab samples (like those in Table 20) are typically skewed towards a greater proportion of larger sediments compared to upstream suspended sediment concentrations, since larger sediment particles tend to settle before smaller particles. Based on the sediment class distribution shown in Table 20 and consultation with experts at ERDC, the boundary sediment was assumed to be 50% Silt and 50% Clay. Sediment parameters are shown in Table 23.

Table 23. Sedimentation model sediment parameters.

Parameter	Silt	Clay
Median Grain Diameter [mm]	3.0E-5	5.0E-6
Specific Gravity [-]	2.72	2.72
Bulk Density [kg/m3]	1400	1200
Critical Shear of Erosion [kPa]	0.67	0.1
Erodibility Factor [-]	1.6E-4	1.6E-4
Critical Shear of Deposition [kPa]	0.1	0.05
Settling velocity [m/s]	2.2E-4	5.0E-5

Like the salinity model, a 1-year spinup simulation was run to determine the initial conditions for the 13-month simulation. The spinup simulation was initiated with zero bed layer thickness and zero sediment concentration in the entire domain and boundary sediments were introduced and allowed to circulate and deposit naturally within the domain. For the spinup simulation, bed updating was disabled, so only the initial distribution of bed layer thickness (i.e. a local source of sediment) was created. One drawback to this method is that high currents in the spinup simulation prevented sediment from naturally settling and developing an erodible layer in the Brazos River, which ultimately restricted the erosion of the Brazos River during the 13-month simulation and resulted in showing no erosion of the river bed.

5.2.2 Calibration & Validation

The sedimentation model was validated by comparing sedimentation rates in each of the zones of influence to calculated sedimentation rates from available surveys. GIWW surveys used to determine the volumetric sedimentation rates in Table 21 were interpolated onto a high-resolution point swath for the West GIWW, Brazos Basin and East-GIWW. The model results were also interpolated onto the same point swath, and the average sedimentation rates for each were compared (Figure 70 and Figure 72). Note in Figure 71, that the model did not capture the

erosion of the Brazos River. This is because of the absence of a bed layer thickness in the Brazos River due to the spinup simulation.

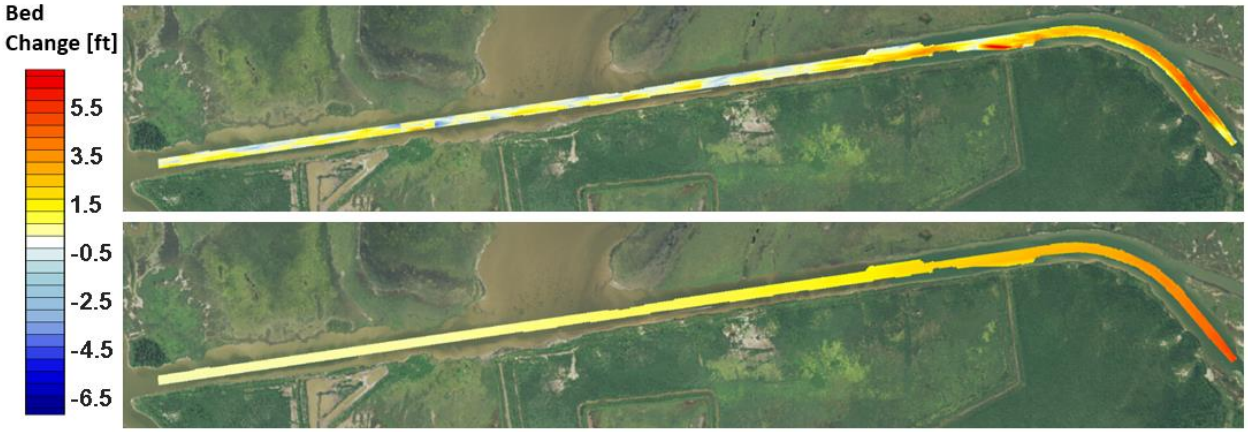

Figure 70. Comparison of measured (top) and modeled (bottom) sedimentation rates in the West GIWW.

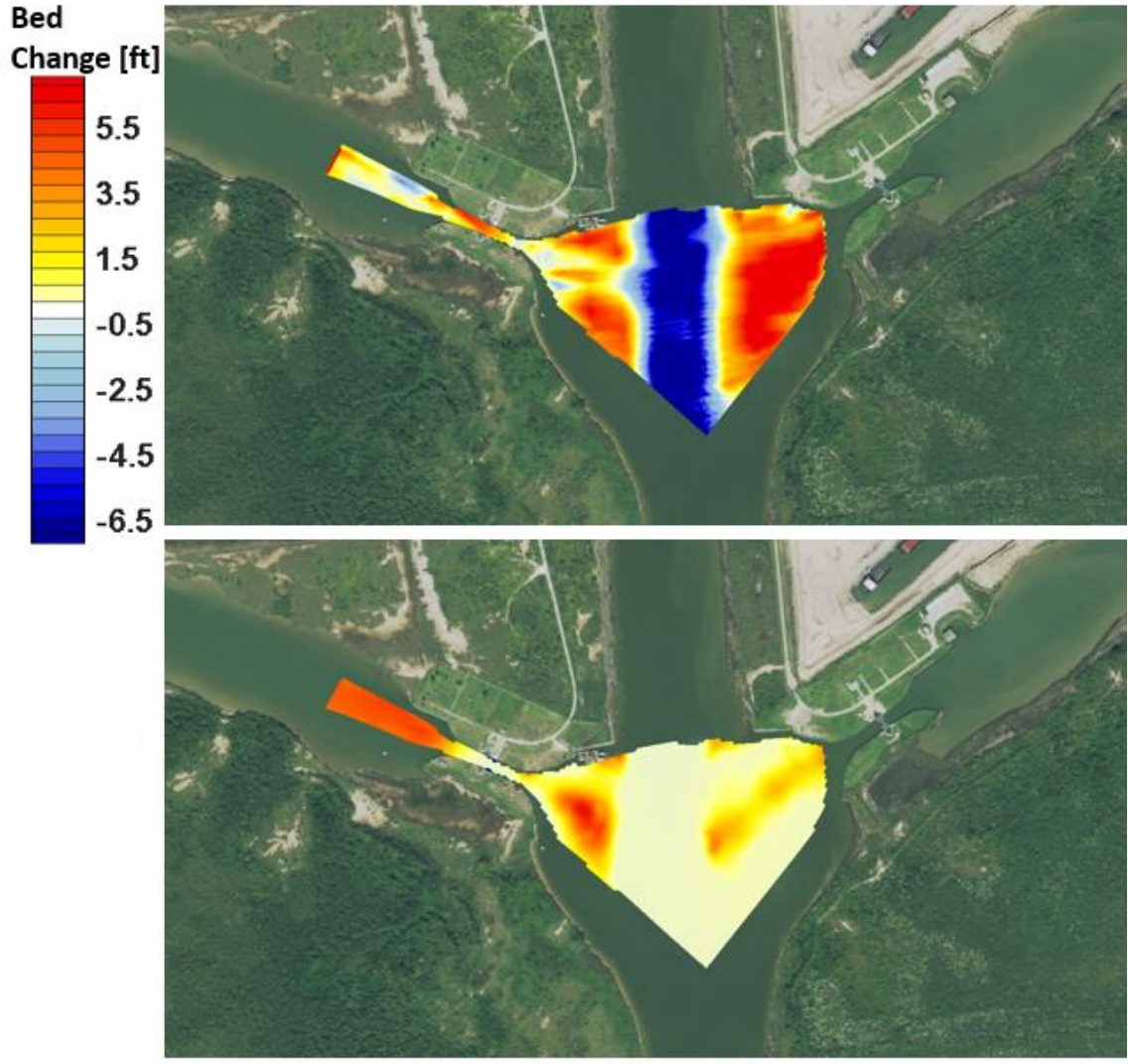

Figure 71. Comparison of measured (top) and modeled (bottom) sedimentation rates in the Brazos Basin.

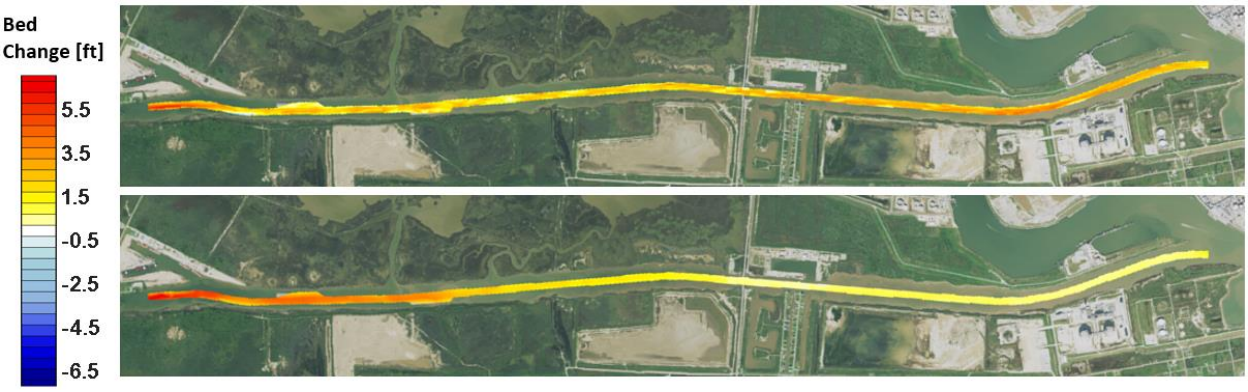

Figure 72. Comparison of measured (top) and modeled (bottom) sedimentation rates in the East GIWW.

Table 24 shows the comparison of volumetric sedimentation rate for the West GIWW, Brazos Basin, and East GIWW. The measured volume in the Brazos Basin was calculated as only the

accreted volume, and erosion of the Brazos River channel as seen in Figure 71 was not included in this volume calculation as it was not simulated. While the model skews the distribution of sedimentation volume towards the west, the total sedimentation volume was underpredicted by about 10%, shown reasonable agreement in the sedimentation in the system overall.

Table 24. Validation of volumetric sedimentation rates in the West GIWW, Brazos Basin, and East GIWW.

	West GIWW	Brazos Basin	East GIWW	Total
Measured	1,502,919	1,076,581	4,232,713	6,812,214
Modeled	2,145,144	454,710	3,563,866	6,163,720
Relative error	43%	-58%	-16%	-10%

Figure 74 shows modeled and measured sedimentation depth compared along the channel centerline (Figure 73). The model does a good job of predicting the sedimentation depth and distribution in the West GIWW (Stations 595+000 – 612+000). In the Brazos Basin (Stations 590+000 – 595+000) the model does not predict the erosion of the Brazos River channel because a lack of sediment layer thickness in the model prevented it, the model does a good job predicting the general sedimentation pattern (accretion in the forebays). In the East GIWW (Stations 567+000 – 590+000), the model predicts sedimentation depth near the East Gate well, but underestimates sedimentation rate farther east towards Freeport. There are a number of factors that could attribute to this, including the influence of vessel traffic on the GIWW on sediment settlement and resuspension, and potential sediment contribution from Oyster Creek east of Freeport. As the goal of sedimentation modeling is to identify potential changes in sedimentation rates and patterns due to project implementation and not to perfectly capture sediment transport dynamics resultant of all possible influences, the model is deemed appropriately calibrated to quantify changes to sedimentation within the system as influenced by the Brazos Floodgates.

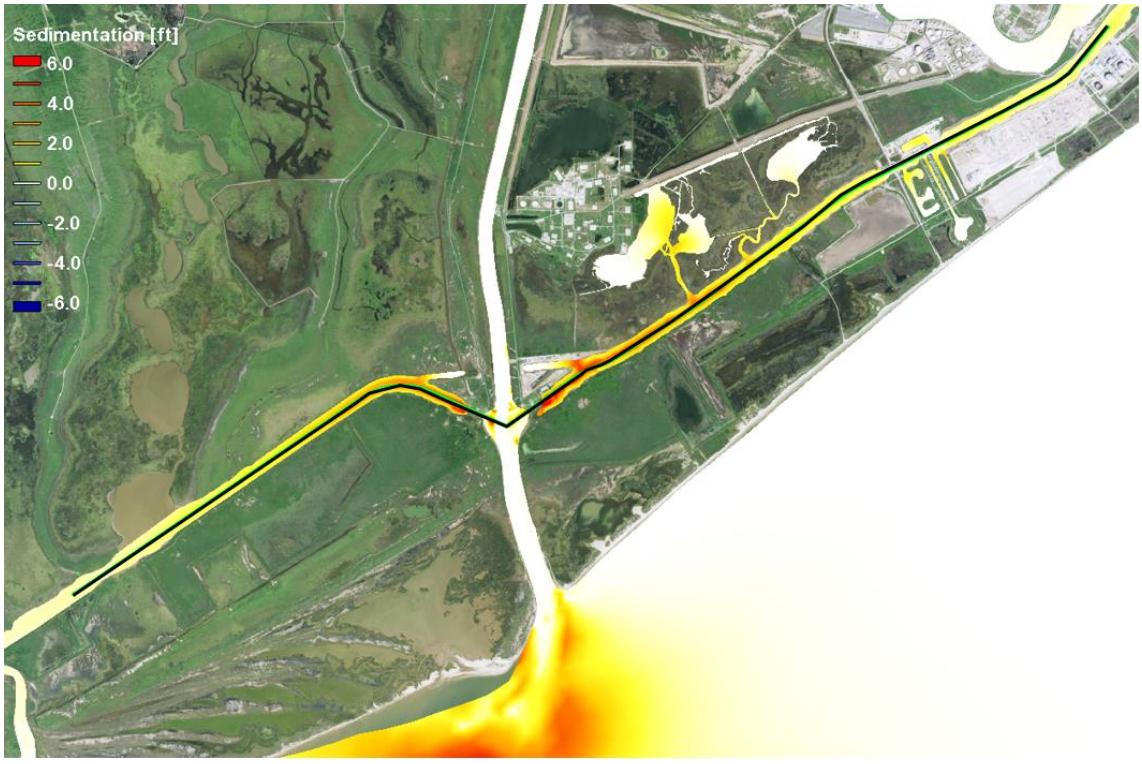

Figure 73. Channel centerline for comparison of modeled vs. measured sedimentation depth between the Freeport Harbor and the San Bernard River.

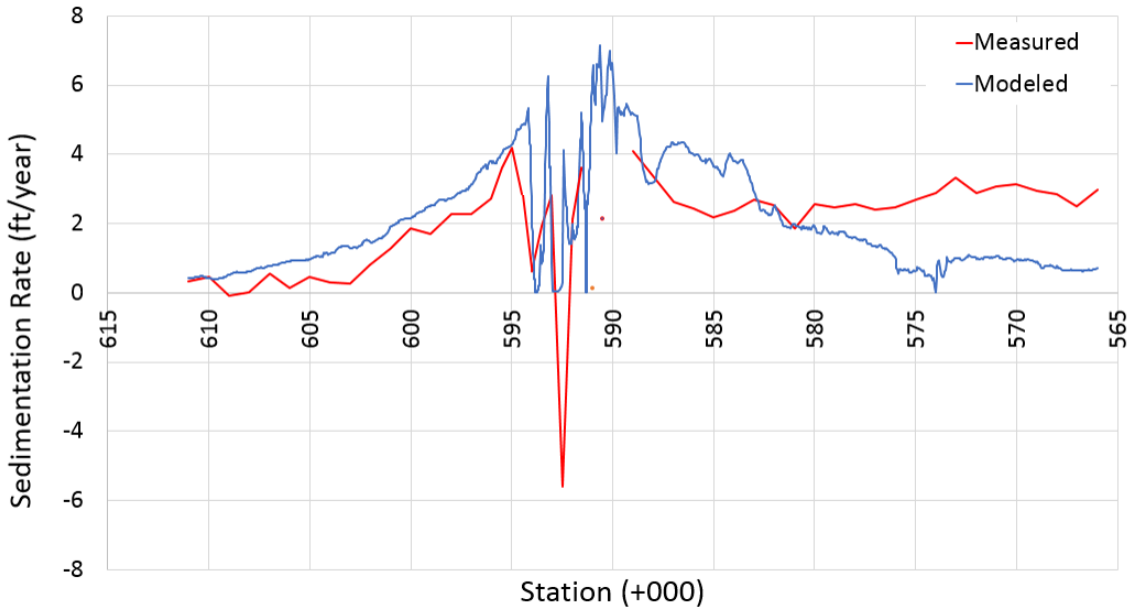

Figure 74. Comparison of measured vs. modeled sedimentation depth along the GIWW channel centerline between the Freeport Harbor and the San Bernard River.

5.2.3 Model Sensitivity to Sand Load

Based on the sediment distributions in Section 5.1.1 and the sediment sampling after Hurricane Harvey, sand was excluded from the sedimentation model since there is a high degree of uncertainty in the boundary sand load and because sand does not penetrate the GIWW and

thus will not have a large impact on the resulting sedimentation volumes. While the existing alignment may not be sensitive to sand load, it is possible that the open channel alternatives may be. Thus, a sensitivity simulation was run with a boundary sand load of 20% the total sediment load (i.e. the total sediment load in increased by 20%). The sediment parameters for the sensitivity simulation are outlined in Table 25.

Table 25. Model sensitivity simulation to sand load sediment parameters.

Parameter	Sand	Silt	Clay
Median Grain Diameter [mm]	2.5E-4	3.0E-5	5.0E-6
Specific Gravity [-]	2.65	2.72	2.72
Bulk Density [kg/m3]	-	1400	1200
Critical Shear of Erosion [kPa]	-	0.67	0.1
Erodibility Factor [-]	-	1.6E-4	1.6E-4
Critical Shear of Deposition [kPa]	-	0.1	0.05
Settling velocity [m/s]	-	2.2E-4	5.0E-5
Total Fraction [%]	16%	42%	42%

The resulting sediment volume in each of the zones of influence was compared to the simulation results without a sand load (Table 26). Based on these results, a 20% sand load leads to a disproportionate increase in sedimentation volume in the Brazos Basin (61% increase), while increasing the sedimentation rate in the other GIWW zones by 10% or less. Thus, if the sediment load of fine sediments was reduced in place of a proportional addition of sand load, the sedimentation volumes would be skewed towards higher sedimentation in the Brazos Basin which is an order of magnitude less than sedimentation in the East GIWW, and towards the Brazos Delta which does not require dredging, thus simulating a less conservative solution.

Table 26. Sedimentation volumes in zones of influence for sensitivity simulations with and without 20% sand load.

	West GIWW	Brazos Basin	East GIWW	Freeport Channel	Brazos Delta	Total
9a [cy./yr.]	775,897	96,903	1,135,209	883,064	37,421,241	40,312,314
9a w/ 20% Sand [cy./yr.]	836,567	155,704	1,251,008	948,638	41,935,363	45,127,279
% increase	8%	61%	10%	7%	12%	12%

Three additional sensitivity simulations were run for Existing Conditions with boundary sediments of 5%, 10% and 20%. The resulting volume increase was evaluated at sediment sample locations BR-05, BR-06, and BR-08 (Figure 60) where measured sand fractions are greatest. A simple linear transfer function was developed for each sample location to relate the boundary sand fraction to the sand fraction at each sample location.

Table 27. Changes in deposition rates based on sand load.

	No Sand	5% Sand ($yd.^3$)	10% Sand ($yd.^3$)	20% Sand ($yd.^3$)	Measured	Target Boundary Sand Fraction
BR-05	7,043 ()	7,454 (6%)	7,880 (12%)	8,885 (26%)	(16%)	(13%)
BR-06	16,470 ()	19,379 (18%)	24,314 (48%)	35,746 (117%)	(7%)	(2%)
BR-08	33,353 ()	35,957 (8%)	38,068 (14%)	42,937 (29%)	(9%)	(6%)

Based on this analysis, the most conservative estimate of boundary sand load would be 13% (at BR-05), meaning that the results of the sensitivity test for Alternative 9a using a 20% boundary sand load would be doubly conservative.

Since there is so much uncertainty in the boundary sand load, and since adjusting the boundary sediment fractions to include sand lead to a less conservative solution, the sedimentation simulations excluding sand load are determined to be acceptable.

5.3 Alternatives Analysis

For all alternatives, a series of sediment load curves were developed to describe the sediment budget around the Brazos Basin. For these load curves, positive values indicate sediment flux into the Brazos Basin and negative values indicate sediment flux out of the Brazos Basin. Similarly, daily sedimentation rating curves were also developed for each of the impact zones.

Figure 75 shows the sediment flux rating curves for Alternative 3a. The sediment flux rating curves show a slight decrease in sediment load into the Brazos Basin at higher flow rates and a comparable decrease in sediment load towards the Gulf. While sediment flux into the West GIWW appears unchanged, the sediment flux into the East GIWW shows a slight decrease at high flow rates. Figure 76 shows the daily sedimentation rating curves for the zones of influence requiring maintenance for Alternative 3a. Based on this figure, there is no noticeable change in sedimentation rates for Alternative 3a.

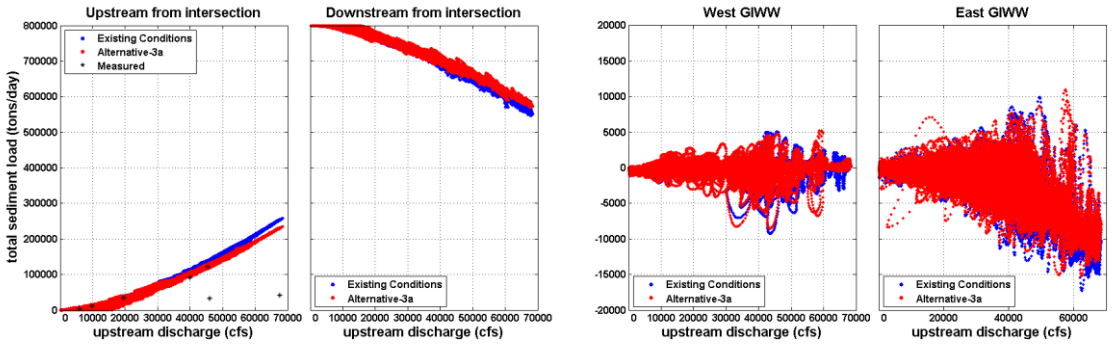

Figure 75. Sediment load vs river discharge for existing conditions and Alt 3a.

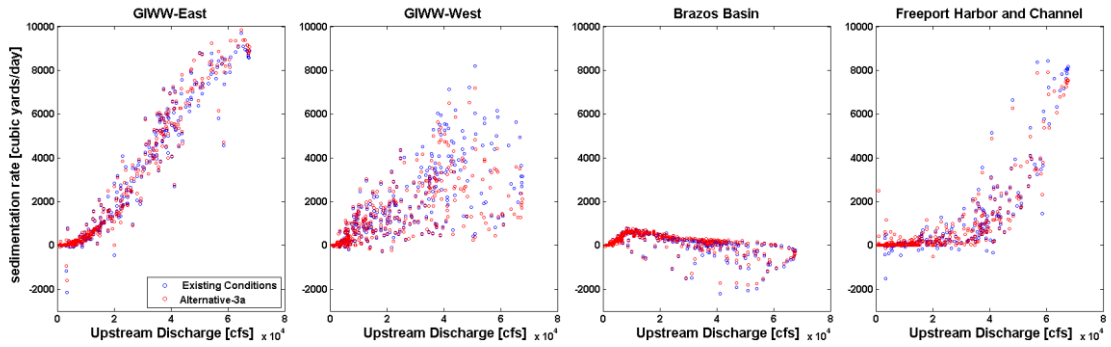

Figure 76. Sedimentation rate vs river discharge for existing conditions and Alt 3a.

Figure 77 shows the sediment flux rating curves for Alternative 3a.1. As with Alternative 3a, there is a noticeable decrease in upstream flux into and downstream flux out of the Brazos Basin at higher flow rates as well as a slight decrease in flux into the East GIWW at high flow rates. However, sediment fluxes both into and out of the West GIWW are increased in magnitude as the absence of the West Gate means there is less damping of tidal flows, which dominates flows and sediment fluxes into the West GIWW. Figure 78 shows the daily sedimentation rating curves for the zones of influence requiring maintenance for Alternative 3a.1. There is no noticeable change in sedimentation rates in the East GIWW, Brazos Basin or Freeport Harbor, however there is a slight increase in sedimentation rate in the West GIWW due to the open channel.

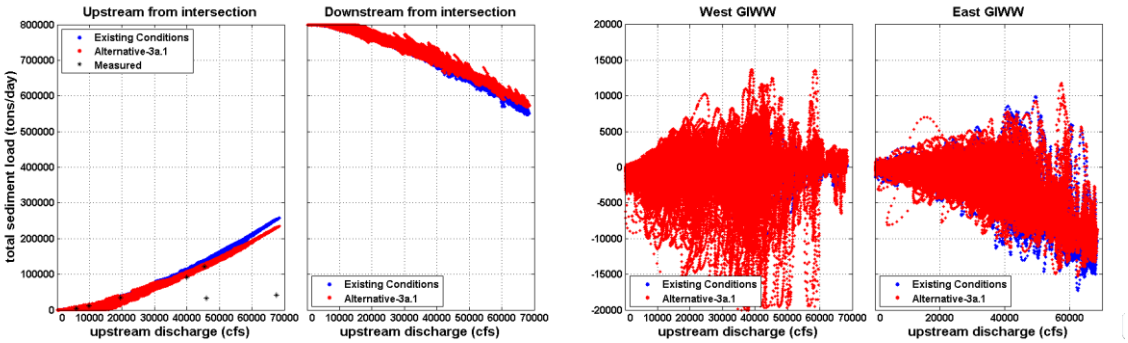

Figure 77. Sediment load vs river discharge for existing conditions and Alt 3a.1.

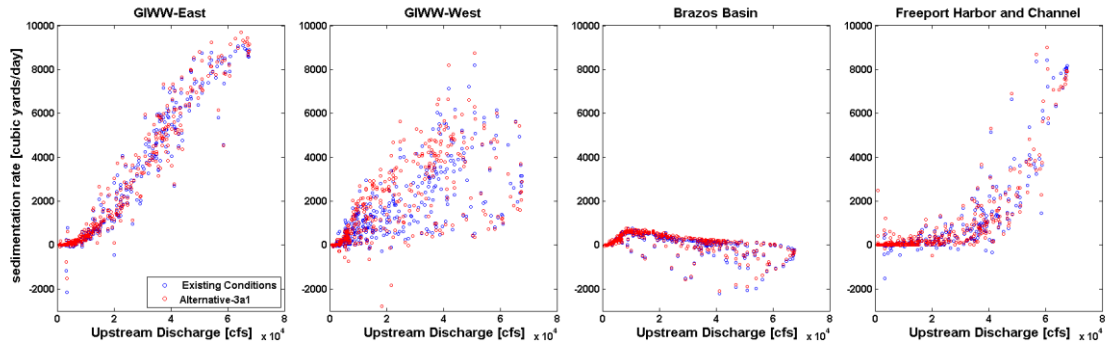

Figure 78. Sedimentation rate vs river discharge for existing conditions and Alt 3a.1.

Figure 79 shows the sediment flux rating curves for Alternative 9a. As with Alternative 3a, there is a noticeable decrease in upstream flux into and downstream flux out of the Brazos Basin at higher flow rates. There is a noticeable increase in sediment flux into the East GIWW at high flow rates, and sediment fluxes both into and out of the West GIWW are increased in magnitude

as the absence of gates means there is less damping of tidal flows, which dominates flows and sediment fluxes into the West GIWW.

Figure 80 shows the daily sedimentation rating curves for the zones of influence requiring maintenance for Alternative 9a. Sedimentation rate in the East GIWW seems to increase at flow rates lower than 4,000 cfs, but decreases at high flow rates when sediment loads are more dramatic. This is intuitive as above a certain flow rate, velocities in the East GIWW will be too high to allow sediment to settle. This observation can be further corroborated by the sedimentation rate in the Freeport Harbor, where flows above 4,000 cfs cause significantly increased sedimentation from Existing Conditions, and lower flows cause negligible sedimentation. The Brazos Basin experiences a noticeable increase in sedimentation rate for flows greater than 1,000 cfs. This can be explained by sediments settling out on the north side of the GIWW just east of the Brazos River – GIWW intersection where higher flows cause a large eddy (as seen in Figure 35). Sedimentation rates in the West GIWW show a slight increase with no real correlation to flow rate.

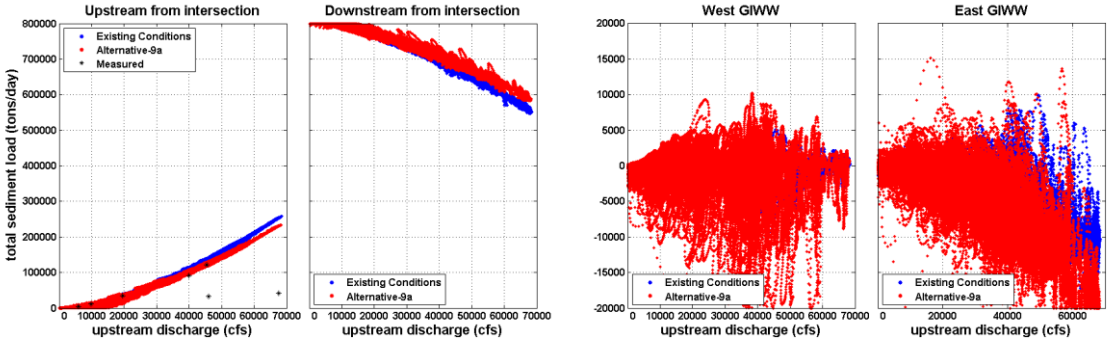

Figure 79. Sediment load vs river discharge for existing conditions and Alt 9a.

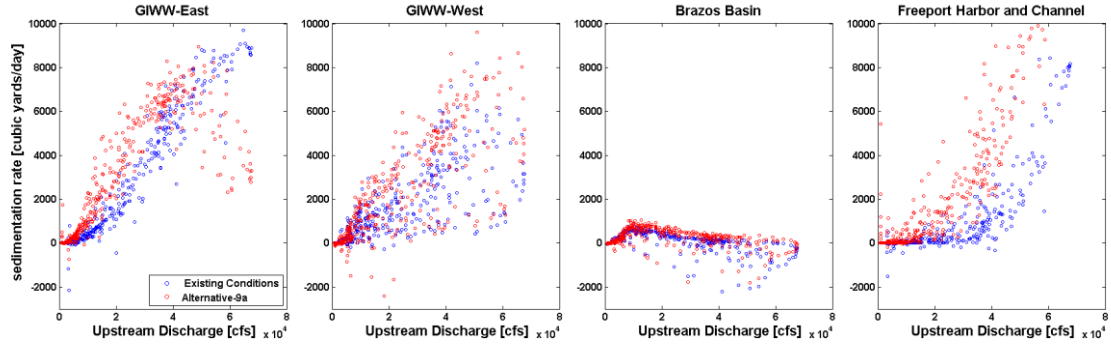

Figure 80. Sedimentation rate vs river discharge for existing conditions and Alt 9a.

Figure 81 shows the sediment flux rating curves for Alternative 9b. As with Alternatives 3a and 9a, there is a decrease in upstream flux into and downstream flux out of the Brazos Basin at higher flow rates. Sediment flux into and out of the west GIWW are increased in magnitude from Existing Conditions, especially at flow rates less than 3,000 cfs. Sediment flux into the East GIWW is increased slightly, especially at high flow rates. Figure 82 shows the daily sedimentation rating curves for the zones of influence requiring maintenance for Alternative 9b. All zones experience an increase in sedimentation rate for flow rates above 2,000 cfs. Like Alternative 9a, at very high flow rates, there is a slight reduction in sedimentation rate in the East GIWW with an accompanying increase in sedimentation in the Freeport Harbor.

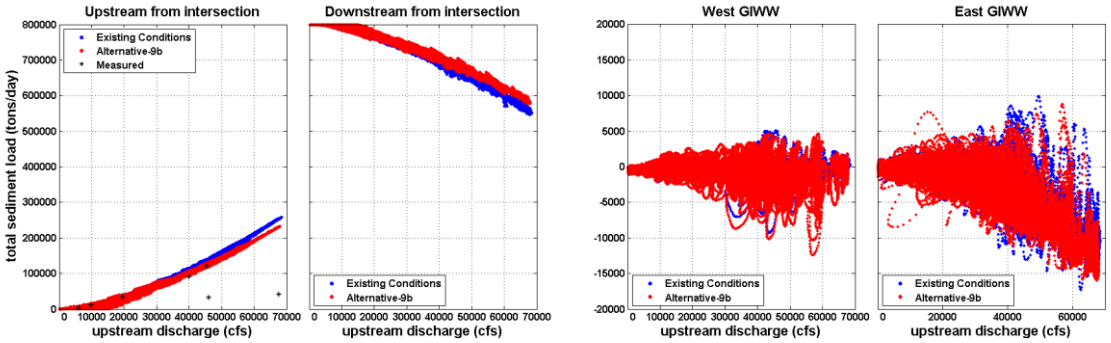

Figure 81. Sediment load vs river discharge for existing conditions and Alt 9b.

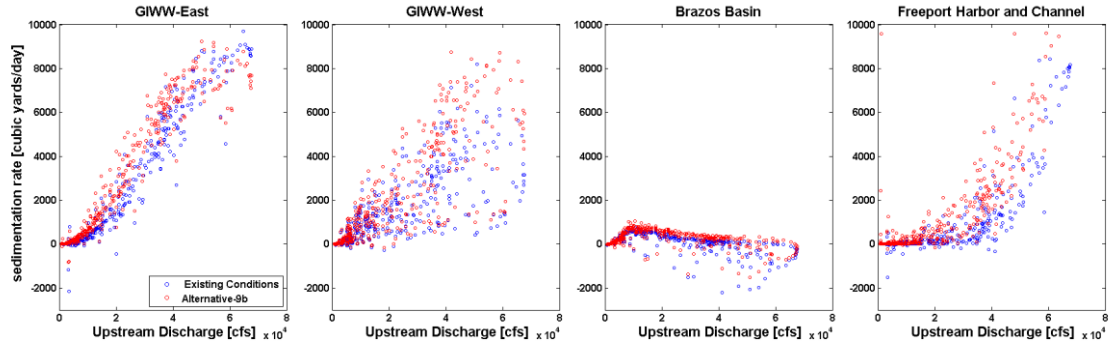

Figure 82. Sedimentation rate vs river discharge for existing conditions and Alt 9b.

Figure 83 shows the sediment flux rating curves for Alternative 9c. The sediment fluxes are virtually identical to Alternative 9b. This is understandable as the only difference between the two alternatives is the sluice gate which is seldom opened and intended to primarily aid in navigation, not to prevent sedimentation.

Figure 84 shows the daily sedimentation rating curves for the zones of influence requiring maintenance for Alternative 9c. As with sediment fluxes, sedimentation rates are very similar to Alternative 9b. The only noticeable difference is that sedimentation rates in the Brazos Basin are slightly for flow rates between 2,000 cfs and 6,000 cfs, which is most likely due to a slight increase in area of the basin near the sluice gate.

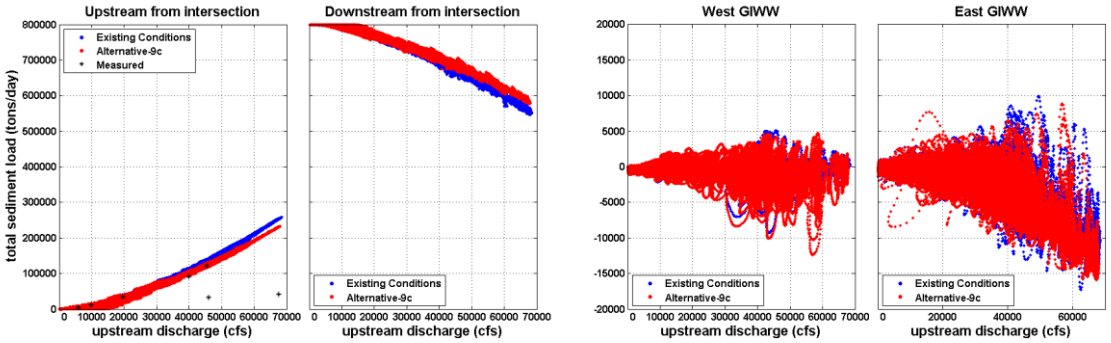

Figure 83. Sediment load vs river discharge for existing conditions and Alt 9c.

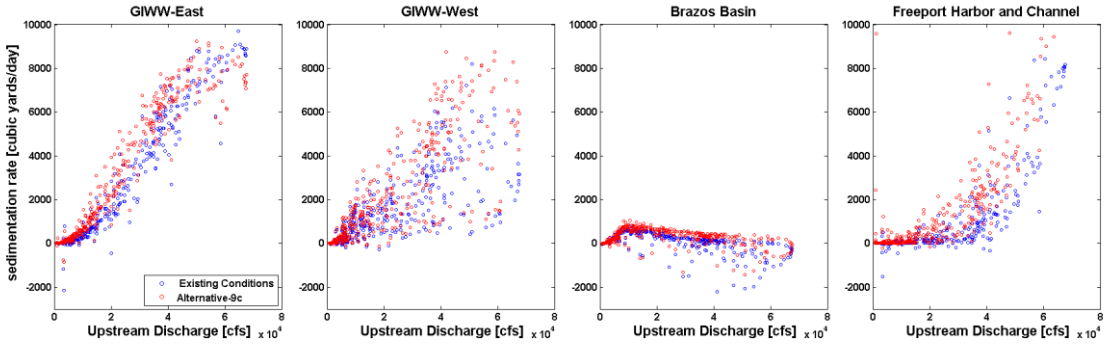

Figure 84. Sedimentation rate vs river discharge for existing conditions and Alt 9c.

Some general trends can be observed for all alternatives. For example, the sediment fluxes upstream, downstream and east of the Brazos Basin generally show an exponential relationship with upstream flow rate, where an increasing flow rate is accompanied by an increase in sediment flux. However, west of the Brazos Basin, there is no apparent relationship between sediment flux and river flow rate. Thus, flow and sediment flux through the west gate seems to be mostly tide-dominated.

Furthermore, based on the sedimentation rating curves, sedimentation rates in the East GIWW increase rapidly between flow rates of 2,000 cfs and 5,000 cfs, and tend to reduce slightly at flow rates greater than 6,000 cfs. In the West GIWW, the relationship is quite scattered. While there is some general increase in sedimentation with increase in flow rate, the large scatter likely indicates that either the tide dominates, or that the San Bernard River influences sedimentation in some way. In the Brazos basin, sedimentation rates increase with and peak at a flow rate of approximately 1,000 cfs at which point they begin to decrease. Negative sedimentation rates indicate erosion of a previously deposited sediment.

In the Freeport harbor, sedimentation rates are negligible for flows less than 2,000 cfs and increase dramatically with flow rates greater than 5,000 cfs. This is intuitive since at low flow rates, sediments heading towards Freeport will instead settle in the East GIWW, and at very high flow rates, sediments are not able to settle in the East GIWW and will instead settle in Freeport.

Table 28 summarizes annualized sedimentation volumes computed in each of the zones of influence. The percent change in total sediment volume in all six zones of influence is less than 1.1% for all alternatives, indicating that the total sediment budget is conserved and local sources of sediment in the model domain are negligible.

Table 29 summarizes the changes in sedimentation volume relative to Existing Conditions for all project alternatives and zones of influence requiring maintenance.

Alternative 3a shows relatively modest changes in sedimentation. There is a small decrease in sediment to the west GIWW and a modest increase to other zones, with an overall slight (negligible) decrease in total sedimentation in zones requiring maintenance dredging. Alternative 3a.1 is very similar to Alternative 3a in the Brazos Basin, East GIWW and Freeport Harbor, in the West GIWW, there is a significant increase in sedimentation rate due to absence of the West Gate.

Alternative 9a had the largest changes in sedimentation both in the GIWW east and west, and had a dramatic increase in sedimentation in the Freeport Channel (231%), and had an overall increase in total sedimentation that requires maintenance of about 64%. In addition, this alternative reduces the sediment to the Brazos Delta, but only by a 5% reduction.

Alternatives 9a and 9b performed nearly identically, with patterns similar to alternative 9a with slightly smaller magnitudes, and an overall increase in sedimentation to be maintained of about 38%. The only substantial difference between 9b and 9c is a slight increase in sedimentation in the Brazos Basin in 9c at the location of the sluice gate. It is hypothesized that the sluice gate allows additional sediment into the basin, possibly recirculated from the western gate around the GIWW and back into the Brazos through the sluice gate.

Table 28. Summary of sedimentation volumes in cubic yards for a one year period for each alternative and all zones of influence.

	West GIWW	Brazos Basin	East GIWW	Freeport Channel	Brazos Delta	Freeport Offshore	Total	% Change
Existing	554,769	48,000	890,769	295,385	44,382,462	208,726	46,379,628	0.0%
3a	493,846	59,077	902,769	316,615	44,332,615	190,864	46,295,289	-0.2%
3a.1	653,130	58,332	902,653	326,420	44,000,887	196,239	46,137,661	-0.5%
9a	781,846	92,308	1,079,077	978,462	42,026,769	854,614	45,813,556	-1.2%
9b	780,923	96,923	1,044,000	550,154	43,232,308	396,989	46,102,044	-0.6%
9c	781,846	107,077	1,044,000	550,154	43,218,462	395,887	46,097,646	-0.6%

Table 29. Summary of sedimentation volume change from existing conditions in cubic yards (and percent) for each alternative and all zones of influence.

	West GIWW	Brazos Basin	East GIWW	Freeport Channel	Brazos Delta	Freeport Offshore	Total Change in Zones Requiring maintenance
3a	-61,000 (-11%)	11,000 (23%)	12,000 (1%)	21,000 (7%)	-50,000 (0%)	-18,000 (-8%)	-17,000 (-0.1%)
3a.1	98,000 (18%)	10,000 (22%)	12,000 (1%)	31,000 (11%)	-381,000 (-1%)	12,000 (-6%)	151,000 (8%)
9a	227,000 (41%)	44,000 (92%)	188,000 (21%)	683,000 (231%)	-2,356,000 (-5%)	646,000 (309%)	1,143,000 (64%)
9b	226,000 (41%)	49,000 (102%)	153,000 (17%)	255,000 (86%)	-1,150,000 (-3%)	188,000 (90%)	683,000 (38%)
9c	227,000 (41%)	59,000 (123%)	153,000 (17%)	255,000 (86%)	-1,150,000 (-3%)	187,000 (90%)	794,000 (39%)

Figure 86 to Figure 89 show a comparison of the modeled sedimentation patterns at the West GIWW, Brazos Basin, East GIWW, and Freeport Harbor respectively. Figure 85 shows the alignment and bounds of each of these figures.

As shown in Figure 86, the most noticeable changes in sedimentation occur near the Brazos River – GIWW intersection. While Alternative 3a experiences a small net decrease in sedimentation volume (Table 29), the volume of sedimentation between the Brazos River and the East Gate has increased dramatically. Thus, while the overall dredge volume required may be decreased, the dredge frequency will increase for that small region.

Figure 87 and Figure 88 show that while the sedimentation near in the GIWW near the Brazos River hasn't changed much for Alternative 9a, while sedimentation father from the Brazos River has increased significantly, particularly in the Freeport Harbor (Figure 89)

Alternatives 9b and 9c show a similar trend to Alternative 9a, but not as pronounced. Also, similar to Alternative 3a, there is significant increase in sedimentation locally just east of the east gate, indicating that dredge frequency in this area would need to be increased.

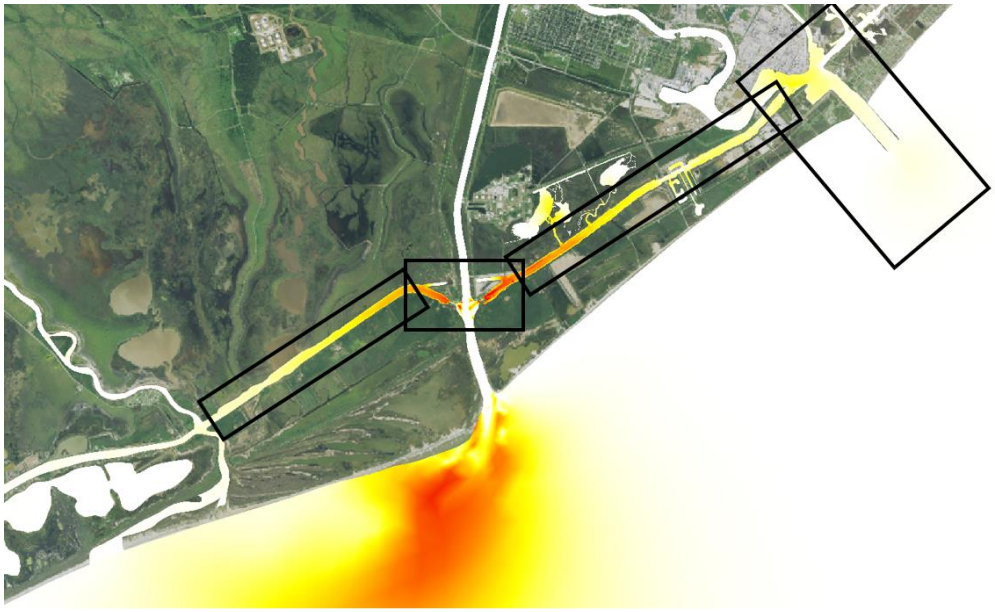

Figure 85. Sedimentation pattern zones master figure.

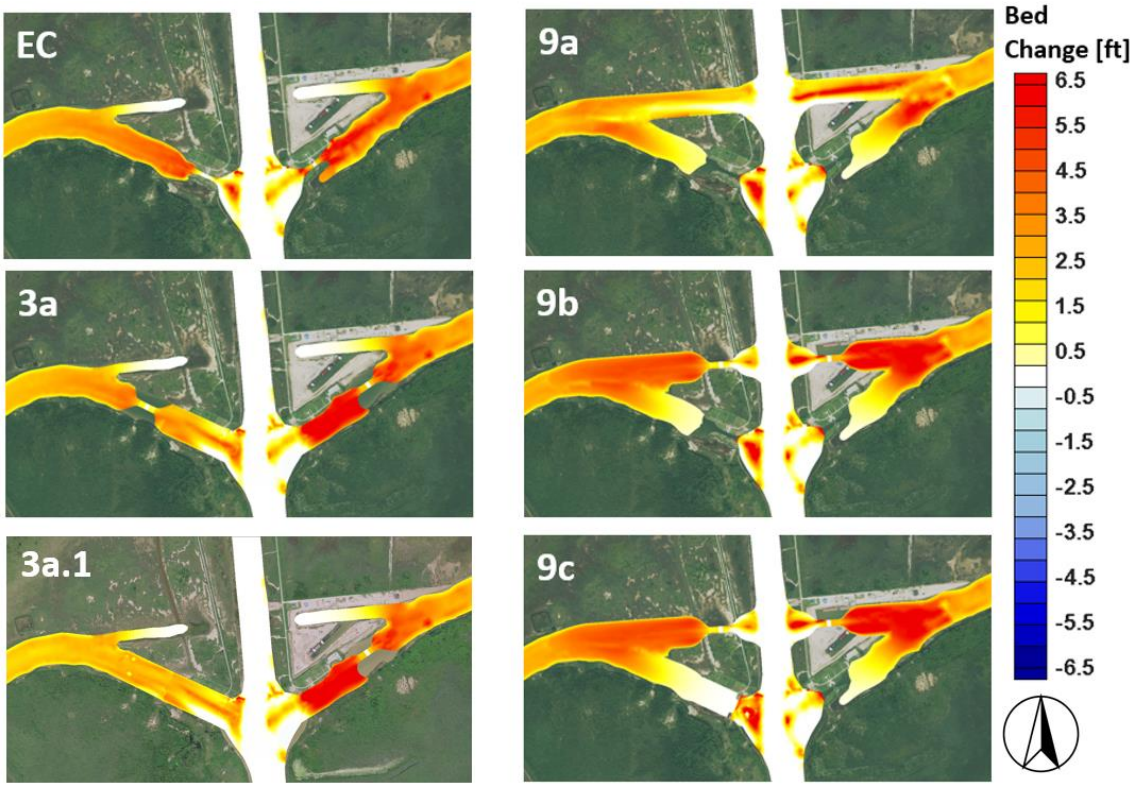

Figure 86. Sedimentation pattern at the Brazos River - GIWW intersection for all alternatives.

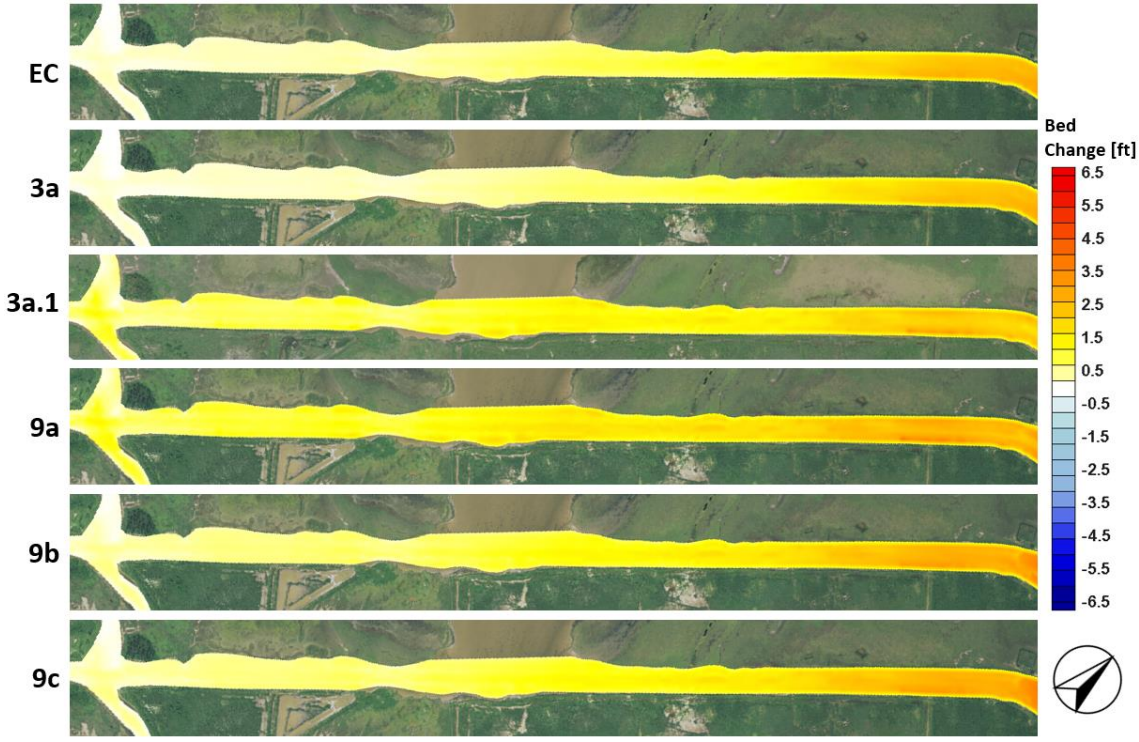

Figure 87. Sedimentation pattern in the West GIWW for all alternatives.

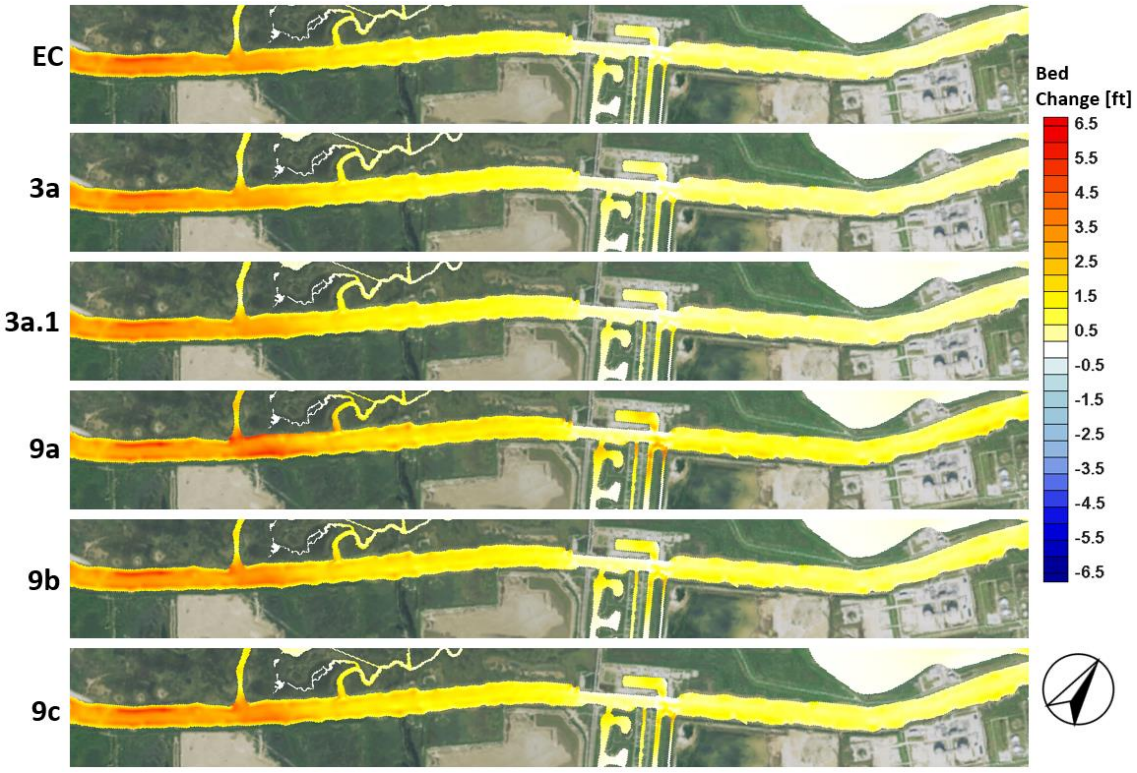

Figure 88. Sedimentation pattern in the East GIWW for all alternatives.

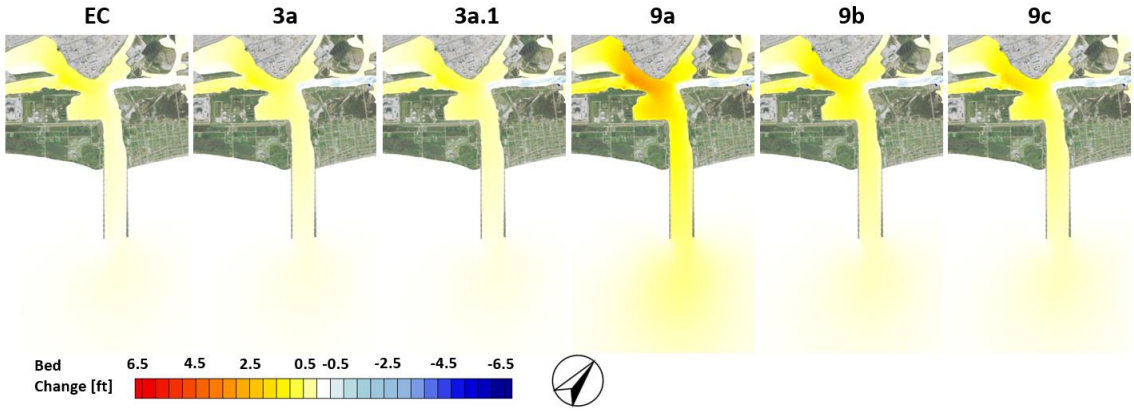

Figure 89. Sedimentation pattern in the Freeport Harbor and channel.

5.3.1 Scaling of Sedimentation Rates

Actual dredging rates for each zone of influence were obtained from the USACE operations department. The annual dredging rates obtained from the USACE operations personnel are provided in Table 30.

Table 30. Scale ratio for East GIWW, Brazos Basin and West GIWW for Existing Conditions to account for the difference between sedimentation volume and dredge volume.

	USACE operations [cu yd/yr]	ADH Model [cu yd/yr]	Scale Ratio [-]
East GIWW	395,000	890,769	0.44
Brazos Basin	110,000	48,000	2.29
West GIWW	360,000	554,769	0.65

Since the modeled sedimentation rates account for all material deposited within each zone (i.e., bank to bank sedimentation) while the USACE operations measure the amount dredged from the channel boundaries only, the modeled sedimentation rates were scaled to match the actual dredging quantities provided by USACE operations. The annual dredging volumes were used to scale the modeled sedimentation rates for existing conditions. The scaling ratio developed for existing conditions was applied to the modeled alternative results. A separate scaling ratio was developed for the East GIWW, Brazos Channel, and West GIWW as shown in Table 30. The sedimentation rates within the Freeport Channel area were not scaled due to limited detailed dredging data in this area. A summary of the sedimentation scaling is shown below in Table 31.

Table 31. Summary of modeled and scaled annual sedimentation rates in cubic yards

	West GIWW		**Brazos Channel & Basin**		**East GIWW**			
	Modeled	**Scaled**	Modeled	**Scaled**	Modeled	**Scaled**	**Freeport Channel**	**Total**[1]
Existing	554,769	**360,000**	48,000	**110,000**	890,769	**395,000**	**295,385**	**1,160,385**
3a	493,846	**320,466**	59,077	**135,385**	902,769	**400,321**	**316,615**	**1,172,787**
3a.1	653,130	**423,828**	58,332	**133,678**	902,653	**400,270**	**326,420**	**1,284,196**
9a	781,846	**507,355**	92,308	**211,539**	1,079,077	**478,503**	**978,462**	**2,175,858**
9b	780,923	**506,756**	96,923	**222,115**	1,044,000	**462,948**	**550,154**	**1,741,973**
9c	781,846	**507,355**	107,077	**245,385**	1,044,000	**462,948**	**550,154**	**1,765,842**

The scaled sedimentation rates were used by the economic team to analyze project costs and net benefits.

5.3.2 Impact of Sea Level Rise on Sedimentation Rate

To bolster posterity of the TSP selection, the sedimentation model was run with a hypothetical relative sea level rise (RSLR) of 1 ft. and 2 ft. Table 32 shows a summary of sedimentation volumes in each zone of influence for all alternatives and relative sea level rise conditions. These data are presented graphically in Figure 90 through Figure 93. Alternative 9c was excluded from this analysis because it assumed to have nearly identical values to Alternative 9b.

Table 32. Summary of sedimentation volumes and percent change from the base condition for all alternatives and RSLR conditions. Percent changes, in parentheses are relative to the base condition for each zone of influence.

	West GIWW			Brazos Basin			East GIWW			Freeport Channel		
	Existing	+1 ft.	+2 ft.	Existing	+1 ft.	+2 ft.	Existing	+1 ft.	+2 ft.	Existing	+1 ft.	+2 ft.
2a	554,769 (-)	701,987 (+27%)	771,263 (+39%)	48,000 (-)	57,366 (+20%)	62,006 (+29%)	890,769 (-)	924,755 (+4%)	986,214 (+11%)	295,385 (-)	239,774 (-19%)	193,047 (-35%)
3a	493,846 (-11%)	655,834 (+18%)	687,736 (+24%)	59,077 (+23%)	71,184 (+48%)	79,948 (+67%)	902,769 (+1%)	1,030,745 (+16%)	1,133,765 (+27%)	316,615 (+7%)	386,029 (+31%)	337,209 (+14%)
3a.1	653,130 (+18%)	820,267 (+48%)	905,365 (+63%)	58,332 (+22%)	69,693 (+45%)	78,301 (+63%)	902,653 (+1%)	943,599 (+6%)	1,018,189 (+14%)	326,420 (+11%)	278,102 (-6%)	239,442 (-19%)
9a	781,846 (+41%)	1,019,896 (+84%)	1,206,746 (+118%)	92,308 (+92%)	111,199 (+132%)	128,972 (+169%)	1,079,077 (+21%)	1,231,424 (+38%)	1,399,920 (+57%)	978,462 (+231%)	948,741 (+221%)	900,053 (+205%)
9b	780,923 (+41%)	1,025,001 (+85%)	1,241,545 (+124%)	96,923 (+102%)	105,580 (+120%)	119,645 (149%)	1,044,000 (+17%)	1,133,113 (+27%)	1,239,575 (+39%)	550,154 (+86%)	473,473 (+60%)	418,966 (+42%)

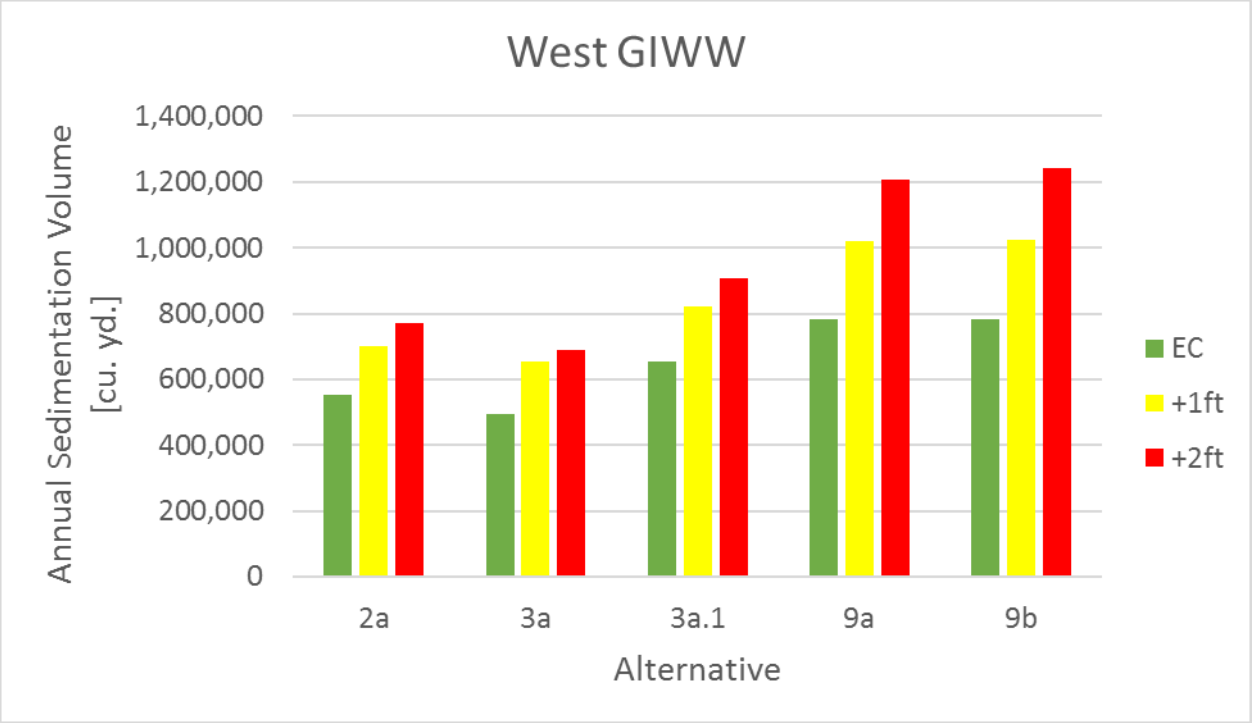

Figure 90. Sedimentation volume in the West GIWW for all alternatives and sea-level conditions.

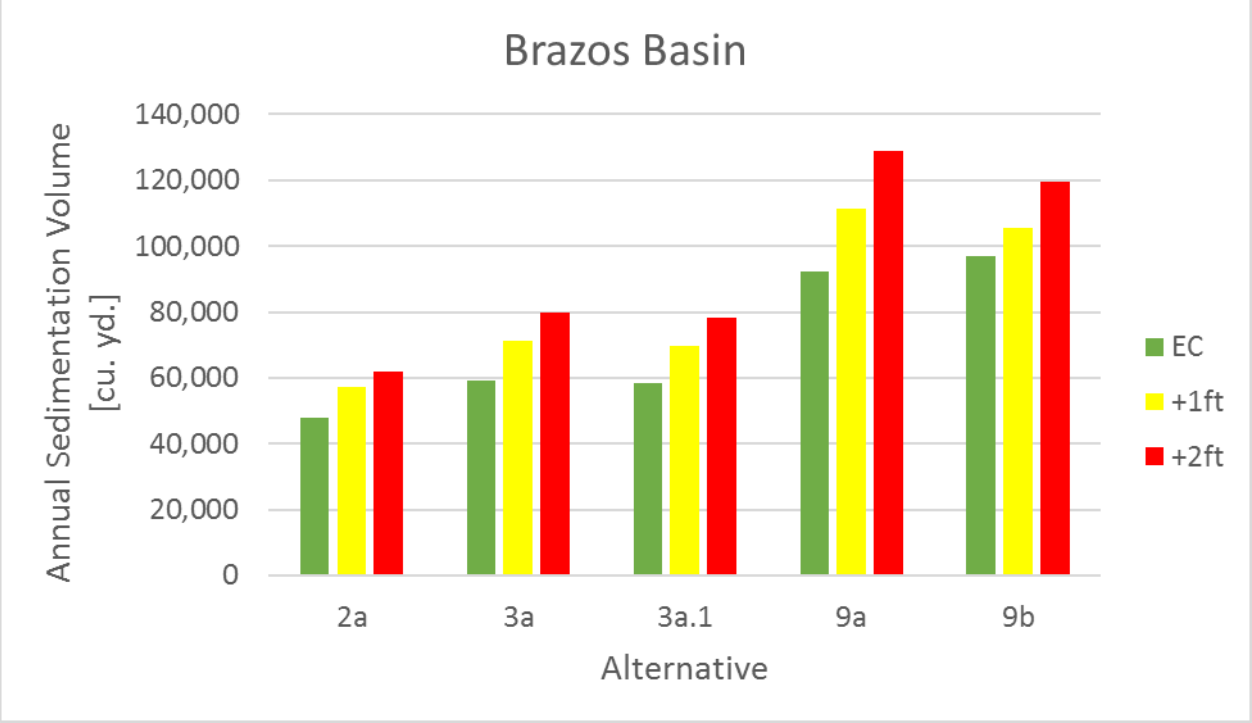

Figure 91. Sedimentation volume in the Brazos Basin for all alternatives and sea-level conditions.

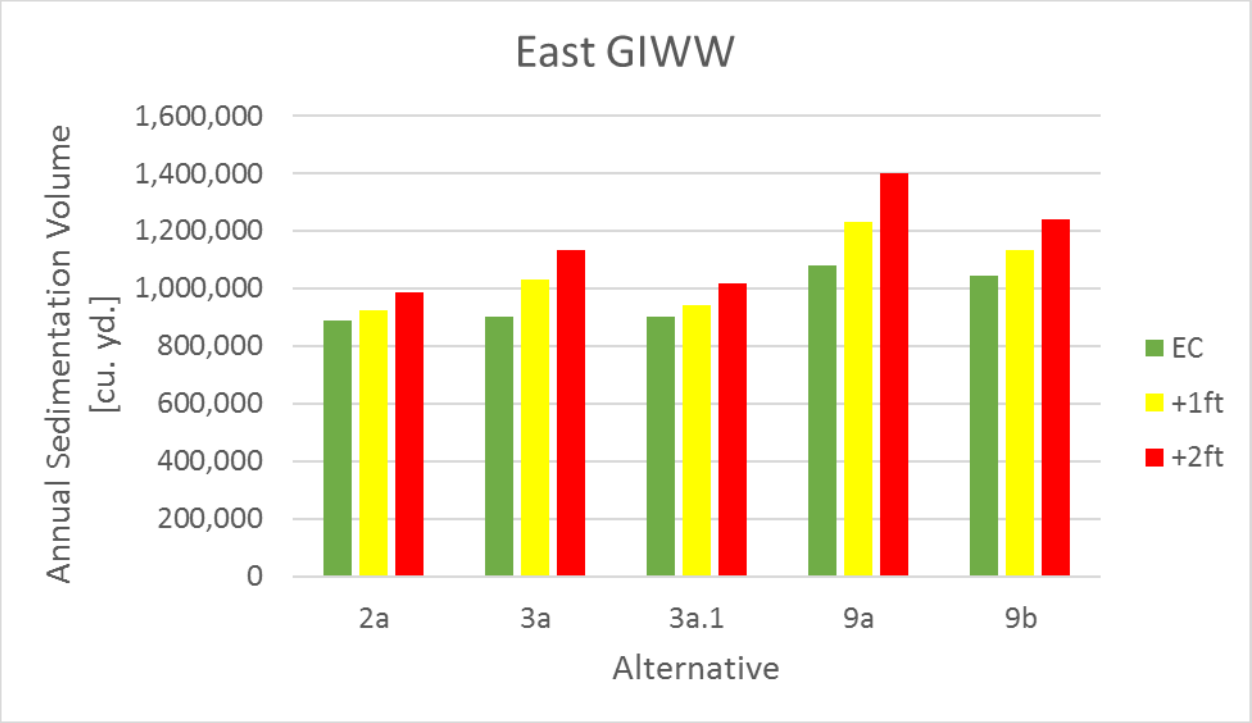

Figure 92. Sedimentation volume in the East GIWW for all alternatives and sea-level conditions.

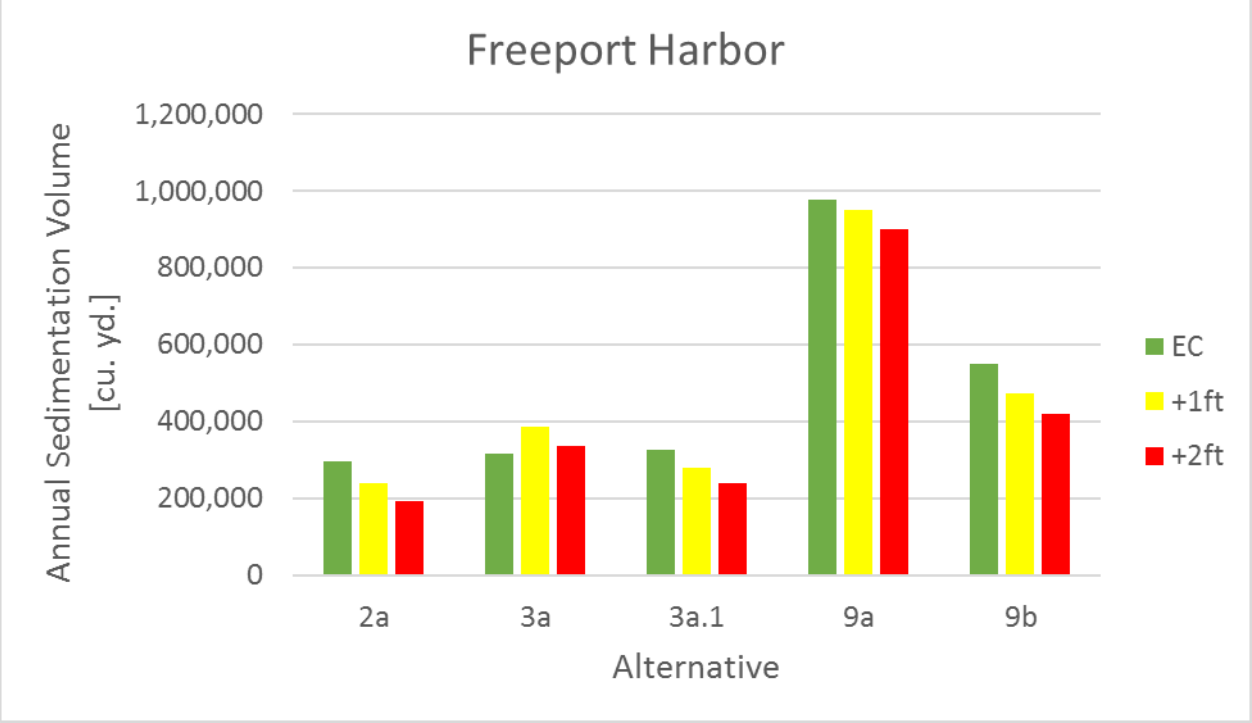

Figure 93. Sedimentation volume in the Freeport Harbor for all alternatives and sea-level conditions.

All alternatives show an almost linear increase in sedimentation volume with RSLR in the East GIWW, West GIWW and Brazos Basin, with a corresponding decrease in sedimentation volume in the Freeport Harbor. This is expected, as the higher sea level would correspond to a lower

velocity in the GIWW which would cause more sediment to fall out of suspension before reaching the Freeport Harbor. The effects of sea level rise are most dramatic in the West GIWW for Alternatives 9a and 9b, where the sedimentation volume increases by nearly 500 thousand cubic yards (about 120% increase from the base condition). Comparatively, Alternative 3a.1 which has an open channel connection to the West GIWW only increases in sedimentation volume by less than 250 thousand cubic yards, indicating that a straight channel is more sensitive to RSLR than a channel along the existing alignment.

While not explicitly included in Table 32, the sedimentation volumes in the Brazos Delta and the Freeport Offshore both tend to decrease with increasing sea level, further compensating for the sedimentation increase in the GIWW. All model scenarios have less than a 2% net change in total sedimentation volume from the base case, so any changes in sedimentation cannot be attributed to a change in the sediment budget of the model. Since the changes in sedimentation volumes appear to be uniform across all alternatives, it is unlikely that the outcome of a TSP selection will change based on RSLR.

5.4 Open San Bernard Mouth Modeling

5.4.1 Sedimentation Modeling

Hydraulic modeling was conducted after the Tentatively Selected Plan (TSP) milestone to determine the impacts of an open San Bernard mouth on the proposed project. This additional modeling was conducted to examine sedimentation patterns in the GIWW if the San Bernard Inlet were opened. It should be noted that currently, the mouth of the San Bernard is not dredged, and is only open following large storm events. The existing AdH model was modified to include an open connection between the San Bernard River and the Gulf of Mexico. Wave driven sediment transport was not included in the model, and the results shown only reflect sedimentation due to river deposition. Much of the morphology of the Sand Bernard River mouth is governed by the littoral processes and therefore this information should not be used to develop any quantitative analysis regarding the impact of the proposed TSP on the duration that the San Bernard River mouth will remain open. Qualitative comparisons were made to analyze the general impact of the proposed TSP on the inlet stability of the San Bernard mouth when compared to existing conditions. Figure 94 shows the open connection to the Gulf at the San Bernard mouth. The connection to the depth was set at a constant 6.6 ft. MSL.

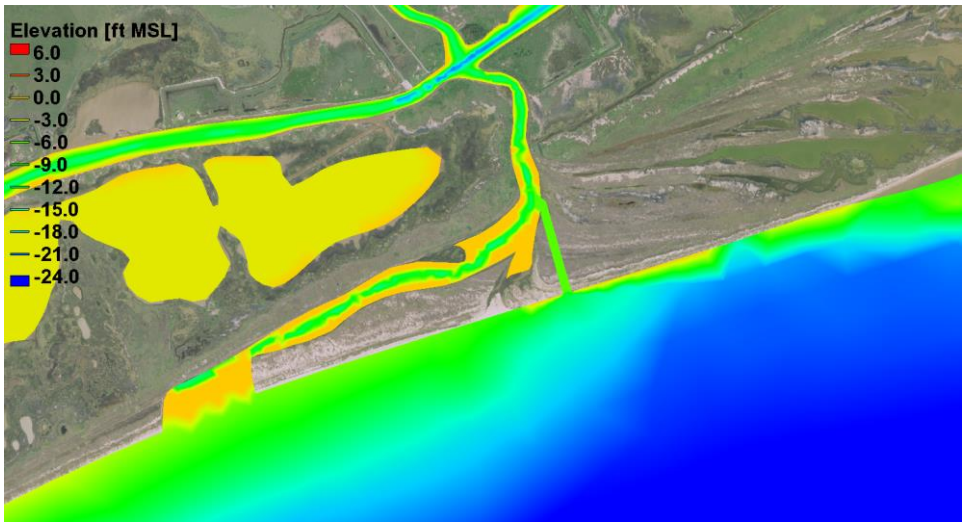

Figure 94. Bathymetry for open San Bernard condition

The calibrated sedimentation model was used to simulate sedimentation patterns and volumes for the open San Bernard mouth condition. Modeling for the open mouth condition was

conducted using the same inputs and timeframe as the closed mouth condition described in the Brazos River Floodgates (BRFG) H&H Appendix. Sediment deposition was quantified in three separate areas of impact for the open mouth condition: The San Bernard Gulf Channel, the San Bernard Inlet, and the West GIWW. Modeled sedimentation in these areas was also calculated for the closed mouth condition. Figure 95 shows the bounds of these impact areas.

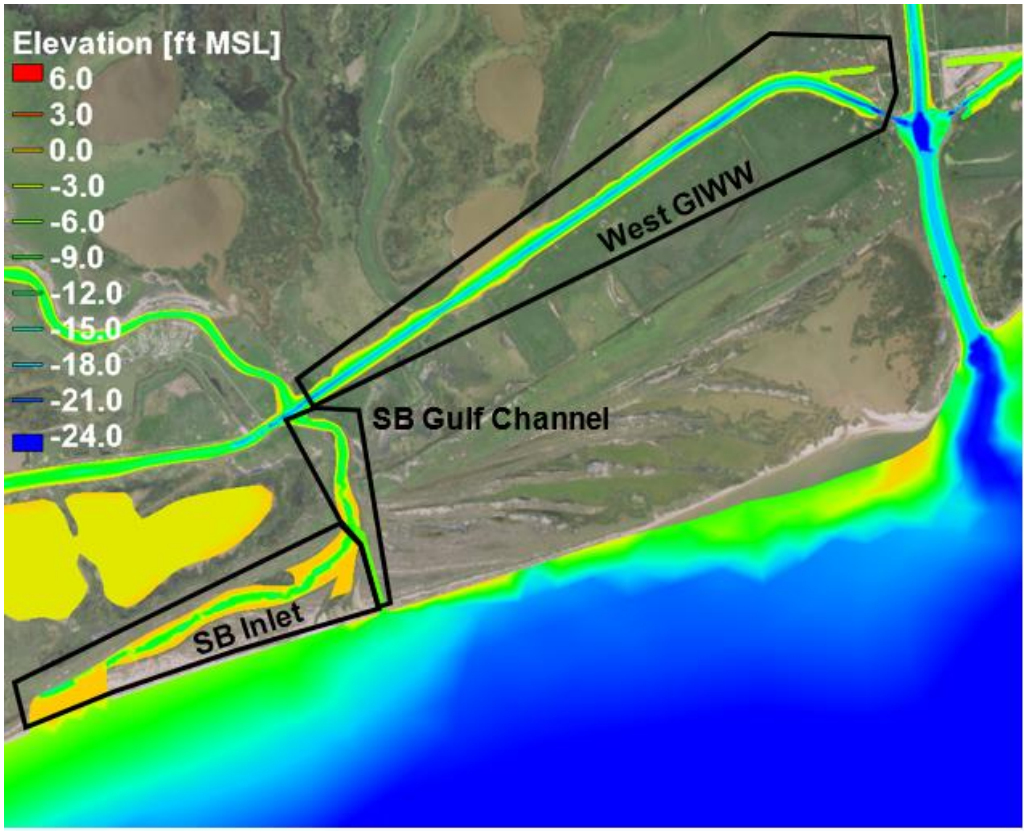

Figure 95. Locations of the West GIWW, San Bernard Gulf Channel, and San Bernard Inlet zones of impact.

Table 33 through Table 35 show the annualized sedimentation rate in the West GIWW, the San Bernard Gulf Channel, and the San Bernard Inlet, respectively.

Table 33. Annualized Sedimentation Rate in West GIWW [Cubic Yards/Year]

Alternative	Closed San Bernard	Open San Bernard	Change (open - closed)
Existing	555,000	689,800	+134,800 (+24%)
Alt. 3a.1	653,100	768,000	+114,900 (+18%)
Change (Alt - Existing)	+98,100 (+18%)	+78,200 (+11%)	

Table 34. Annualized Sedimentation Rate in San Bernard Gulf Channel [Cubic Yards/Year]

Alternative	Closed San Bernard	Open San Bernard	% Change (open vs closed)
Existing	10,100	1,200	-8,900 (-88%)
Alt. 3a.1	30,600	10,900	-19,700 (-64%)
% Change (Alt vs Existing)	+20,500 (+203%)	+9,700 (+808%)	

Table 35. Annualized Sedimentation Rate in San Bernard Inlet [Cubic Yards/Year]

Alternative	Closed San Bernard	Open San Bernard	% Change (open vs closed)
Existing	13,500	12,000	-1,500 (-11%)
Alt. 3a.1	26,000	24,200	-1,800 (-7%)
% Change (Alt vs Existing)	+12,500 (+93%)	+12,200 (+102%)	

In general, the open San Bernard condition resulted in increased sedimentation in the West GIWW when compared to closed conditions. This was true for existing conditions (24% increase) and Alternative 3a.1 (18% increase). The open San Bernard reduced sedimentation in the San Bernard Gulf Channel when compared to the closed condition, which is to be expected due to increased flowrates and velocities in this area. Overall an open San Bernard mouth shows the potential to increase sedimentation in the West GIWW, which could increase maintenance dredging costs. Presently for existing conditions, there are closures due to head differential at the west gate, often resulting from high San Bernard River flows traveling east and backing up against the closed west gate structure. Due to the removal of the west gate for the TSP, an open San Bernard is expected to have minimal impacts to navigation at the Brazos River Crossing for future with project conditions.

Note that when the San Bernard is open, the TSP (Alternative 3a.1) shows an increase in sedimentation of approximately 9,700 cy/year in the San Bernard Gulf Channel when compared to existing conditions. Overall, model results show that opening the San Bernard mouth causes additional sedimentation in the West GIWW, approximately 134,800 cy/year for existing conditions, and 114,900 cy/year for alternative 3a.1. Based on historical aerial examination, previous dredging attempts, and previous literature (Kraus and Lin, 2002), the controlling process for the morphology of the San Bernard mouth was found to be the net westward transport of sediments deposited by the Brazos River into the Gulf of Mexico, and not sediment deposition via in the San Bernard channel via the GIWW. Again, note that wave driven sediment transport was not included in the model, and the results shown here only reflect sedimentation due to river deposition.

5.4.2 Water Surface Elevation Analysis

Water surface elevations were investigated with an open and closed San Bernard mouth for both existing conditions and for the proposed TSP (Alternative 3a.1). Similar to the analysis performed in Section 3.2, water surface elevations were extracted from the model results at Sanders Road and Rivers End along the San Bernard River. The CDF curves at each location are shown below in Figure 96 and Figure 97.

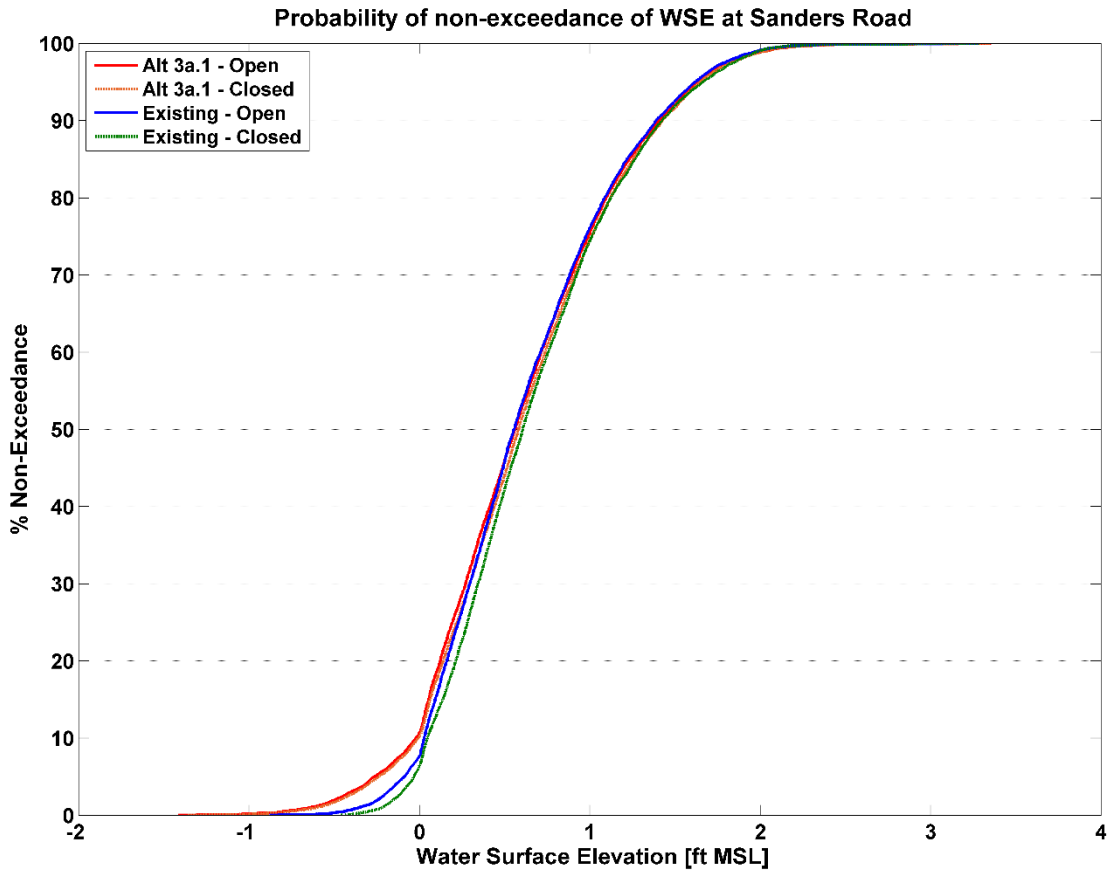

Figure 96. Probability of Non-Exceedance at Sanders Road for open/closed conditions.

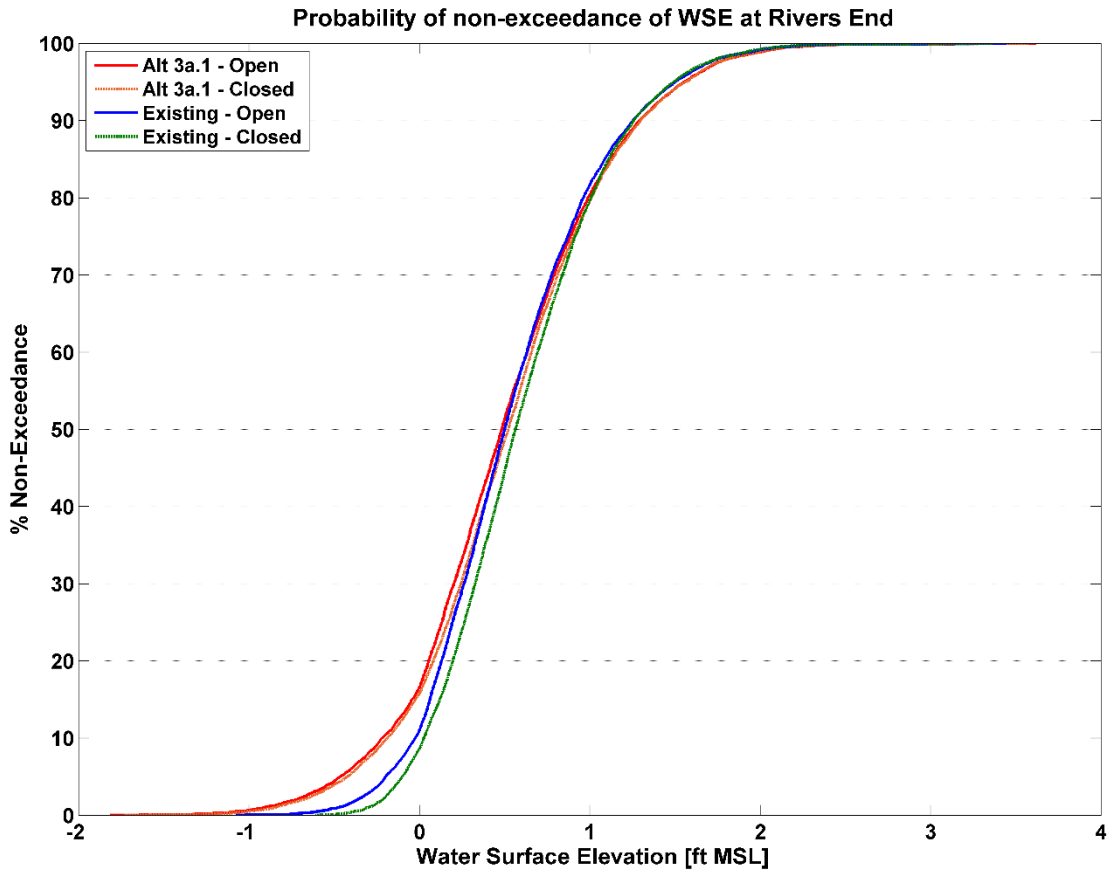

Figure 97. Probability of Non-Exceedance at Rivers End for open/closed conditions.

Table 36 and Table 37 show the change from existing closed for Alt 3a.1 (open), Alt 3a.1 (closed) and Existing (open) for selected intervals along the CDF curve.

Table 36: Rivers End change in WSE [ft.] from existing (closed) conditions for selected CDF intervals.

PNE Percentile	Alt3a1 Open	Alt3a1 Closed	Existing Open
5%	-0.11	-0.10	-0.03
10%	-0.08	-0.07	-0.02
25%	-0.04	-0.03	-0.02
50%	-0.03	-0.01	-0.02
75%	-0.01	0.00	-0.01
90%	0.01	0.01	0.00
95%	0.02	0.02	0.00
100%	0.08	0.06	0.03

Table 37: Sanders Road change in WSE [ft.] from existing (closed) conditions for selected CDF intervals.

PNE Percentile	Alt3a1 Open	Alt3a1 Closed	Existing Open
5%	-0.07	-0.06	-0.02
10%	-0.02	-0.02	-0.01
25%	-0.03	-0.02	-0.02
50%	-0.01	-0.01	-0.02
75%	-0.01	0.00	-0.01
90%	-0.01	0.00	-0.01
95%	-0.01	0.00	-0.01
100%	0.02	0.02	0.00

5.4.3 Inlet Stability Analysis

The hydraulic modeling described in Section 5.4.3 was further analyzed to provide a qualitative estimate of the proposed TSP's impact on the inlet stability of the San Bernard River. Inlet stability was investigated to determine whether the proposed TSP caused the San Bernard River mouth to change from a stable to an unstable inlet. Various methodologies have been proposed relating to inlet stability. Bruun and Gerritson (1960) and Bruun (1978) introduced a relationship between the tidal prism (Ω) and the annual gross littoral drift (M). Bruun (1978) proposed the following relationships for inlet stability based on historical inlet observations:

- Ω/M > 150: Good Inlet Stability
- 100 < Ω/M < 150: Fair Inlet Stability
- 100 < Ω/M < 150: Fair to Poor Inlet Stability
- Ω/M < 50: Poor Inlet Stability

Tung (2011) further investigated the stability relationships proposed by Bruun (1978) by conducting morphodynamic modeling using the Delft-3D system. The model tide period, amplitude, basin area, river discharge, and inlet dimensions were varied to test the stability of various inlet configurations. Tung (2011) conducted seven simulations with varying Ω/M ratios to test the relationships developed by Bruun et al. (1978). In general, Tung (2011) showed that higher Ω/M ratios resulted in good location stability, while lower ratios resulted in closure prone inlets with highly variable channel locations, which is in agreement with the relationships proposed by Bruun et al. (1978).

Flowrates along the open San Bernard channel south of the GIWW were extracted for use in the inlet stability analysis. Figure 98 shows the extraction location used for this analysis.

Figure 98. Extraction Arc Used for Inlet Stability Analysis

These flowrates were used to calculate the tidal prism for each tidal cycle in during the model simulation period. Previous research by Kraus & Lin (2002) quantified the eastward and westward littoral drift near the mouth of the San Bernard River. These quantities were added to determine the annual gross littoral drift. Table 38 summarizes the longshore transport results at the mouth of the San Bernard from 1990-1999.

Table 38: Annual Sediment Transport Rates at the Mouth of the San Bernard (from Kraus & Lin, 2002)

Year	Eastward [cu m/yr]	Westward [cu m/year]	Gross [cu m/yr]
1990	58,860	259,390	318,250
1991	65,250	309,340	374,590
1992	74,290	257,050	331,340
1993	68,750	253,030	321,780
1994	58,630	298,740	357,370
1995	81,750	287,800	369,550
1996	96,060	208,220	304,280
1997	87,660	242,050	329,710
1998	60,710	285,370	346,080
1999	73,370	224,520	297,890
Mean	**72,533**	**262,551**	**335,084**
Max	**96,060**	**309,340**	**374,590**
Min	**58,630**	**208,220**	**297,890**

Source: Kraus & Lin (2002)

The minimum, mean, and maximum gross transport rates shown in Table 38 were used in the inlet stability analysis. Figure 99 shows the results of the inlet stability analysis. The box and whisker plot shown in Figure 99 summarizes the range of Ω/M ratios from the model simulation.

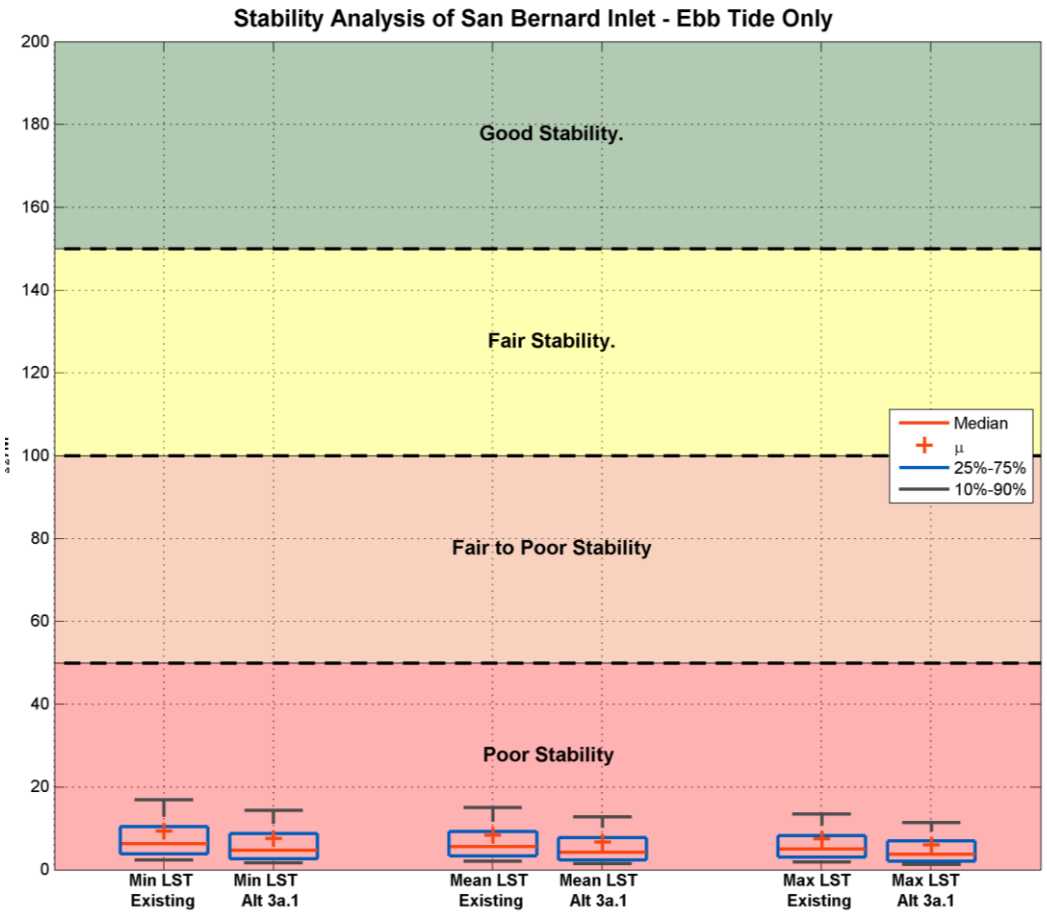

Figure 99. Box and whisker plot showing the range of inlet stability

The results in Figure 99 show poor stability for both existing and proposed conditions. The maximum stability number noted during the simulation corresponds to an approximate 5-year flow. The Ω/M ratio for the 5-year flow event is shown in Table 39. Table 39 shows the absolute change in the Ω/M ratios for existing and proposed conditions. Note that the maximum stability ratio corresponds to an approximate 5-year flood event in the San Bernard River and is not representative of the typical stability of the inlet.

Table 39: Summary of Ω/M ratios for existing and proposed conditions

Condition	Existing Conditions Ω /M	Alternative 3a.1 Ω /M	Change Ω /M
25th Percentile	3.9	2.7	-1.2
Mean	8.4	6.8	-1.6
75th Percentile	10.4	8.8	-1.6
95th Percentile	20.7	15.2	-5.5
Max*	237.6	205.3	-32.3

Note*: Maximum Ω/M ratio corresponds to 5-year flood event in San Bernard River and is not representative of typical stability of the inlet.

The results shown in Figure 3 and Table 39 indicate that San Bernard inlet has poor stability during existing conditions as well as for the proposed TSP. Any changes in stability (Ω/M

ratio) due to the proposed TSP are expected to be minor, and do not change the stability regime of the San Bernard Inlet.

6 Navigation Analysis

6.1 Introduction

Closures and delays at the Brazos River floodgates are often caused by hydraulic conditions. This Section of the report quantifies these closure and delay conditions for existing conditions, and uses the results of the hydraulic model to quantify those conditions for the proposed alternatives. The following sub-sections examine project site conditions, provide an assessment of existing navigation regulations, provide a methodology for analyzing the hydraulic model results, calibrate the model for existing conditions, and perform an analysis of the navigation conditions for all proposed alternatives.

6.2 Project Site Conditions

This Section examines existing conditions at the Brazos River Floodgates (BRFG). In this Section, closure and delay criteria are described and a summary of the available data is provided.

6.2.1 Existing Closure & Delay Criteria

Delay conditions at the Brazos River Floodgates are caused by numerous factors including high velocities in the Brazos River, head differential between the river and GIWW side of the gate structure, and accidents. This memorandum investigates closures due to river velocity and head difference. Closures due to accidents are included in economic analysis and models developed under task 100.3 – Economics. The closure criteria guidelines for hydraulic conditions as listed in 33 CFR 207.187 are shown in Table 40 (USACE, 1969). Note that the closure criteria for river velocities is based upon the High Water Operations Policy Memorandum CESWG-OD-O (11-2-240a) (USACE2016).

Table 40. Closure criteria.

Condition	Description	River Conditions
Unlimited passage	No restrictions on passage.	River current below 2 mph and head differential is less than 0.7 feet.
Limited Passage	Passage allowed for single vessels with a single loaded barge or two empty barges	River current between 2-5 mph (daylight) or 2-7 mph (night) or the head differential is between 0.7-1.8 feet.
Gate Closures	Closed to navigation.	River current exceeds 7 mph (daylight) or 5 mph (night). Head differential exceeds 1.8 feet.

6.2.2 Available Data for Navigation Analysis

Each of the Brazos floodgates were individually removed for maintenance between 2009 and 2013. Thus, the gages were analyzed in the period between March 2015 and April 2016 to determine typical hydrodynamic conditions at the Brazos gates.

6.3 Navigation Assessment

This Section assesses the navigation standards to characterize the safe inland waterway navigation criteria through the Brazos River Floodgates. The goal of this section is to understand how the navigation threshold criteria are set relative to the standards in order to understand how they may change with future alternative conditions.

Currently the GIWW is maintained to a bottom width of 125 feet. Depths along the GIWW are maintained at a project depth of 12 feet mean low water. As shown in Table 40, there are regulations on the operations of the floodgates that fall into three categories. Proposed alternatives include a 125-foot-wide gate structure, which is 50 feet wider than the existing alignment. It is possible that the closure conditions may change under the proposed wider gate alignment. For the purposes of this analysis, closure and limited passage conditions were assumed to remain the same for all alternatives. Shipping industry members were consulted during a Project Delivery Team (PDT) meeting held on October 5th, 2017. Industry members were consulted regarding closure restrictions for the with-project conditions. Industry members present at the October 5th meeting recommended maintaining the current restriction and closure criteria for all with project alternatives.

6.4 Navigation Analysis Methodology

The goal of this analysis is to determine delays at the Brazos River floodgates for the existing configuration due to conditions exceeding the limitations stated in 33 CFR207.187. Closure data during the model simulation period was obtained from the USACE and used to calibrate the navigation analysis (USACE, 2017).

Modeling of hydrodynamic processes at the project site was conducted using the ADH model as described in Section 3.1. The modeled flow conditions were analyzed for delay events and compared to the measured closures. The following methodology is proposed to compare the recorded closures to the modeled closures.

- Outlier processing was conducted to remove unrealistically high or low spikes in modeled data. Closure or limited passage events less than a 30-minute duration were removed from the modeled dataset. Events with less than a 45-minute time between them were grouped into a singular event.
- The modeled data was processed through a low pass to remove the higher frequency fluctuations due to gate operations, discussed in Section 6.5.2.
- Recorded closure data due to head differential and river velocity was obtained from the USACE. The filter scheme that provided the highest correlation between the modeled and recorded closures and limited passage conditions was selected.
- A comparison between the recorded and modeled closure data was conducted to determine the percent error of modeled closures when compared to recorded closures.

6.5 Existing Condition Results

This Section discusses the analysis conducted to determine closures of the existing BRFG system. The goal of the analysis of existing conditions analysis are to develop understanding of hydrodynamic conditions causing closures of the BRFG system crossing during a variety of conditions. This methodology will be used to quantify closures for proposed array of alternatives

6.5.1 Measured Data Delays

6.5.1.1 Limited Passage & Closure Data

As shown in Table 40, limited passage due to river velocity occurs when the river velocity is between 2 mph and 5 mph during nighttime hours, or between 2 mph and 7 mph during daylight hours. Limited passage due to head differential occurs when the head differential at the gates is between 0.7 and 1.8 feet. Limited passage requires "… passage afforded only for single vessels or towboats with single loaded barges or two empty barges. When two barges are

rigidly assembled abreast of each other and the combined width is 55 feet or less, they are considered a single barge". Limited passage requires additional tripping of barges, and is therefore a key variable when determining the delays related to the hydrodynamics at the BRFG system.

Complete closure of the gates due to river velocity occurs when the river velocity is greater than 5 mph during nighttime hours, or above 7 mph during daylight hours. Closures due to head differential occur when the head differential at the gates is greater than 1.8 feet. Recorded closures and limited passage conditions were analyzed for the model simulation period of March 1, 2015 to April 1, 2016 (USACE, 2017). A summary of the recorded limited passage conditions and closure during the model simulation period of March 1, 2015 to March 31st, 2016 (396 days) is shown below in Table 41.

Table 41. Recorded limited passage delays and closure conditions between March 2015 and April 2016 when the threshold head difference and velocity for limited passage was exceeded.

Condition	Number of days with Delay	% of total time delay occurs
Limited Passage	186	43%
Closures	23	2%
Total	209	45%

Note that the number of days shown in column one of Table 41 represent the number of days over the evaluated time period (396 days occur between 3/1/15 and 3/31/16) when at least one instance of limited passage or closure conditions occur. The percent of total time with a delay column shown in Table 41 represent the percent of total time where a given delay condition was met. The results show that approximately 45% of the time limited passage or closure conditions occur at the Brazos River Floodgates.

6.5.2 Modeled Delays

Output results for existing conditions were extracted from the hydraulic model to determine the modeled downtime due to head differential (>1.8 feet) and river velocity (> 5 mph during daylight or >7mph during nighttime). Statistics on limited passage due to head differential (>0.7 feet) and river velocity (2-7 mph during daylight or 2-5mph during nighttime) were also developed. The extraction points used for delay calculations are shown in Figure 100. To determine river velocity criteria, the velocity used was derived from the total flow divided by the flooded area of the river cross section rather than a singular point extraction. This better represents the overall velocity of the river. The point data shown in Figure 100 represent a singular point along the flow extraction line.

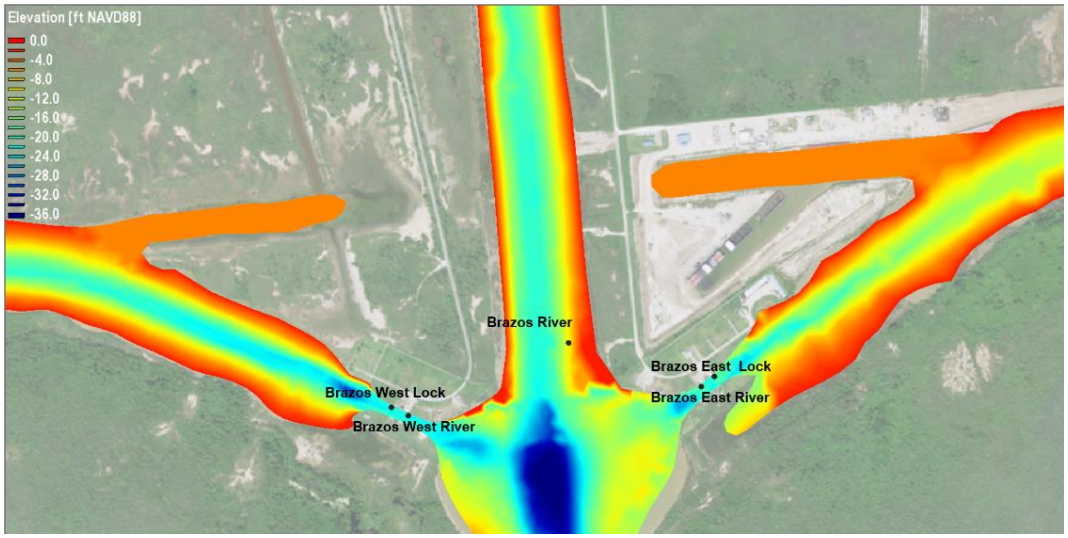

Figure 100. Existing condition model bathymetry and extraction points for navigation analysis.

An example of the raw modeled water surface elevation data and the filtered data is shown in Figure 101. A 3-hour moving average window was used to filter the data shown in Figure 101. Note the large spikes in the raw data. Several filtering schemes were tested and the selected scheme was chosen based on agreement with the recorded closure data. The filtered data was used to calculate the modeled delays and compare them to the known delays as recorded by the USACE. The selected filtering scheme (a moving average window of 3 hours) was able to predict 100% of the limited passage events, and 31% of the closure events. While the closure event prediction rate is fair, the model was able to identify these known closure times as at least limited passage. So, while the closure was not identified for 69% of events, all these events were identified as limited passage (i.e., some navigation impact). The recorded restricted navigation events occur for 45% of the time; the model predicts restricted navigation 48%. Overall the methodology captures the major trends in the navigation restrictions. The results of the modeled closure analysis for limited passage and closure conditions using a 3-hour moving average filter are shown in Table 42 and Table 43, respectively.

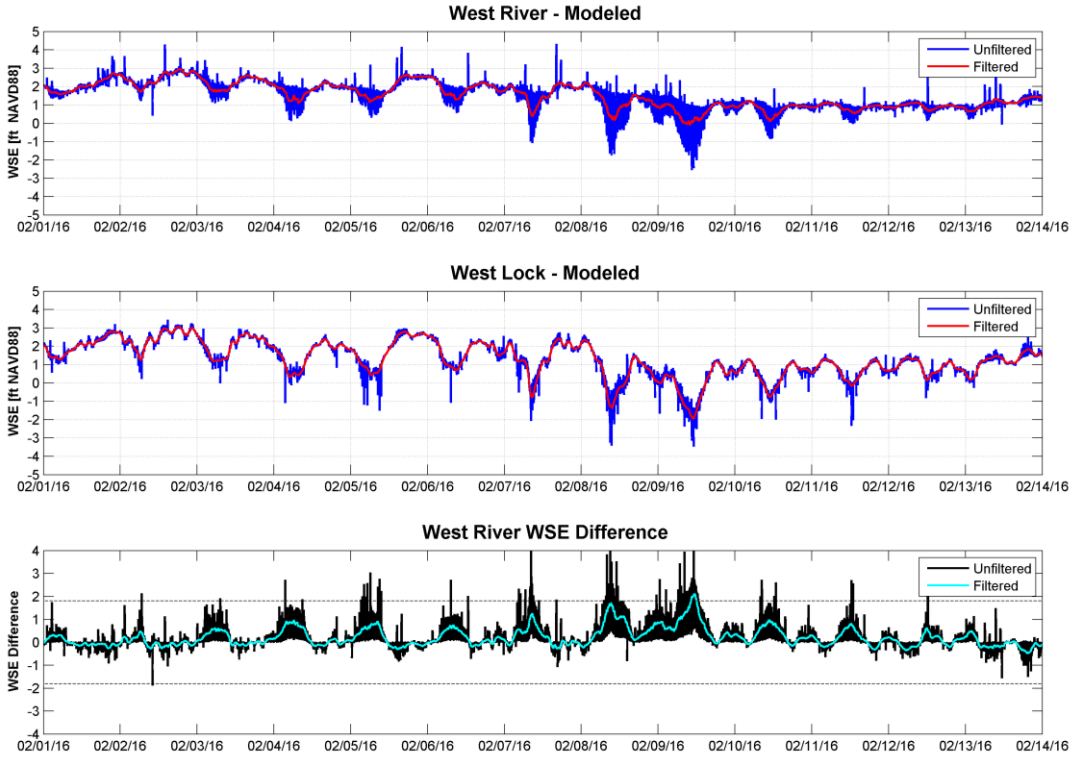

Figure 101. Filtering results for west river extraction point (top), west lock extraction point (middle), and the water surface elevation difference (west river – west lock) between the two gages (bottom).

Table 42. Comparison of what causes modeled limited passage conditions.

Condition	Number of days with delay	% of total time delay occurs
West Gate >0.7ft and <1.8ft on river side	200	5.2%
West Gate >0.7ft and <1.8ft on GIWW side	9	0.03%
East Gate >0.7ft and <1.8ft on river side	11	0.05%
East Gate >0.7ft and <1.8ft on GIWW side	3	0.04%
River Velocity >=2mph	185	41.1%

Table 43. Comparison of what causes modeled closures.

Condition	Number of days with closure	% of total time closure occurs
West Gate >= 1.8 ft. on river side	5	0.1%
West Gate >= 1.8 ft. on GIWW side	0	0.0%
East Gate >= 1.8 ft. on river side	0	0.0%
East Gate >= 1.8 ft. on GIWW side	0	0.0%
River Velocity >=5mph	37	3.5%

The results shown in Table 42 and Table 43 illustrate that limited passage and closures conditions are controlled by head differential at the west gate and velocity in the river. The

majority of closures and limited passage conditions are due to the river velocity being above the specified thresholds. The second most common cause of both closure and limited passage conditions is the water surface elevation of the river being higher than the water surface elevation of the GIWW at the west gate. Potential causes of these delay conditions are examined later in this Section. A comparison of the modeled closure and limited passage conditions is shown in Figure 102.

Modeled limited passage conditions (light blue) show significant overlap with recorded limited passage conditions (dark blue). Modeled closure conditions (red) show less overlap with recorded closures (pink). The largest discrepancy between recorded and modeled closure conditions occurs in mid-June to early July. There is a modeled closure condition during this time due to high river velocity, while the recorded closure data showed limited passage during this time. Despite this discrepancy, when you combine closure and limited passage conditions, the modeled results show 100% overlap with the recorded results. The model results do show several brief limited passage events from July to November and from February to March that are not in the recorded data; this may be due to the high temporal resolution of the model compared to the manual measurement and implementation of actual limited passage criteria on the ground. Figure 103 shows the modeled head differential at both gates, as well as modeled river velocity plotted against the recorded closure and limited passage conditions obtained from the USACE. Note that the head differential at each gate is calculated by subtracting the river elevation from the GIWW elevation resulting in positive values indicating the GIWW is higher than the river.

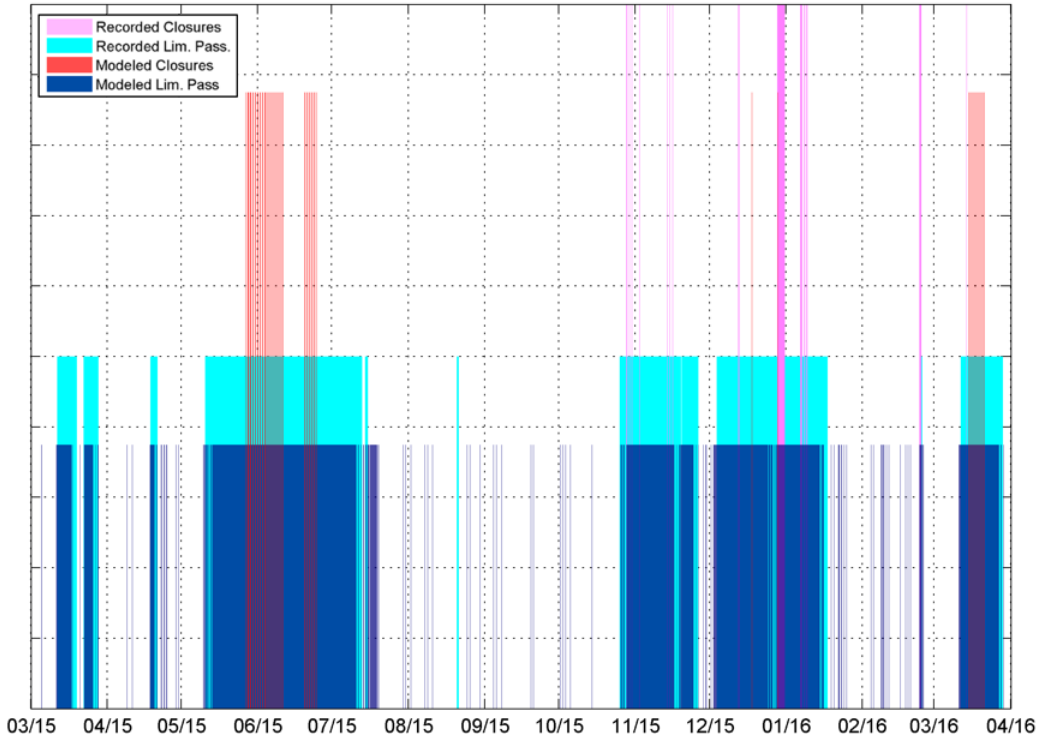

Figure 102. Comparison of recorded and modeled close and limited passage events.

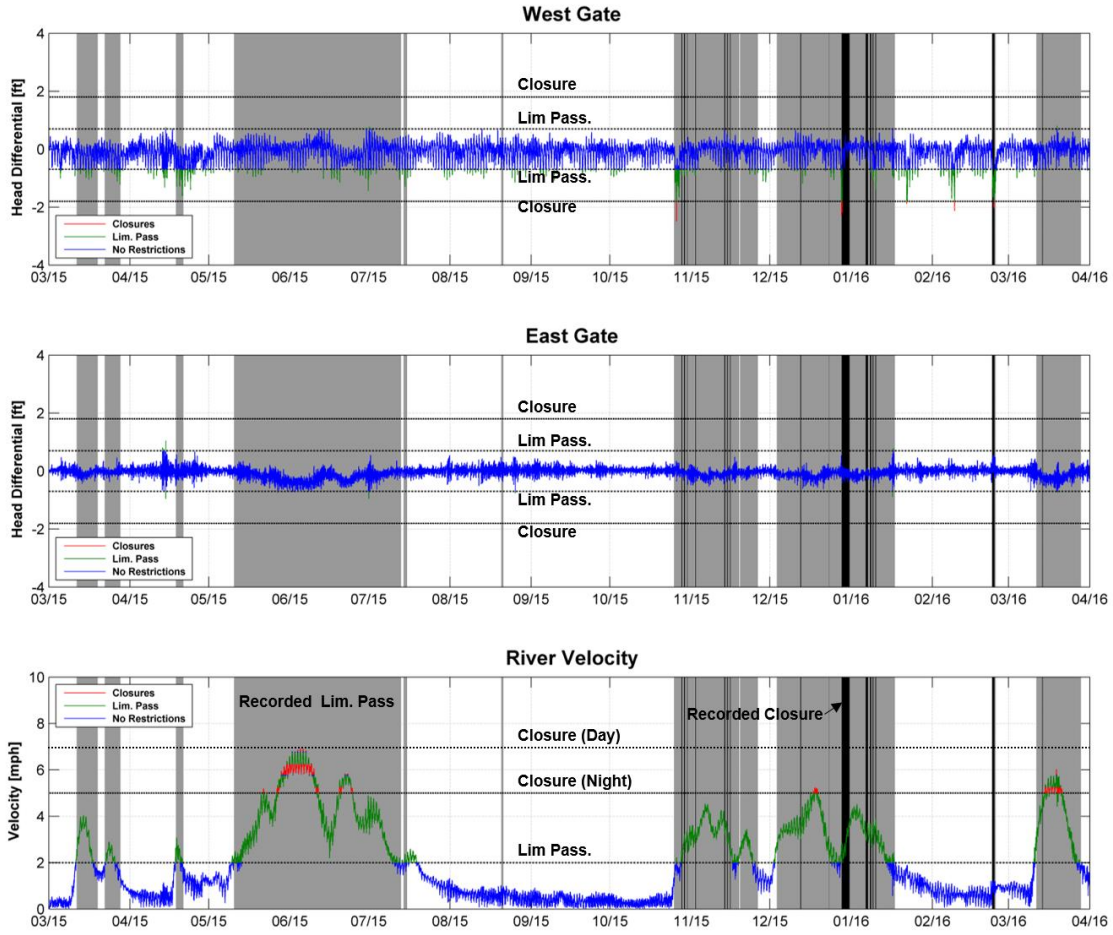

Figure 103. Modeled head differential (River – GIWW) at west gate (top), east gate (middle), and modeled river velocity. Grey shaded areas represent recorded limited passage conditions, while black shaded areas represent recorded periods of closure.

These results show limited modeled closure conditions due to head differential. The only modeled closure events due to head differential occur at the west gate, when the Brazos River is at a higher elevation than the GIWW.

Closure and limited passage events were compared to river conditions to examine the relationship between different types of river events and river flow to quantify any patterns. Figure 104 shows the relationship between days on which a modeled gate closure condition occurs and the time series of flow rates in the Brazos River and San Bernard River and the observed tidal elevation. This figure also shows the relationship between the combined flow rates in the Brazos River and the San Bernard River on days when a gate closure condition occurred.

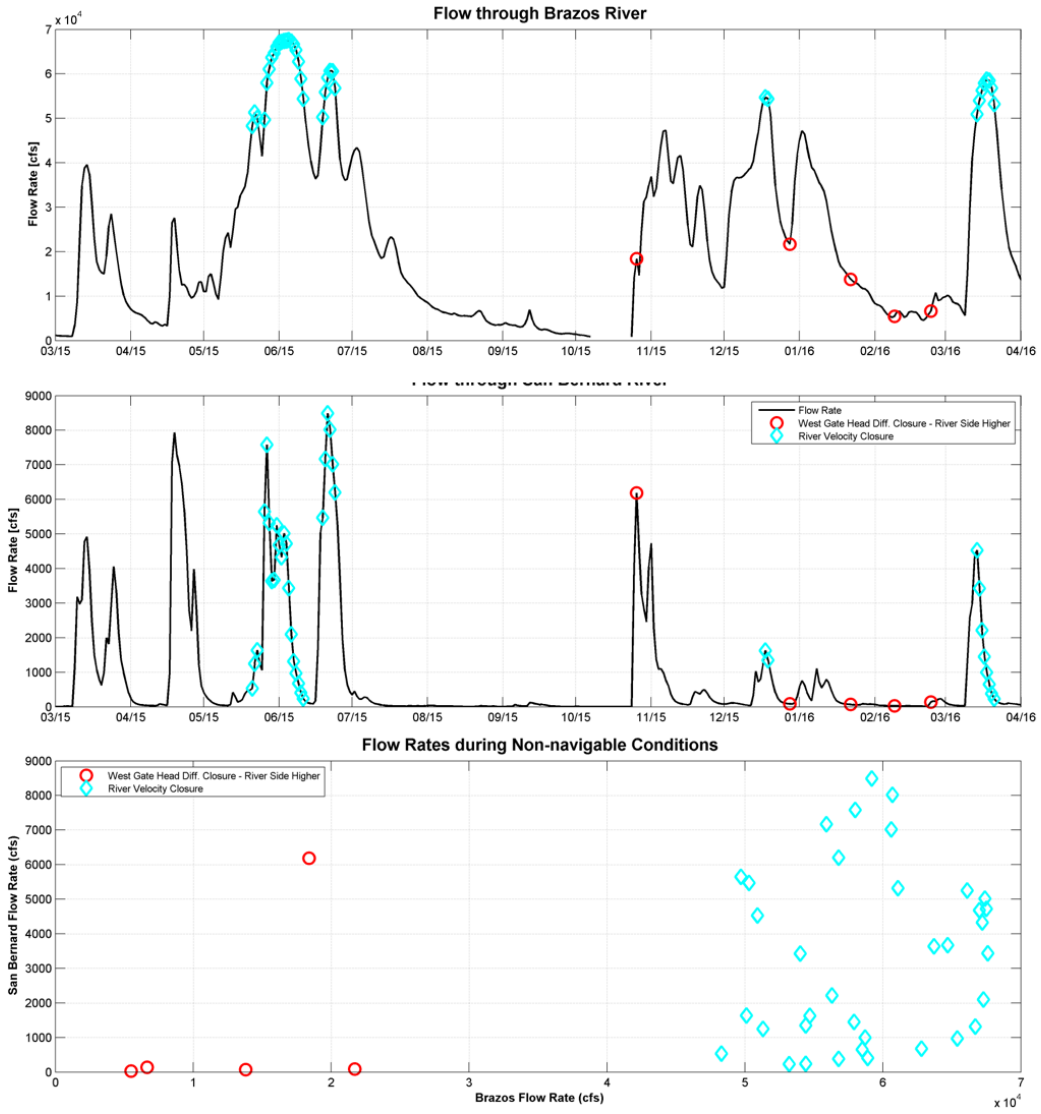

Figure 104. Relationship between modeled gate closure conditions and flow rate in the Brazos River (top), flow rate in the San Bernard River (middle), and the combined flows in both rivers (bottom).

Based on Figure 104, the following can be observed about the relationship between the river flows and what condition caused the closure during the model simulation period:

- **Condition 1) Brazos River head exceeds GIWW head at the West Gate:** The majority of these closures tend to occur during times when the flow in the San Bernard River is low relative the flow in the Brazos River. This closure condition seems more dependent on very low flows in the San Bernard River than very high flows in the Brazos River.
- **Condition 2) River Velocity exceeds threshold:** Closures due to high river are solely dependent on high flows in the Brazos River. It appears that when the input flow into the modeling grid at Rosharon, TX is approximately above 50,000 cfs that the river velocity at the gates meets the closure condition.

Limited passage conditions and river flow velocities were also investigated. The results of the limited passage analysis are shown below in Figure 105.

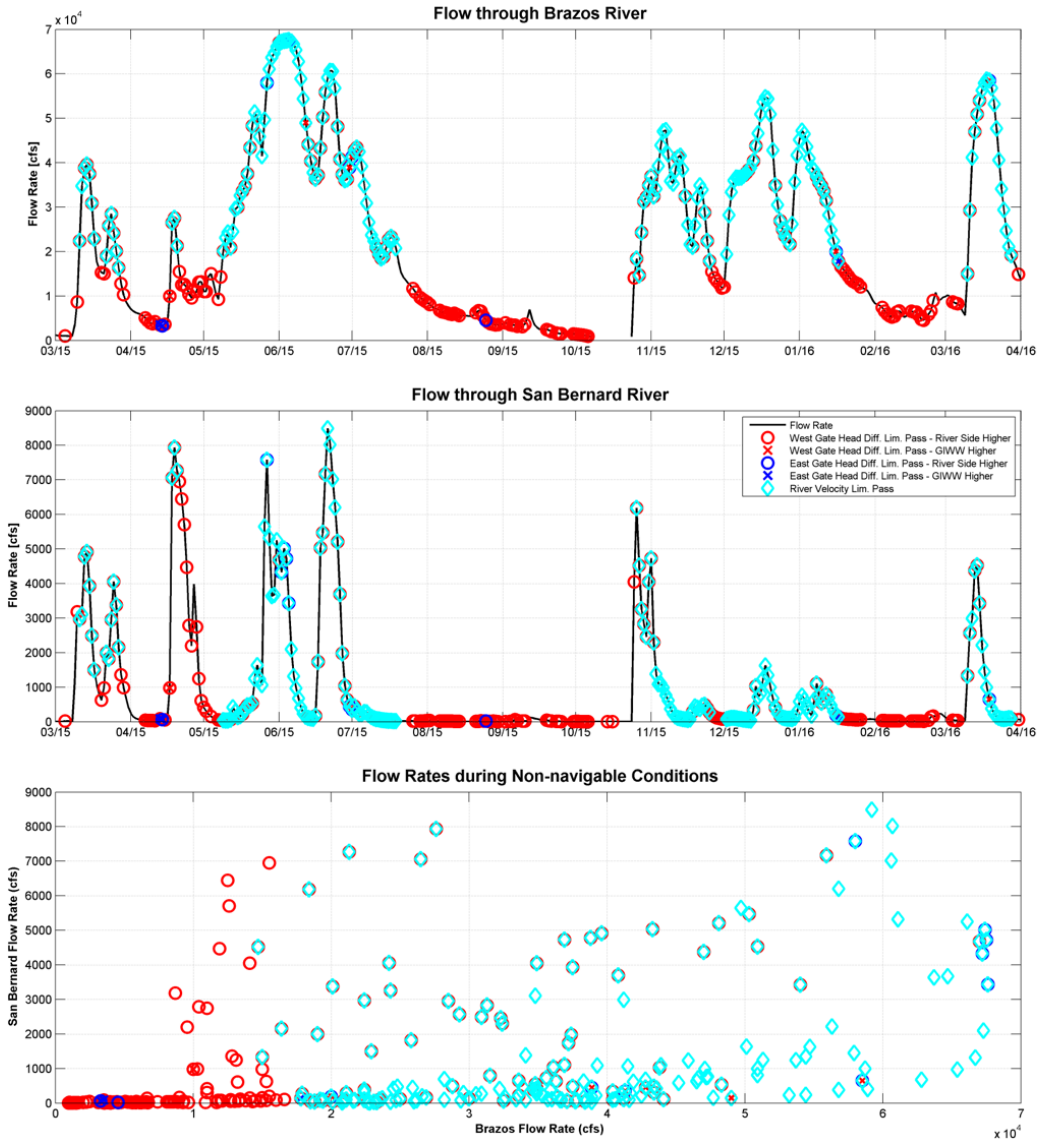

Figure 105. Relationship between modeled limited passage conditions and flow rate in the Brazos River (top), flow rate in the San Bernard River (middle), and the combined flows in both rivers (bottom).

Based on Figure 105, the following can be observed about the relationship between the river flows and what condition caused the limited passage event during the model simulation period:

- **Condition 1) Brazos River head exceeds GIWW head at the West Gate:** Similar to the closure analysis, the majority of these closures tend to occur during times when the flow in the San Bernard River is low relative the flow in the Brazos River. During high flow events, this condition seems to coincide with the river velocity condition.
- **Condition 2) River Velocity exceeds threshold:** Limited passage events due to high river are solely dependent on high flows in the Brazos River. It appears that when the input flow into the modeling grid at Rosharon, TX is approximately above 15,000-20,000 cubic feet per second (cfs) that the river velocity at the gates meets the limited passage condition. At higher flow rates in the Brazos, this condition has large amounts of overlap with limited passage events due to the Brazos head exceeding the GIWW head at the west gate.

- **Condition 3) Brazos River exceeds GIWW head at the East Gate:** Limited passage events due to the Brazos exceeding the GIWW at the east gate are rare, however they seem to occur only when the flow in the Brazos is extremely high. The flow in the San Bernard river does not appear to influence these events.

The model is well suited for prediction of limited passage, but poor in prediction of closures. We hypothesize that much of the lack of skill in the prediction of closures is due to at least three factors. One factor is no knowledge of actual gate operations; instead we use only a schematized approach. Gate operations impact hydraulics. In the runup to an event, if the gates are actually closed more than are being simulated, this may result in an increase in head difference which results in closure that may not have occurred if the gates were operating at regular intervals as they are in the model. The opposite is true as well: in the runup to an event if the gates were operating more frequently than simulated, this may reduce head difference compared to the model. Second, we have only very noisy measured hydraulic data resulting from gages sampling too infrequently and located too close to the gates that provides little insight into the actual hydraulics at closures. Finally, the recording of events has a coarse temporal resolution. In other words, the declaration of events is based on human sampling of the head and velocity, and is updated at unknown frequency, is recorded at an unknown time relative to onset of the event, and ends at an unknown time relative to the actual end of the event. Given these challenges, the model's ability to predict restricted navigation is reasonable for comparison purposes. However, we recommend improving these limitations after a Tentatively Selected Plan (TSP) is selected for a more quantifiable comparison of delay events.

6.6 Navigation Hindcasting

An Artificial Neural Network (ANN) was developed to hindcasting head differentials at each gate and river velocity from 1980-2016. An ANN is a machine learning technique that uses a series of input data to perform "training examples". The training examples are organized into layers of nodes, that are calibrated to the training dataset. Once trained, the ANN can be used to predict results outside of the training set. At the BRFG, the modeled head differential at each gate and the river velocity were used to train the ANN. The input conditions fed into the ANN during the training period are the wind velocity, Brazos River flowrate, San Bernard River Flowrate, change rate of the harmonic tide, and harmonic tidal elevations. Using these variables as input conditions and the modeled head differential or velocity as output, the ANN was trained for the model simulation period of March 2015 to April 2016. Once trained, the ANN was used to hindcast river velocity and the head differential at each gate Figure 106 shows the results of the neural network training for head differential at each gate and river velocity. River velocity shows the greatest correlation with modeled results, with an index of agreement of 1.00. The index of agreement between hindcast and modeled head differential is 0.94 at the west gate and 0.81 at the east gate. The lower index of agreement at the east gate suggests that head differentials are less correlated with the training parameters than the river velocity and west gate head differential. Model results show that delays are mostly caused by head differential at the west gate and river velocity, with little impact from the east gate head differential. Therefore, the lower index of agreement between the modeled and hindcast results at the east gate is not expected to greatly affect the hindcast accuracy.

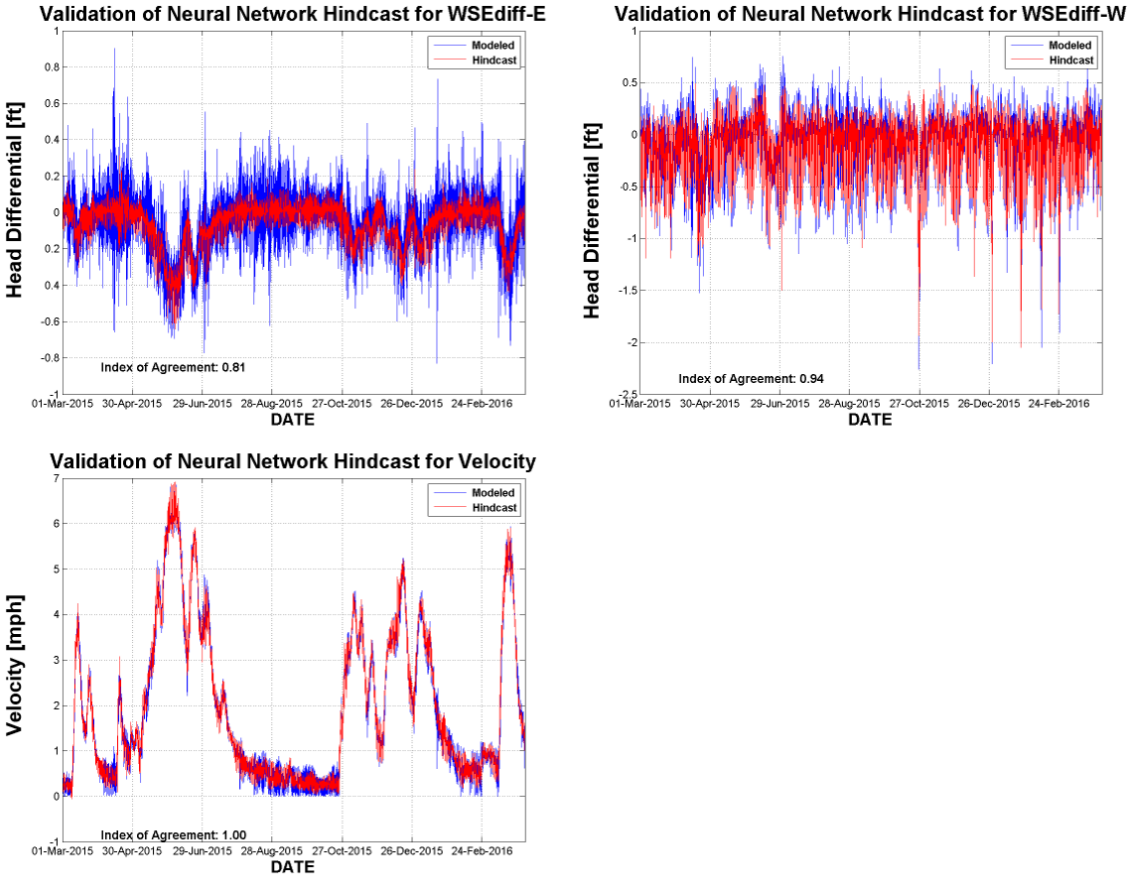

Figure 106. Existing condition hindcast training results.

Once validated, the trained neural network was used to hindcast river velocity and head differentials at each gate from 1980-2016. The hindcast results from this 36-year period were then used to form closure and limited passage statistics for existing conditions. A comparison of the delay statistics for the hindcast (1980-2016) and modeled (2015-2016) results is shown in Table 44.

Table 44. Comparison between modeled and hindcast delay statistics.

Method	Limited Passage	Closure	Total
Model 2015-2016	44%	4%	48%
Hindcast 1980-2016	24%	4%	27%

Note that the hindcast delays for existing conditions are significantly less than the modeled delays. This is likely explained by the fact that the modeled year (March 2015-April 2016) was an unusually wet year, with 3 flood events greater than the 1-year event in the Brazos and 4 such events in the San Bernard.

6.7 Alternatives Analysis

The hydraulic conditions were extracted from the alternatives and filtered using the same methodology as existing conditions. The results of the alternatives analysis are described in the following Section.

Alternatives were analyzed for closure and limited passage delay events. The proposed alternatives were simulated using the hydrodynamic model results. All alternatives were filtered using the same methodology stated in the previous section. The filtered results for each alternative were then passed through the neural network, which was trained separately for each alternative. The trained neural network was then used to hindcast the gate head differentials and river velocities from 1980-2016. Figure 107 shows the extraction points used for navigation analysis as well as the bathymetry used to model each alternative.

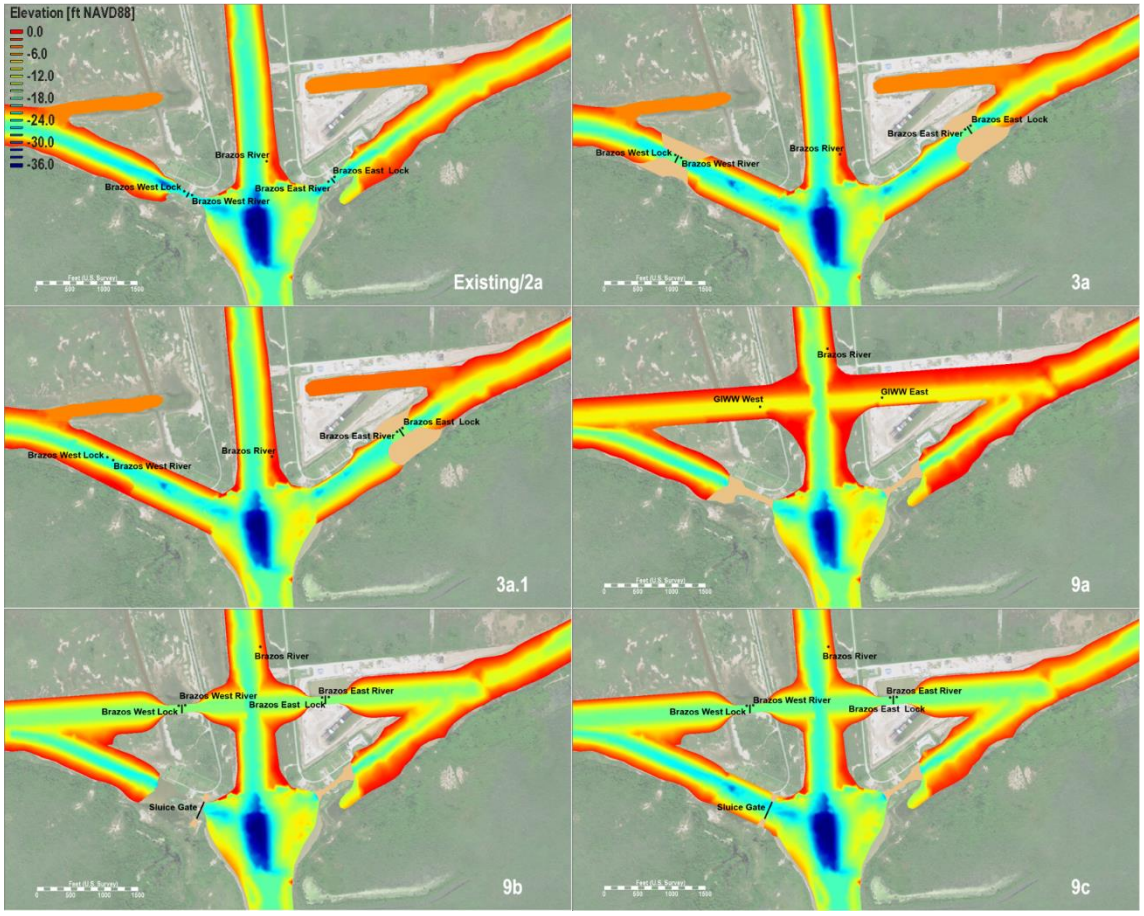

Figure 107. Alternatives modeled and extraction points for navigation analysis.

A summary of the closure conditions during the hindcast period (1980-2016) due to head differential, velocity and total closures is shown in Table 45. A summary of the limited passage occurrence rate during the simulation period due to head differential, velocity, and total is shown in Table 46. Note that the total closure and limited passage columns in each table employ the filters described earlier in this Section and only count the instances when head differential and velocity delays occur simultaneously as one event. Due to the filtering scheme described earlier in this section, a summation of the head differential and velocity closure percentages may not equal to total closure percentage shown in the tables below.

Table 45. Summary of closure condition causes and total closure % for alternatives.

Alternative	Closure % Head Differential	Closure % Velocity	Total %
Existing/2a	3.1%	1.0%	3.8%
3a	0.0%	0.7%	0.6%
3a.1	0.0%	0.9%	0.9%
9a	0.0%	1.8%	1.7%
9b	0.3%	1.7%	1.8%
9c	0.2%	1.6%	1.6%

Table 46. Summary of limited passage conditions and % of time under limited passage restrictions for alternatives.

Alternative	Limited Passage % Head Differential	Limited Passage % Velocity	Total %
Existing/2a	14.5%	10.6%	23.5%
3a	7.5%	10.0%	16.6%
3a.1	0.2%	9.7%	9.8%
9a	0.0%	12.3%	12.2%
9b	7.5%	12.5%	18.9%
9c	6.2%	12.6%	17.4%

Based on the hindcast results shown in Table 45, all proposed alternatives are expected to significantly reduce closures due to head differential. Changes in closure conditions due to river velocity remain relatively unchanged, except for Alternative 9a, 9b, and 9c. Increased closures due to velocity are noted for these alternatives, however overall closure rates are lower than existing conditions. Note that for Alternative 9a there is a potential for higher velocities through the GIWW due to the lack of gates. This is investigated later in this Section.

Limited passage occurrences due to head differential are also decreased with all proposed alternatives as show in Table 46. Limited passages due to velocity follows similar trends to the closure statistics. Alternatives along the existing alignment (Alternative 3a and 3a.1) show little change, while Alternatives 9a, 9b, and 9c show an increase in velocity closures. The total percent of the model simulation where limited passage or closure conditions occur is shown in Table 47.

Table 47. Summary of limited passage conditions, closure conditions, and total event conditions as a percentage of the model simulation period.

Alternative	Limited Passage %	Closure %	Total %	% Change from Existing
Existing/2a	23.5%	3.8%	27.3%	--
3a	16.6%	0.6%	17.2%	-10.0%
3a.1	9.8%	0.9%	10.7%	-16.6%
9a	12.2%	1.7%	13.9%	-13.3%
9b	18.9%	1.8%	20.7%	-6.5%
9c	17.4%	1.6%	19.1%	-8.2%

Based on the results shown in Table 47, Alternative 3a.1 provides the greatest reduction in total events (16.6% reduction), followed by Alternative 9a (13.3% reduction).

Head differentials at the gates were analyzed and are shown in the form of cumulative distribution function (CDF), with probability of non-exceedance for the range of water surface elevations in Figure 108. The CDF curves for head differential were based on the hindcast results. The CDF curves developed during this analysis show the probability of non-exceedance at various head differentials. The alternatives show reduction in head differential at the west gate from existing conditions, while all alternatives with a gate on the east side of the Brazos show similar results to existing conditions.

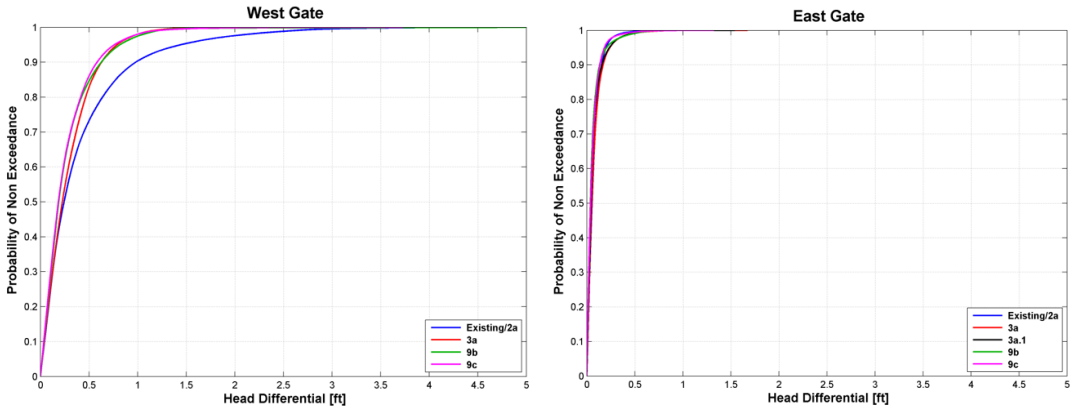

Figure 108. Probability of Non-Exceedance for head differential at west gate (top) and east gate (bottom).

The CDF curves were also developed for velocities at the intersection of the GIWW and the Brazos River. Hindcasting was not performed on these velocities due to a due to a lack of measured data for calibration of the model results. The CDF velocity curves shown in Figure 109 were developed using model output. The CDF curves for velocities at the GIWW and Brazos intersection were extracted riverward of the gates for Alternatives 2a, 3a, 3a.1 east, 9b, and 9c. The velocities were extracted near the intersection of the GIWW and Brazos for Alternatives 3a.1 west and 9a since there are no gate structures. The results of the CDF curves at the intersection of the Brazos River and GIWW are shown in Figure 109. Alternative 3a.1 west shows slightly decreased velocities at the intersection of the west location under daily conditions, even when compared to the open channel alternative. This is likely due to the lack of a gate constriction causing increased velocities. In addition, Alternative 3a.1 shows lower velocities in the west GIWW immediately adjacent to the Brazos River when compared to Alternative 9a. This reduction in velocity is hypothesized to be directly related to the angled intersection with the Brazos, as well as the wider opening at the crossing from the open channel. The angled intersection reduces the amount of flow that can enter the GIWW, resulting in the lower velocities seen for Alternative 3a.1 (west side) when compared to

Alternative 9a (west side). Alternative 3a.1 shows a reduction in velocities when compared to existing conditions.

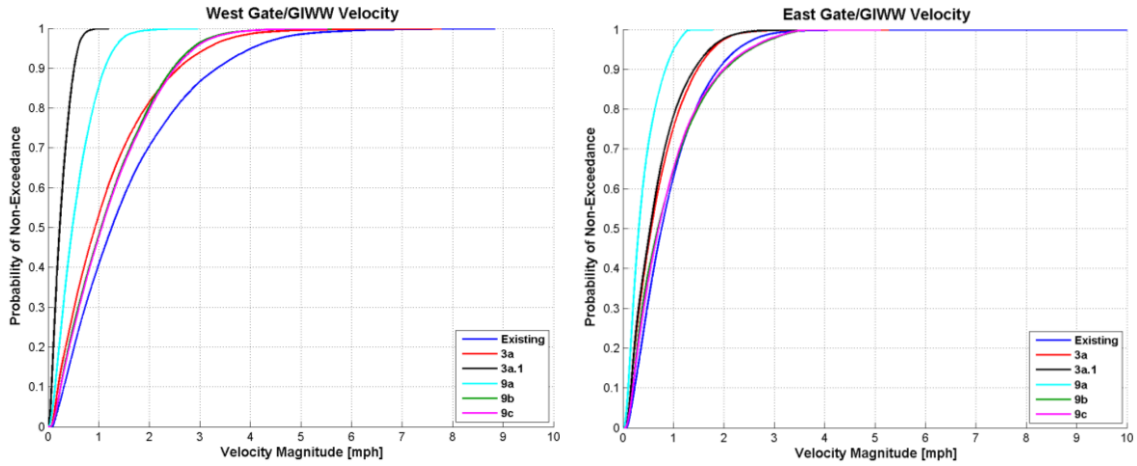

Figure 109. Probability of Non-Exceedance of velocity at gate locations (Existing/2a, 3a, 3a.1 east, 9b, 9c), and open GIWW (3a.1 west, 9a).

6.8 GIWW & Freeport Velocity Analysis

After the TSP milestone, further investigation into the velocity impacts of the proposed TSP (Alt. 3a.1) was conducted. Two areas of concern were identified during the comment period. First, there were concerns that the proposed removal of the west gate would cause elevated velocities in the section of the GIWW west of the Brazos River intersection. To investigate this concern, velocities were extracted from the 13-month modeling simulation described in Section 3. Velocities were extracted for existing conditions and the proposed TSP. CDF curves were extracted at stations spanning from the Brazos River to the San Bernard river to analyze any velocity impacts of the TSP. Figure 110 shows spatial distribution the 25th percentile, 50th, and 95th percentiles of river velocity at all extraction points all the West GIWW.

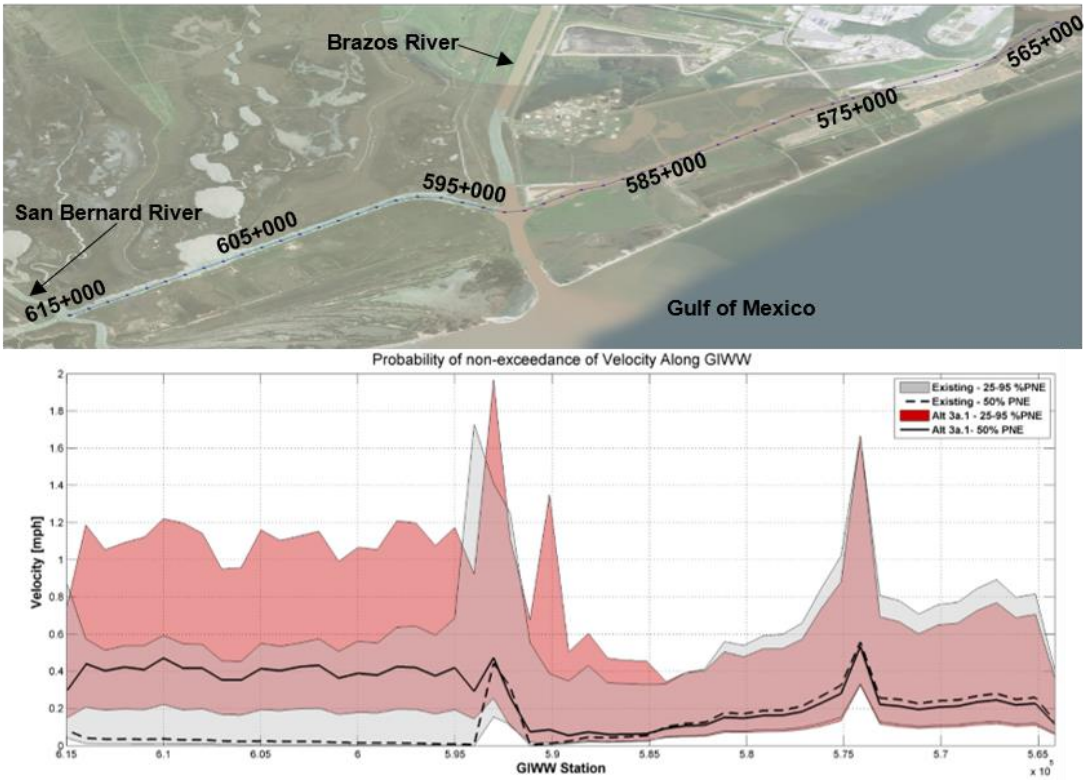

Figure 110. Spatial distribution of the 25th, 50th, and 95th percentiles of river velocity along the west GIWW for existing conditions (grey) and the TSP (red).

The TSP shows slightly increased velocities along the west GIWW. Based on previous project experience by the USACE, 2 mph was indicated as the velocity that could cause navigation concerns. There was less than a 0.1% change in the time above 2mph for the TSP, indicating that there are expected to be minimal impacts due to elevated velocities in the west GIWW as a result of the TSP.

In addition to the concerns about velocities in the west GIWW, the team extracted velocities along the Freeport Channel to determine if the wider gate, which was increased to 125' from the existing 75' gate, would increase velocities in the channel. Velocities were extracted at 16 locations along the Freeport Channel centerline for the full 13-month model simulation. CDF curves were developed at each point. Figure 111 shows the spatial distribution of the 25th, 50th, and 95th percentiles of river velocity at all extraction points in the Freeport Channel for existing and TSP conditions.

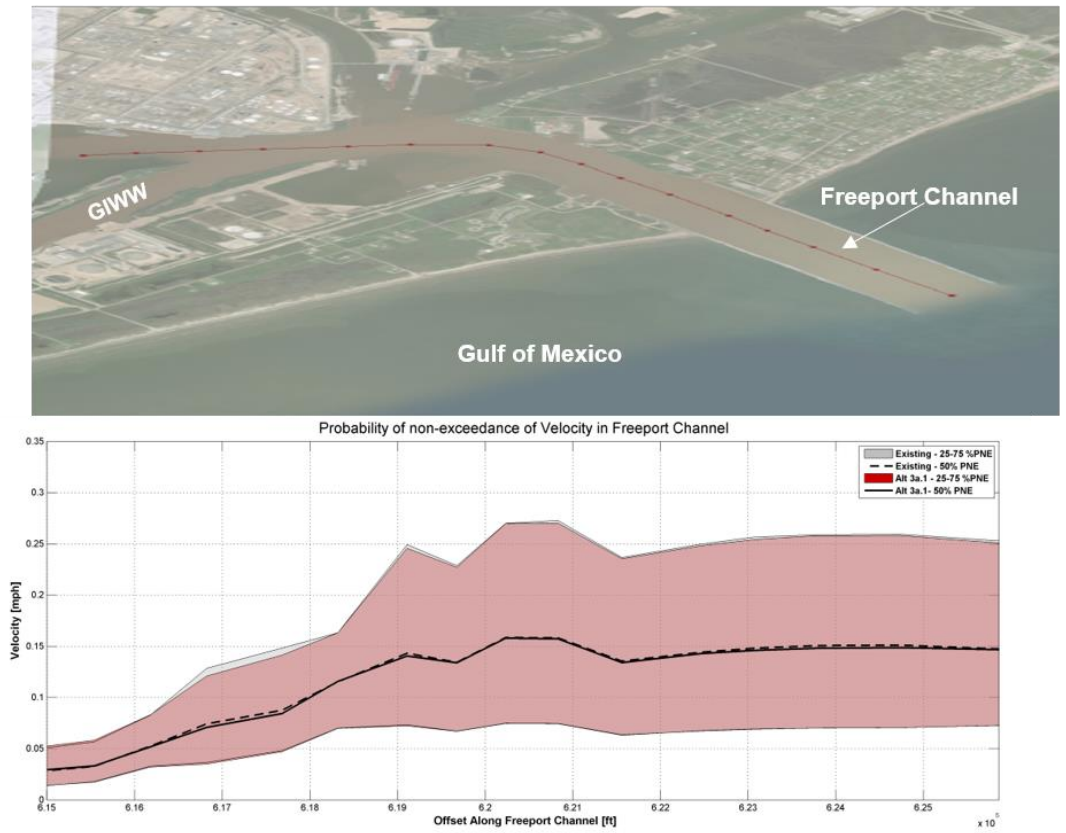

Figure 111. Spatial Distribution of the 25th, 50th, and 95th percentiles of river velocity along the Freeport Channel for existing conditions (grey) and the TSP (red).

Figure 112 shows CDF curves of velocity at two selected extraction points in the Freeport Channel.

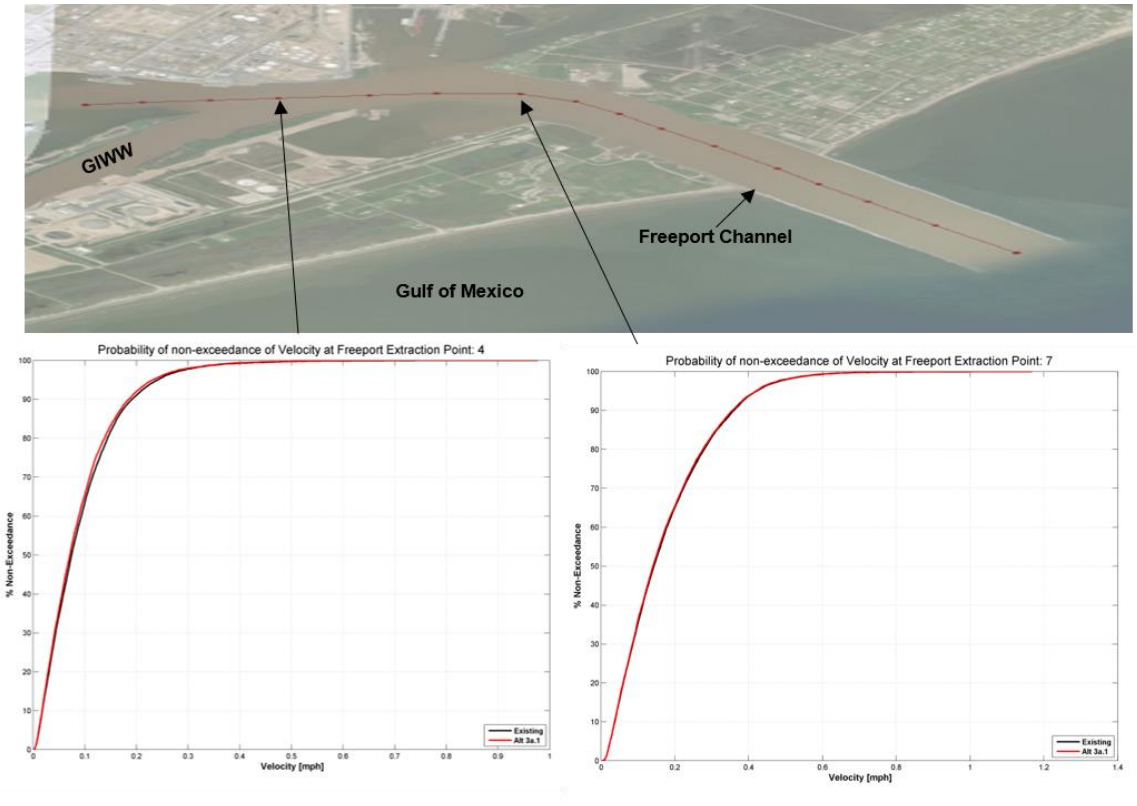

Figure 112. CDF curve for selected extraction points along Freeport Channel comparing velocity for existing conditions (black) and alt. 3a.1 (red).

Note the overlap between the CDF lines for existing conditions and the proposed TSP, indicating that any changes in velocity due to the proposed TSP are expected to be minimal.

7 References

Beven., J. (2003). *Tropical Cyclone Report Hurricane Claudette.* National Hurricane Center.

Bruun, P. a. (1960). Natural Bypassing of Sand at Coastal Inlets. *North Holland Publishing Co., Amsterdam*.

Bruun, P. M. (1978). Stability of Tidal Inlets: Theory and Engineering. *Developments in Geotechnical Engineering*.

Carlin, J. D. (2015). The influence of a salt wedge intrusion on fluvial suspended sediment and the implications for sediment transport to the adjacent coastal ocean: A study of the lower Brazos River TX, USA. *Marine Geology*, (Issue 359) 134-147.

FEMA. (1999). *Flood Insurance Study Brazoria County, Texas and Incorporated Areas.*

IPCC: Church, J., Clark, P., Cazenave, A., Gregory, J., Jevrejeva, S., Levermann, A., . . . Sta, D. (2013). *Sea Level Change. In: Climate Change 2013: The Physical Science Basis. Contribution of Working Group I to the Fifth Assessment Report of the Intergovernmental Panel on Climate Change (IPCC).* Cambridge, United Kingdom and New York, NY, USA.: Cambridge University Press.

Jeffery, E. (2015, December). Personal communication USGS gages at the intersection of the San Bernard River and the Gulf Intracoastal Waterway, Texas.

Kraus, N. a. (2002). *Coastal Processes STudy of San Bernard River Mouth, Texas: Stability and Maintenance of Mouth.* US Armer Corps of Engineers.

Texas Water Development Board. (2011). *Texas Water Development Borad, Surface Water, Bays, Coastal Hydrology*. Retrieved from http://www.twdb.texas.gov/surfacewater/bays/coastal_hydrology/index.asp

Tung, T. (2011). *Morphodynamics of Seasonally Closed Coastal Inlets at the Central Coast of Vietnam.* UNESCO-IHE, Delft.

TXDOT. (2015). *Request for Qualifications, Professional Engineering Procurement Services, Solicitation Number: 0000000986, .* Texas: TXDOT.

USACE. (1966). *33 CFR 207.187 - Gulf Intracoastal Waterway, Tex; special floodgate, lock, and navigation regulations.* USACE.

USACE. (1988). *Analysis of Sediment Transport in the Brazos River Diversion Channel Entrance Region.* Galveston: USACE.

USACE. (1999). *Engineering and Design for Civil Works Projects (EC 1110-2-1150).* Washigton, DC: USACE.

USACE. (2002). *Coastal Processes Study of San Bernard River Mouth, Texas: STability and Maintenance of Mouth.* Galveston: USACE.

USACE. (2014). *Coastal Modeling System Draft User Manual.* Vicksburg: USACE.

USACE. (2014, November 19). *Response to Climate Change, Comprehensive Evaluation of Projects with Respect to Sea-Level Change, Sea Level Change Curves*. Retrieved October 2015, from http://www.corpsclimate.us/ccaceslcurves.cfm

USACE. (2015). *Recent Climate Change and Hydrology Literature Applicable to US Army Corps of Engineers Missions.* USACE.

USACE. (2016). *High Water Operations Policy Brazos River Floodgate Colorado River Locks.* Corps of Engineers Project Operations.

USACE. (2017). Recorded Closure & Limited Passage Data at Brazos River Floodgates.

USGS. (2015). *USGS, Texas Water Science Center, Texas Real Time*. Retrieved November 2015, from http://tx.usgs.gov/infodata/basins.html

USGS. (2017, March). *USGS, Texas Water Science Center, Texas Real Time*. Retrieved from http://tx.usgs.gov/infodata/basins.html

USGS. (undated). *Status Report: Stream Velocity, Discharge, and Water-Quality Parameters at the Intersection of the San Bernard River and the Gulf Intracoastal Waterway, near River End, Texas, October 2003-September 2005.* USGS.

Zervas, C., Gill, S., & Sweet, W. (2013). *Estimating Vertical Land Motion from Long-Term Tide Gauge Records, NOAA Technical Report NOS CO-OPS 065.* NOAA National Ocean Service Center for Operational Oceanographic Products and Services.